The Dissertation Committee for Yinghui Li Certifies that this is the approved version of the following dissertation

FAST AND ROBUST PHASE BEHAVIOR MODELING FOR COMPOSITIONAL RESERVOIR SIMULATION

Committee:

Russell T. Johns, Supervisor

Steven L. Bryant

Larry W. Lake

Quoc P. Nguyen

Kamy Sepehrnoori

Birol Dindoruk

FAST AND ROBUST PHASE BEHAVIOR MODELING FOR COMPOSITIONAL RESERVOIR SIMULATION

by

Yinghui Li, B.S., M.S.

Dissertation

Presented to the Faculty of the Graduate School of

The University of Texas at Austin

in Partial Fulfillment

of the Requirements

for the Degree of

Doctor of Philosophy

The University of Texas at Austin

December 2007

Dedication

This dissertation is dedicated to my wife, Litao and my daughter, Grace. I would never have so much pleasure without you.

Acknowledgements

First and foremost, I appreciate all the guidance and education I received from my advisor, Dr. Russell Johns throughout my research. Without his dedication and constructive instruction, I would not have the opportunity to learn and mature, and my life in Austin would not have been so colorful.

I thank my wife, Litao and my little one, Grace for the endless pleasure and encouragement they brought me through all the ups and downs. I would also give my heartful thanks to my parents and my parents-in-law, for their help in the past years.

I thank my committee members, Dr. Lake, Dr. Sepehrnoori, Dr. Bryant, Dr. Nguyen and Dr. Dindoruk for their advice and time. In addition, I thank all other faculty members in the department who taught helpful knowledge to me. I also would like to thank Ms. Schenck, Ms. Kruzie, Ms. Pettengill and Dr. Terzian and all the administrative staff. Without their help, the dissertation process would have been much harder.

I thank Mr. Okuno and Mr. Ahamdi for their help. I also thank my friends in our group, department and school, who bring fresh air to my life everyday and make my studies bright. I especially thank the generous financial support from Dr. Johns, the Department of Petroleum and Geosystems Engineering and the Department of Energy under grant number DE-RA26-98BC15200. With the burnt orange running in my veins, I am thankful for the irreplaceable opportunities I received.

FAST AND ROBUST PHASE BEHAVIOR MODELING FOR COMPOSITIONAL RESERVOIR SIMULATION

Publication No._____

Yinghui Li, Ph.D

The University of Texas at Austin, 2007

Supervisor: Russell T. Johns

A significant percentage of computational time in compositional simulations is spent performing flash calculations to determine the equilibrium compositions of hydrocarbon phases in situ. Flash calculations must be done at each time step for each grid block; thus billions of such calculations are possible. It would be very important to reduce the computational time of flash calculations significantly so that more grid blocks or components may be used.

In this dissertation, three different methods are developed that yield fast, robust and accurate phase behavior calculations useful for compositional simulation and other applications. The first approach is to express the mixing rule in equations-of-state (EOS) so that a flash calculation is at most a function of six variables, often referred to as reduced parameters, regardless of the number of pseudocomponents. This is done without sacrificing accuracy and with improved robustness compared with the conventional method. This approach is extended for flash calculations with three or

more phases. The reduced method is also derived for use in stability analysis, yielding significant speedup.

The second approach improves flash calculations when *K*-values are assumed constant. We developed a new continuous objective function with improved linearity and specified a small window in which the equilibrium compositions must lie. The calculation speed and robustness of the constant *K*-value flash are significantly improved. This new approach replaces the Rachford-Rice procedure that is embedded in the conventional flash calculations.

In the last approach, a limited compositional model for ternary systems is developed using a novel transformation method. In this method, all tie lines in ternary systems are first transformed to a new compositional space where all tie lines are made parallel. The binodal curves in the transformed space are regressed with any accurate function. Equilibrium phase behavior calculations are then done in this transformed space non-iteratively. The compositions in the transformed space are translated back to the actual compositional space. The new method is very fast and robust because no iteration is required and thus always converges even at the critical point because it is a direct method.

The implementation of some of these approaches into compositional simulators, for example UTCOMP or GPAS, shows that they are faster than conventional flash calculations, without sacrificing simulation accuracy. For example, the implementation of the transformation method into UTCOMP shows that the new method is more than ten times faster than conventional flash calculations.

Table of Contents

List of Tables

List of Figures

Chapter 1: Introduction

Enhanced oil recovery (EOR) processes will be very important to lessen the gap between oil supply and demand. Many EOR processes, such as gas injection, result in complex interactions of flow with phase behavior. This is mainly because reservoirs are operated at conditions where miscibility is developed between the injection gas and the reservoir fluid. Depending on production pressure and gas composition, there are two different miscibility mechanisms: first-contact miscibility (FCM) and multi-contact miscibility (MCM). For FCM, the reservoir hydrocarbon is miscible with the injection gas in any proportion so that a piston-like or quasi-piston-like displacement occurs. First contact miscible displacements often require very high pressures that are usually not obtainable. For MCM, miscibility is developed in situ by repeated contacts between the injection gas and the reservoir fluid. Compositional changes are the important driving force for enhanced recovery, and distinguish gas injection from immiscible water floods.

Reservoir simulation is often performed to evaluate the oil reservoirs and production strategies, and to give valuable insights into the displacement mechanisms. Despite simplicity and speed, black oil models are typically too simple to accurately account for the compositional changes that occur in gas flooding simulations. Since most EOR processes are compositional in nature, we need compositional simulations to model them.

In compositional simulation, we need to solve for the following at each time step for each grid block: (1) When the injection solvent contacts with the reservoir fluid, does the mixture split into multiple phases or not? (2) If the overall composition is not stable, how many phases will form? (3) For each phase, what are the equilibrium compositions? (4) What are the phase saturations and densities? Equations-of-state

(EOS) are used to test the stability of a single-phase mixture and also to determine equilibrium compositions by flash calculations if Np>1. The first two questions are answered with stability analysis calculations, and the remaining with phase-split calculations.

A significant disadvantage of fully compositional simulations, however, is that they are much more computationally intensive than black-oil simulations. Thus there is a great need for faster and more robust compositional simulators. The primary reason for the increased computational time is the result of solving iterative flash calculations in each time step for each grid block. For example, for an IMPEC (implicit pressure explicit compositions) type simulation with grid blocks of 200 × 200 × 25 and 2000 time steps, about two billion flash calculations are performed. A linear solver to update reservoir pressure for the same case would be done 2000 times. In general, flash calculations using cubic EOS can occupy a significant percentage of total computational time in IMPEC compositional simulations (Stenby and Wang, 1993; Chang, 1990).

Repeated flash calculations with cubic EOS are also needed in other problems such as multi-phase flow in pipelines (Lityak and Wang, 1998) and determination of minimum miscible pressure (MMP) or minimum miscible enrichment (MME) by an analytical method (Jessen *et al.*, 1998; Yuan and Johns, 2005).

There are a few standard methods used to reduce computation time in flash calculation. The first is to use fewer pseudocomponents. However, this approach results in less accuracy and requires significantly more tuning (Hong, 1982; Liu 2001; Egwuenu *et al.* 2005). This is especially true in MCM displacements, in which miscibility is developed by a combined condensing/vaporizing (CV) drive process (Zick, 1986; Johns *et al.*, 1992; Johns *et al.* 1993; Johns and Orr, 1996). Fluid characterization for these models can be improved by tuning to the analytical MME or MMP (Egwuenu *et*

al. 2005), but those models still require significant computational time even with fewer pseudocomponents.

Another way to decrease computation time is to reduce the number of grid blocks. With coarser grids, however, numerical dispersion is unrealistically large, which will result in poor prediction from simulation (Solano *et al.* 2001). Ideally, fine grids should be used that can better match the level of dispersion found at field scale.

In this dissertation, we focus on three different approaches for rapid calculations: (1) phase-split calculations and stability analysis using EOS models; (2) constant *K*-value models, and (3) simplified phase behavior models for limited compositional simulation.

1.1 TWO-PHASE SPLIT CALCULATIONS USING EQUATIONS-OF-STATE

In compositional simulation, we often assume that the reservoir fluid and injection gas are at thermodynamic equilibrium in each grid block at each time step. Equilibrium compositions depend on reservoir temperature, pressure and overall composition given by mass balance equations (governing equations in IMPEC type reservoir simulators). Two distinct methods are used to calculate equilibrium compositions. The first is to minimize Gibbs free energy of the mixture, because Gibbs free energy should be a minimum when the mixture is at equilibrium (Heidemann, 1974; Gautam and Seider, 1979; Trangenstein, 1985). The other uses the equality of fugacity for each component at different phases and solves these nonlinear fugacity equations to find equilibrium compositions (Michelsen, 1982a, 1982b). In conventional flash calculations, there are N_C primary variables, for example equilibrium *K*-values for each pseudocomponent, where N_C is the number of pseudocomponents. As a result, the speed of flash calculations usually decreases quadratically as a function of N_C.

More recently, reduced methods are of growing interest, because they can significantly decrease the number of primary variables for flash calculations, and thus greatly save computation time. In these methods, we can write excess Gibbs energy and fugacities in terms of a few groups that are called reduced parameters or reduced variables.

For example, when all binary interaction parameters (BIPs) are zero, the speed of phase-split calculations can be significantly improved by finding three reduced parameters using the standard van der Waals mixing rules (Michelsen, 1986). The number of primary variables is therefore independent of the number of pseudocomponents. The assumption of all zero BIPs is not realistic, however, when CO_2, nitrogen or other non-hydrocarbon components are injected or present.

Jensen and Fredenslud (1987) extended Michelsen's approach (1986) by using two more reduced parameters when only one column of the BIP matrix is non-zero. For example, when CO_2 is injected, they obtained five reduced parameters. All other BIPs between the remaining components, however, must be zero, which again limits its usefulness. Their method quickly becomes cumbersome when there are many pseudocomponnets with non-zero BIPs. For an N_C-component system, if there are m columns or rows in the BIP matrix that have non-zero elements, the total number of reduced parameters is $2m+3$. When m is large, the number of reduced parameters can be a large value, and thus no or little improvement in speed compared with the conventional method.

Recently, a different diagonalization method for the BIP matrix is proposed using linear transformation techniques (Nichita, 2006). This model solves a set of linear functions for the BIP matrix. Although this method maintains the diagonal BIP elements, it provides no further reduction compared with the model developed by Jensen

and Fredenslund (1987). We still need $2m+3$ reduced variables for m components that have non-zero BIPs with other components (Jensen and Fredenslund, 1987; Nichita and Minescu, 2004; Nichita, 2006).

Hendricks (1988) used an eigenvalue analysis method to identify the dominant BIPs in phase-split calculations. The binary interaction parameter matrix is recalculated by setting all small eigenvalues to be zero, using some predetermined criterion (that are often uncertain). Hendricks and van Bergen (1992) later applied this procedure using Newton-Raphson (NR) iteration. Although this method is faster than conventional flash calculations, zeroing of eigenvalues can lead to non-physical BIPs in that the diagonal elements of the BIP matrix have small nonzero values. In addition, their method is only an approximation at its best to the original phase behavior characterization. Pan and Firoozabadi (2001) formulated phase-split calculations using the same reduced parameters of Hendricks (1988) with a general cubic EOS (Coats, 1985).

The comparison of the BIP modeling methods (Michelsen, 1986; Jensen and Fredenslund, 1987; Nichita, 2006) and the dominant eigenvalue decomposition methods (Hendricks, 1988; Pan and Firoozabadi, 2001; Nichita et al. 2004) from the previous research indicates that: (1) both approaches significantly reduce the number of primary variables. Dominant eigenvalue decomposition methods require the elimination of small eigenvalues to achieve this objective, while BIP modeling methods require a strong interrelationship in BIP elements. (2) Dominant eigenvalue decomposition is only an approximation at its best, and may often lead to non-zero diagonal BIPs. (3) If BIPs are required to change frequently as reservoir pressure and temperature change, determining the dominant eigenvalue is required for each grid block in each time step. As a result, this method can be very computationally intensive. (4) BIP modeling method may

provide easier and systematically accurate regression than dealing with individual BIP elements. The regression process is empirical subject to experience, but a strong interrelationship, although still ambiguous, may be an appropriate approach accounting for the physical forces between hydrocarbon molecules.

The global minimization method for flash calculations can also be applied in both actual compositional space (Nagarayan *et al.*, 1991; Bullard and Biegler, 1993, Han and Rangaiah 1997) and reduced space (Pan and Firoozabadi, 1998; Firoozabadi, 1999; Nichita *et al.*, 2002). These methods are of great value and some reservoir simulators use these methods (only available in actual compositional space) over direct solution methods. For simplicity and better speed, however, we only consider direct solution methods to calculate equilibrium compositions in this dissertation. In addition, the purpose of this dissertation is not to examine the difference by using various iterative methods, but to propose a practical EOS model for compositional simulators. This new EOS model can be optimized by applying different iterative techniques, which may be a topic of future research.

1.2 STABILITY ANALYSIS CALCULATIONS USING REDUCED METHOD

Stability analysis is very important in reservoir simulations because slow phase-split calculations that are unnecessary can be eliminated. In addition, stability analysis can often provide a better initial guess for phase-split calculations. Stability analysis should be done for each grid block at each time step. As a result, phase-split calculations are performed only when (1) stability analysis shows that the mixture of the reservoir fluid and injection gas is unstable; or (2) the grid block has multiple phases in the previous time step (Voskov and Tchelepi, 2007).

Similar to phase-split calculations, there are two different approaches for stability analysis. The first approach focuses on finding the minimum of the tangent plane distance (TPD) function and the second focuses on finding the stationary points of TPD and then evaluates the TPD values at those stationary points. The tasks are similar in both approaches. In the first approach, we need to find the global minimum rather than local minima. In the second approach, we need to locate all the stationary points.

Baker *et al.* (1982) examined the Gibbs free energy surface and the tangent plane to that surface at calculated equilibrium compositions. When the Gibbs free energy surface is always above the tangent plane, tangent points are the correct equilibrium solutions. When Gibbs free energy surface is below the tangent plane at any composition, the equilibrium solution is incorrect, although that solution satisfies both mass balance and equal-fugacity constraints.

Further based on this Gibbs free energy analysis, Michelsen (1982a) formulated phase stability analysis by calculating the distance between Gibbs free energy surface and the tangent plane, called the tangent plane distance (TPD). Stability analysis is to locate the minimum of the TPD at all compositions. He further suggested that the check of positivity at stationary points is sufficient. In addition, Michelsen (1982a) suggested that it is sufficient to determine the stationary points by the initial guesses using a composition made up of either the most or least volatile components. This approach is widely used in stability analysis calculations owing to its simplicity.

Hua *et al.* (1996) found all stationary points of the TPD by an interval Newton/Bisection method. However, their approach requires significant calculations because the actual compositional space is divided into many small sub-domains and Newton/Bisection calculations are then applied in each of them. This approach is very

expensive in reservoir simulations because billions of these stability analysis calculations are executed.

Rasmussen et al (2006) identified a problematic region for stability analysis calculations, which is located close to the two-phase boundary. In this region, a slight overshooting of the Newton step may force convergence to the trivial solution where $y_i = z_i$ rather than to the correct solution.

All the methods above used compositions of the trial phase as primary variables. That is, an N_C-component system requires N_C primary variables. As a result, stability analysis calculations are still relatively very slow.

Some researchers have extended stability analysis calculations in reduced space by the dominant eigenvalue decomposition of the BIP matrix using Lagrange multipliers (Firoozabadi and Pan, 2002) or direct solution methods (Nichita *et al.* 2004; Hoteit and Firoozabadi, 2006). In addition, Hoteit and Firoozabadi (2006) also identified the trivial solution problem mentioned by Rasmussen *et al.* (2006) in reduced space. Nevertheless, they showed that the reduced method is much faster with a speedup ratio that depends on the number of pseudocomponents. This is mainly because the reduced method uses significantly less primary variables and thus a much smaller Jacobian matrix (in direct solution approach) or Hessian matrix (in minimization approach).

The global minimization method, although not a topic in this dissertation, has attracted some interest as well to be used both in actual compositional space (McDonald and Floudas, 1995; Sun and Seider, 1995; Hua *et al.*, 1996; Hua *et al.*, 1998; Harding and Floudas, 2000) and in reduced space (Firoozabadi and Pan, 2002; Nichita *et al.*, 2002; Nichita *et al.* 2006). Stability analysis calculations that are currently performed in reduced space employ the same reduced variables using the dominant eigenvalue decomposition method as described by Hendricks and van Bergen (1992). Firoozabadi

and Pan (2002) also observed that the TPD surface is smoother in the reduced space than in compositional space. Because of the same concern we have in phase-split calculation, we only focus on direct solution methods in this study.

1.3 PHASE-SPLIT CALCULATIONS USING REDUCED METHOD FOR THREE OR MORE PHASES.

Phase-split calculations for three or more phases have important applications as well. For example, CO_2 injection can result in the formation of three hydrocarbon phases — two oleic phases and one gaseous phase — under realistic reservoir temperatures and pressures.

Conventional phase-split calculations can be extended to three or more phases. However, for an N_C-component system with N_P phases, the conventional method requires iterations on $(N_P - 1)N_C$ primary variables, i.e., the *K*-values of each component in each phase (expect those in the reference phase). As a result, phase-split calculations are much slower than that in the two-phase region. This is mainly because of the significantly increased size of the Jacobian matrix.

We can also extend the reduced method to phase-split calculations in three or more phases, similar to that in two-phase flash calculations. Since the number of primary variables is greatly lowered compared with conventional flash calculations, the speedup could be much more than two-phase flash calculation.

Nichita *et al.* (2005) used the same reduced parameters as described by Hendricks and van Bergen (1992) for phase-split calculations in three or more phases. They showed that, similar to that in two-phase flash calculations, both computation speed and robustness are significantly increased compared with the conventional phase-split method.

1.4 FLASH CALCULATIONS WITH CONSTANT K-VALUES

Flash calculations with constant *K*-values play an important role as well in reservoir simulations in that: (1) in each of the conventional flash step 5, we need to use this iterative routine to update *K*-values; (2) for grid blocks where pressure is much lower than MMP, constant *K*-values is a good approximation for the phase behavior. Constant *K*-value flash calculations are much faster than EOS flash calculations. Even though this flash calculation is easier to formulate than EOS flash calculations, there are potential problems that can lead to the wrong solutions.

Rachford and Rice (1952) derived a simple objective function assuming constant *K*-values to calculate phase compositions for two equilibrium phases. They used an iterative bisection method where phase molar fraction, either the liquid phase or the vapor phase, is constrained to lie in the range from 0.0 to 1.0. Equilibrium phase compositions are then calculated by mass balance equation from the converged phase saturation and overall compositions. The objective function of Rachford and Rice (1952), however, has many poles and roots and is often very nonlinear. As a result, the convergence to the correct root by bisection method can be very slow. Further, when the overall composition lies outside the two-phase zone, the correct root is not between 0.0 and 1.0.

Li and Nghiem (1982) extended the Rachford-Rice method (1952) to negative flash calculations, where the overall composition can be outside two-phase zone, but within the region of tie-line extensions. They also improved the speed of convergence by using Newton-Raphson (NR) iterations. There is no guarantee with their method, however, that NR will converge to the correct root because of the multiplicity of poles and roots.

Whitson and Michelsen (1989) made a significant improvement in the robustness of negative flash calculation by specifying a range or window in which the correct root of the phase molar fraction should lie. Furthermore, they showed that there are no poles within that range. Because of the nonlinearity of the Rachford-Rice (1952) objective function, however, their improvement still suffers from many of the same disadvantages as the original Rachford-Rice method (1952).

Several authors (Von Rossenberg, 1963, 1977; Warren and Adewumi, 1993; Monroy-Loperena and Vargas-Villamil, 2001) derived a new objective function by multiplying the Rachford-Rice (1952) function by its denominators (poles). This approach makes the new objective function more continuous than the Rachford-Rice objective function (1952). However, this objective function is much more computationally intensive and nonlinear than the original Rachford-Rice (1952) function. Thus, this approach offered no significant advantages over the Rachford-Rice (1952) function with the Whitson and Michelsen (1989) window.

Leibovici and Neoschil (1992) continued this approach. They multiplied the Rachford-Rice objective function (1952) by the denominators of poles corresponding to the lightest and heaviest components, instead of all the pseudocomponents. They gave a smaller window for phase mole fraction than that of Whitson and Michelsen (1989) and showed some improvement in average computational time for the flash calculations considered. Their method, however, still has problems with the nonlinearity of the objective function, especially when the lightest and heaviest components are present in small amounts and the overall composition is close to either the bubble-point or dew-point curves. Their method also suffers from increased computational cost per iteration and in most cases of practical interest will not be faster than Rachford-Rice (1952).

Last, their method cannot be extended to equilibrium calculations with more than two phases (Leibovici and Neoschil, 1995), and is therefore not a general approach.

Wang and Orr (1997, 1998) used the same Rachford-Rice (1952) objective function, but iterated on the liquid equilibrium phase composition of the lightest component (x_1) instead of vapor phase molar fraction. Their goal was primarily to improve the convergence for overall compositions outside of positive composition space where at least one overall composition is negative. For practical flash calculations, however, their method is similar to that of Rachford-Rice (1952). In addition, this approach suffers from a trivial solution at $x_1 = 0$.

1.5 LIMITED COMPOSITIONAL RESERVOIR SIMULATION

Comparison of EOS compositional simulators and black-oil models indicates that the difference in computational time of a simulation largely depends on phase behavior calculations. In EOS compositional simulators, equilibrium phase compositions are calculated iteratively by solving equal-fugacity equations. In black-oil models, phase behavior calculations are much faster using some simple relationships, for example, solubility as a function of the pressure.

There are many simulation projects that black-oil models are inappropriate to use even though they are faster than compositional models. For example, in CO_2 sequestration in an oil reservoir, the phase behavior is often considerably much more complicated than that used in black-oil models. However, the reservoir itself may require so many grid blocks and time steps that prohibit the use of expensive EOS compositional simulators. Even if we can lump the reservoir fluids using only a few pseudocomponents or use reduced methods, flash calculations are still iterative, and thus fully compositional simulation is still slow. It is obvious that an accurate non-iterative

phase behavior model is very desirable. One approach is to use simplified phase behavior models for a limited number of pseudocomponents, but where the key compositional effect such as vaporization are retained.

Limited compositional reservoir simulators (LCRS) could be used to fill the gap between EOS compositional and black-oil models. There are some three- or four-components LCRS available, and the major difference among them is usually the phase behavior calculations. The required flash calculations for each grid block must be: (1) very efficient in that no fugacity calculations should be used to determine equilibrium compositions; (2) very fast in that no or only a few iterations are needed in flash calculations; (3) unique in that only the correct solution(s) can be determined for any given overall composition, and no tie line can intersect in the multi-phase region; and (4) reasonably accurate in that the intersection of tie lines and binodal curves (bubble point and dew point curves) can represent experimental data or EOS flash calculation results.

There are two different pieces of information required to calculate equilibrium phase compositions. One is for the shape of the binodal curves and the other is for the slope of the tie line passing through the specified overall composition. In LCRS, both information is significantly simplified, so that direct solution is possible.

One common practice is compositionally independent *K*-values, which are the ratio of equilibrium vapor compositions to liquid compositions. This type of flash calculation is outlined in section (1.4), and in more detail in Chapter 4 for a newly developed model. In this type of model, the binodal curves are straight lines (or plains), and the tie lines are defined by these *K*-values (Fig. (1.3)). However, we still need iterations for equilibrium computations using this model, although the calculation is much faster compared with EOS compositional model because only one primary variable is used for the two-phase flash calculations. Flash calculations with compositionally

independent *K*-values are sometimes good approximations when reservoir pressure is significantly lower than MMP (and thus it is immiscible flood or when the composition path avoids the critical region.), for example, for the case of ternary systems as shown in Fig. (1.1). However, when reservoir pressure is greater than the MMP during gas flooding, it is impossible for these *K*-values to be compositionally independent. For example, it is very inaccurate if we assume constant *K*-values for the ternary system shown in Fig. (1.2).

Similar approaches include solubility models that can only simulate partial miscible floods. In solubility models, solvent solubility in the oleic phase is calculated using a similar way of calculating the solution gas-oil ratio in black-oil models. However, solubility is no longer defined under miscible flooding conditions. In reservoir simulation, if the pressure is less than the MMP, we often use these models; and when the pressure is higher than MMP, we could use Todd-Longstaff mixing rule (1972) or other approaches to correct for miscibility.

Phase behavior for a ternary diagram could also be simplified by assuming the dew-point and bubble-point curves are straight lines. For example, a phase envelope with this assumption is shown in Fig (1.4). There are several major drawbacks of this model: (1) no critical point can exist. (2) For a single phase composition close to the critical point, this model mistakenly treats it as two phases, and thus may yield inaccurate results; and more importantly (3) no tie-line information is given, and thus intensive iterations are still required.

An alternative approach to model a miscible flood is described by Tang and Zick (1986) for ternary systems. In their model, tie lines are assumed to converge to a common point, known as the pivot composition, which is taken to be the dead oil pseudocomponent. Binodal curves are assumed to be piecewise linear to the critical

point as is shown in Fig. (1.5). This model is relatively inaccurate because the pivot point assumption is usually invalid for most miscible floods. Further, if we use multiple linear segments, the pressure dependence of these connecting points requires significant computation time.

1.6 HAND'S METHOD

Another simple representation of binodal curves and tie lines are made by Hand (1930). He found that certain ratios of equilibrium compositions in a ternary system are sometimes straight lines on a log-log scale (see Fig. (1.6)). His method to determine equilibrium compositions generally requires an iterative approach. For some cases, iterations are not required for example in surfactant flooding, when (1) the critical point is at one of the apexes; and (2) the binodal curves are symmetric. With these assumptions, the new phase envelope can be solved directly by a quadratic solver. This simplified phase behavior is shown in Fig. (1.7).

Hand's model (1930) requires that two components are fully immiscible with each other such that the tie line at the bottom extends to both apexes. However, in gas floods even the most and least volatile components have some mutual solubility. This limitation, however, can be lifted by altering the apexes of the ternary diagram to the solubility limits on the base tie line (Welch, 1982). Direct solution also requires that all tie lines converge to one of the apexes, which may be accurate enough for some surfactant cases, but not in gas floods. In addition, for a simple ternary gas flooding, it has been shown that the straight-line assumption in Hand's plot (1930) is largely inaccurate. For example, for a ternary system composed of C_1, nC_4 and nC_{10} at 2000 psia and 150^{o}F, bubble point and dew point curves are shown in Fig. (1.8). If we

implement Hand's method (1930) on this ternary system, it does not accurately predict the equilibrium compositions as shown in Fig. (1.9).

In the same paper, Hand (1930) gave another approach to simplify phase behavior. This approach assumes equilibrium compositions for the intermediate components are same at fixed temperature and pressure for both phases. This assumption essentially implies that all tie lines in compositional space have the same slope, i.e., are parallel. However, this approach is typically invalid for gas flooding or surfactant flooding cases of practical interest. In this dissertation, we extend this idea from Hand (1930), however, to model accurately real phase behavior data.

1.7 OBJECTIVES AND OUTLINE OF DISSERTATION

The objective of this research is to develop simple, fast, robust and accurate flash calculation models that can be applied for compositional simulation. Chapter 2 describes EOS compositional phase-split calculations based on our new reduced method. We develop a new BIP model that lead to a maximum of six reduced parameters even when all BIP elements are non-zero. Our research shows that this model is very accurate compared with other reduced methods. This new model is also significantly faster than conventional phase-split calculations. We also formulate phase-split calculations in three or more phases using the same BIP model. In Chapter 3, stability analysis calculations for EOS compositional simulators based on the same reduced model are described using a direct Newton-Raphson method. The stability analysis is also much faster and more robust compared with conventional stability analysis. In Chapter 4, a new phase flash calculation with constant K-values is outlined. This new objective function is faster and more robust than Rachford-Rice (1952), which is currently used in most simulators. In Chapter 5, we develop a simplified phase behavior model for

ternary systems using a new transformation method. As a result, flash calculations are non-iterative and can account for different reservoir pressures. Simulation results show that this model is very accurate compared with EOS models. Last, we draw some conclusion and outline possible future research.

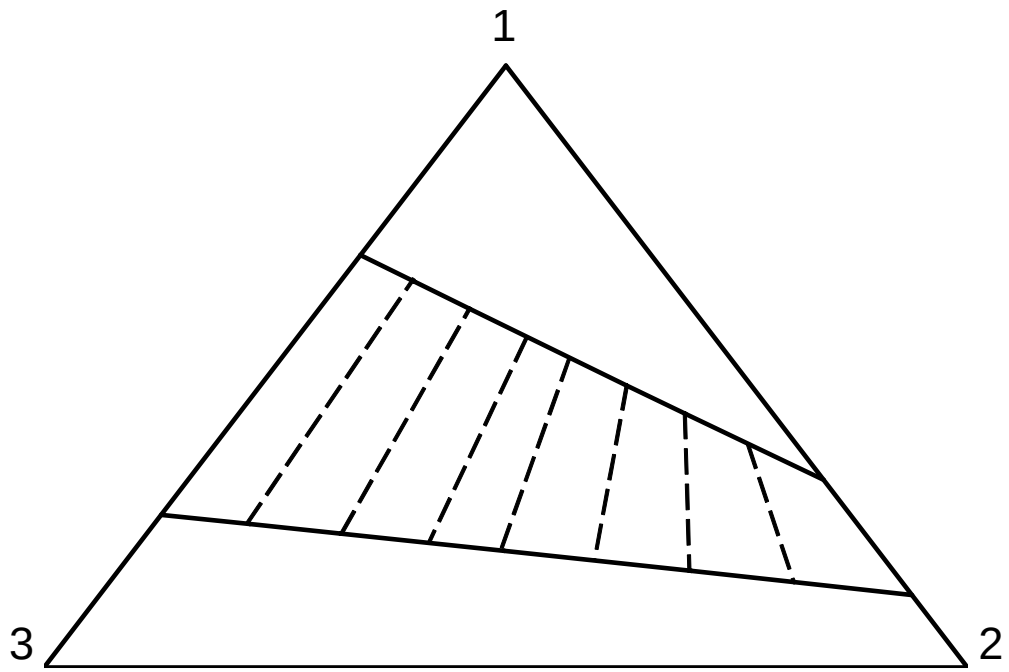

Fig. 1.1 A ternary system without a critical point. *K*-values for the tie lines are composition dependent.

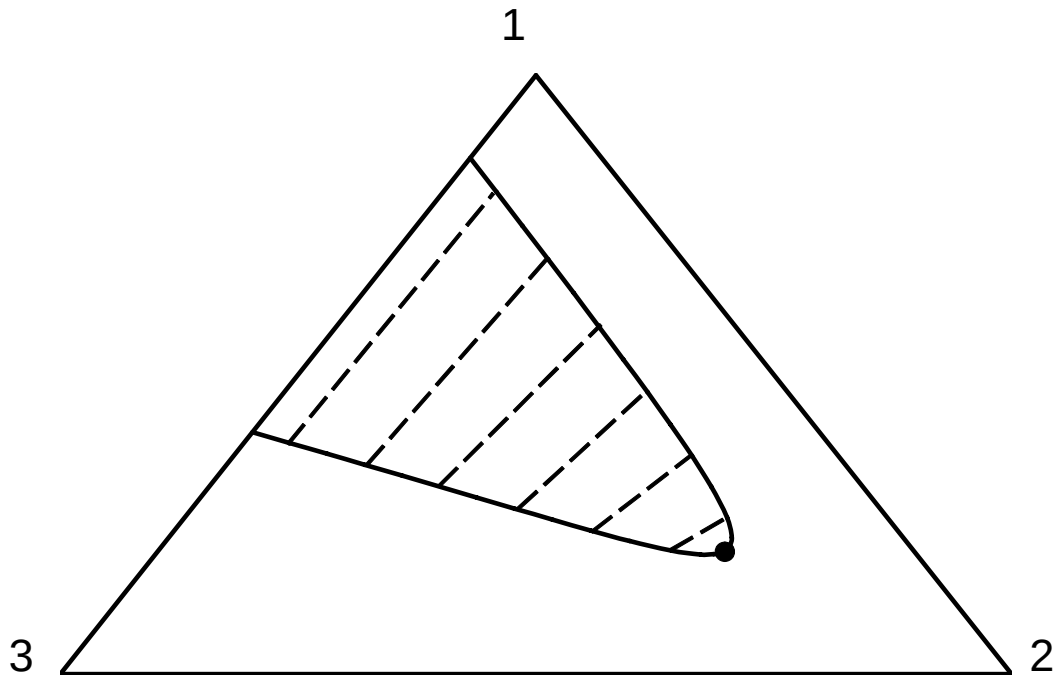

Fig. 1.2 Ternary diagram with a critical point. K-values along different tie lines are composition-dependent. The critical point is shown by the solid circle.

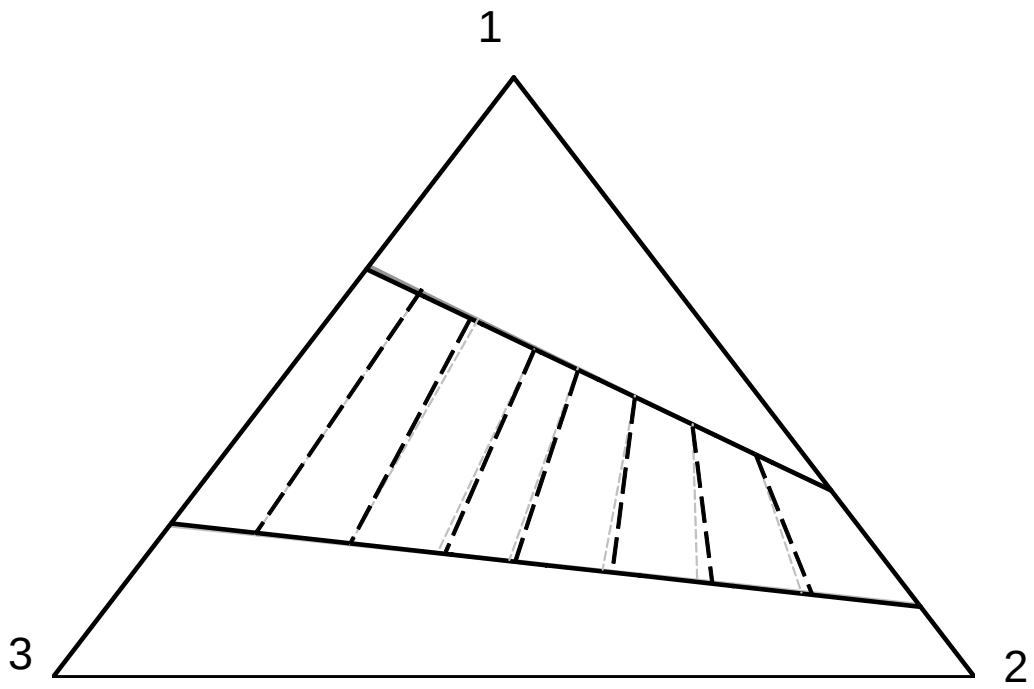

Fig. 1.3 Constant *K*-value approximation for the ternary system shown in Fig. (1.1). The original tie lines and binodal curves are shown in grey, and the current simplification is shown in black.

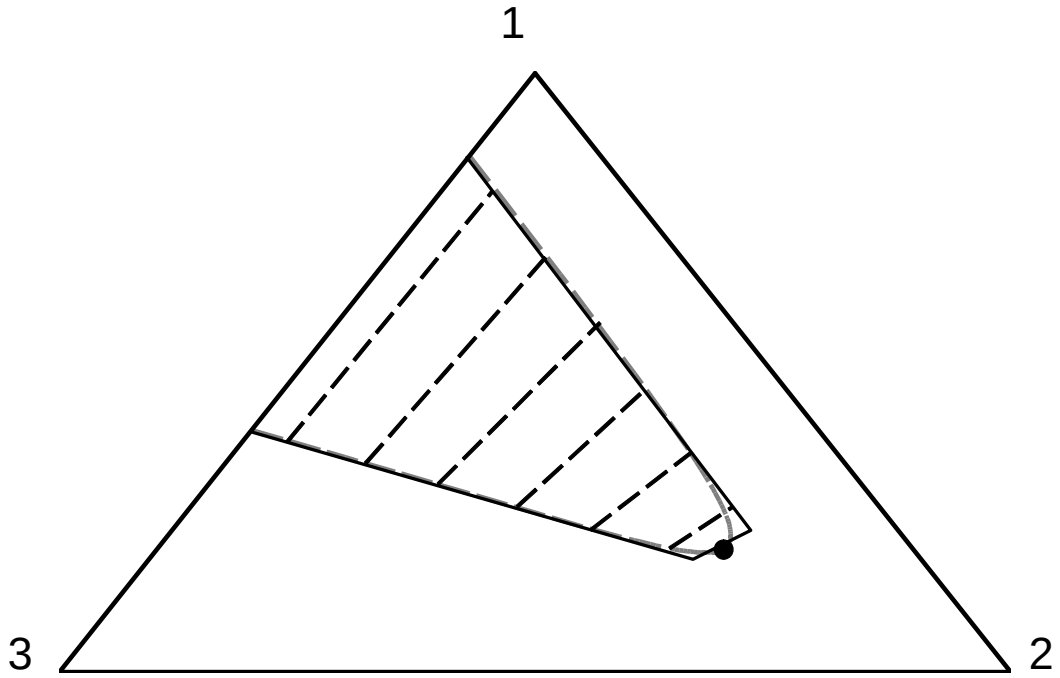

Fig. 1.4 Simplified ternary diagram for Fig. (1.2). The critical point is replaced by a limiting tie-line, and the binodal curves are straight lines. The original phase envelope is shown in grey.

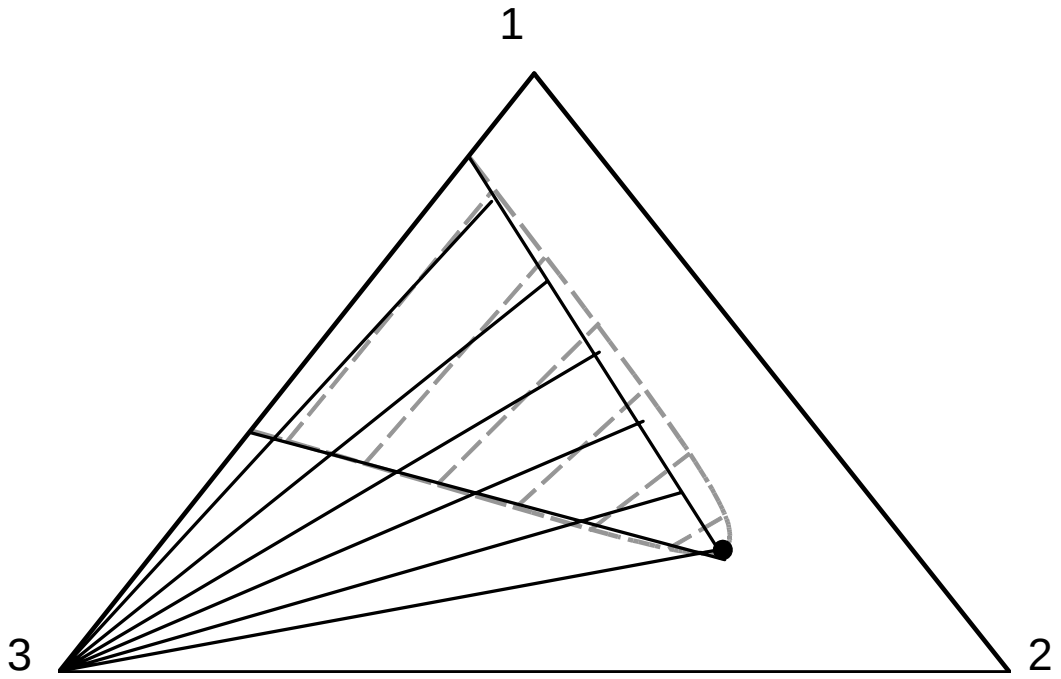

Fig. 1.5 Phase behavior model of Tang and Zick (1985). In this model, all tie lines go to the pivot composition (the dead oil pseudocomponent). The original phase envelope is shown in grey, and Tang and Zick's binodal curves in black.

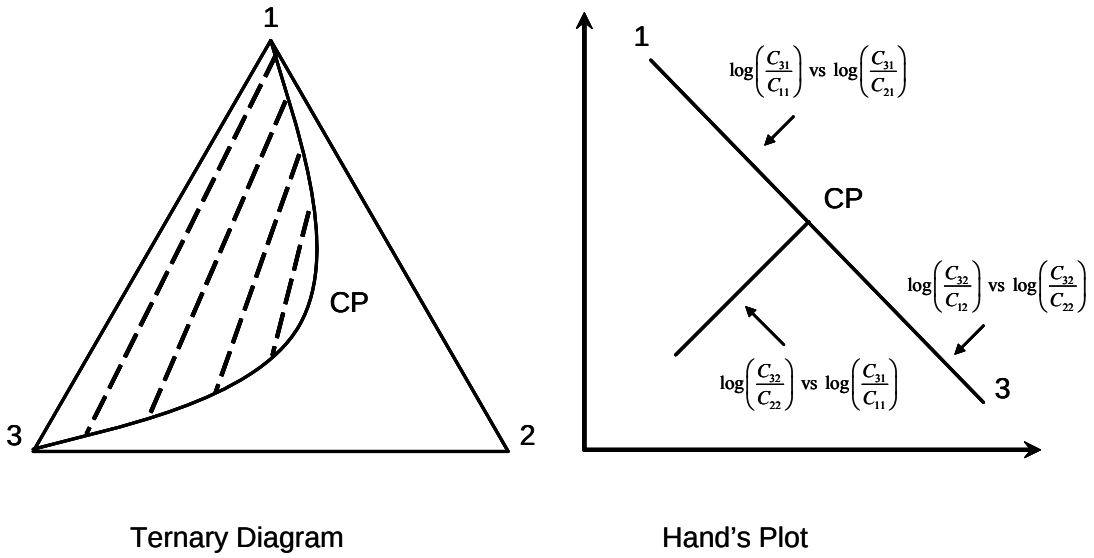

Fig. 1.6 Ternary diagram described by Hand's simplification (1930). The solution requires iteration of the non-linear equations that fit Hand's plot.

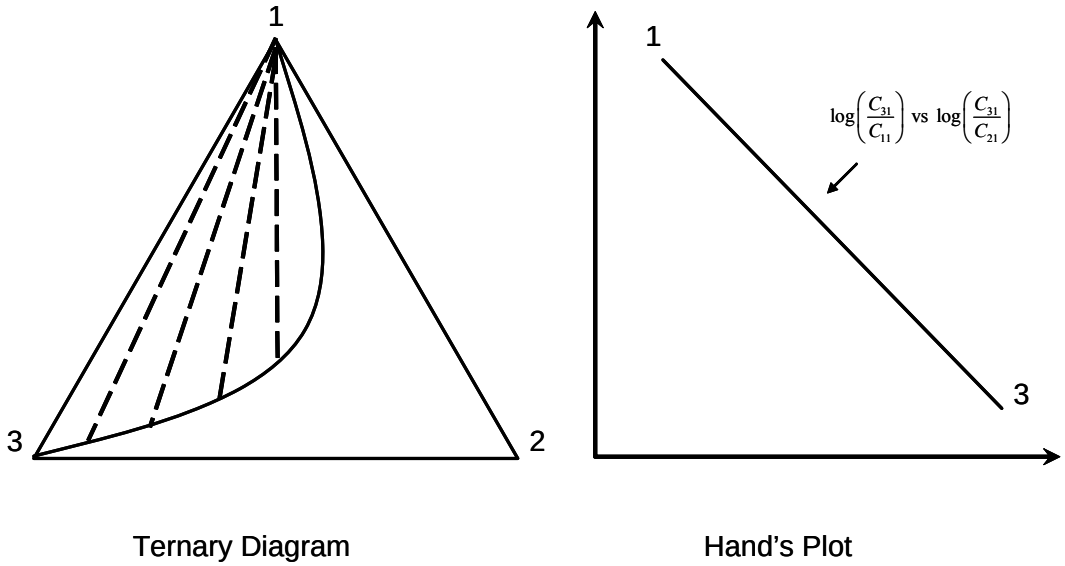

Fig. 1.7 Ternary diagram described by Hand's model that requires no iterations. The critical point is at the apex where all tie lines intersect. The ratios of specified compositions have a unit slope.

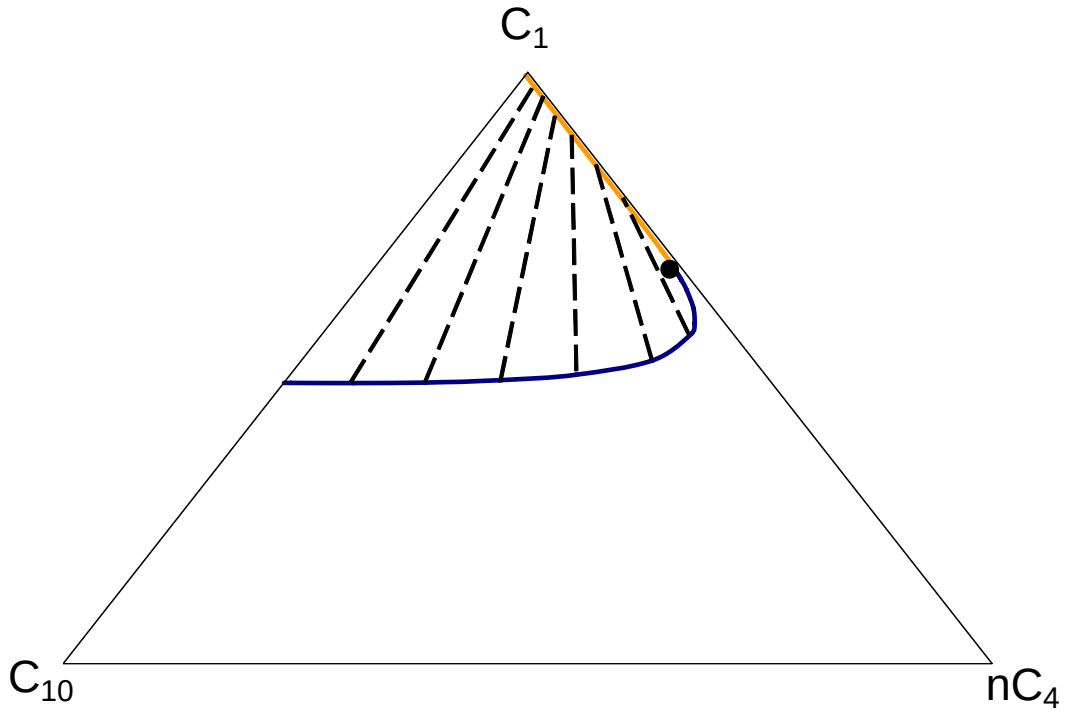

Fig. 1.8 Ternary diagram for C_1-nC_4 –nC_{10} at 2000 psia and 150^{o}F. The critical point is shown by the black circle.

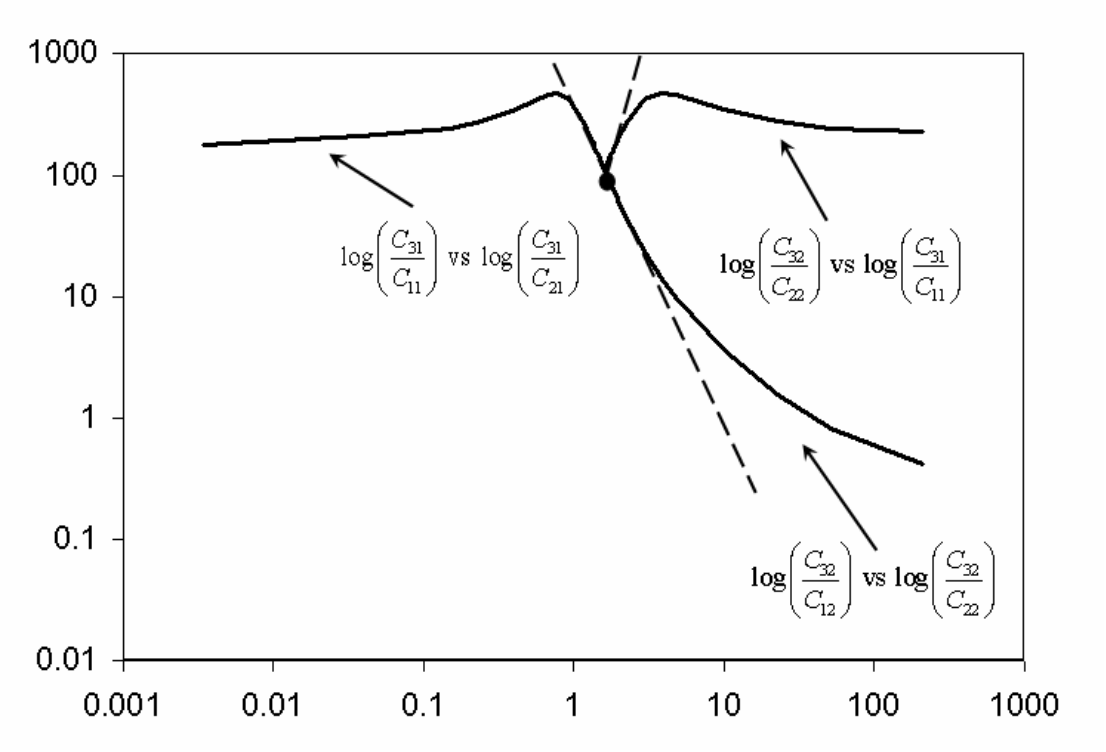

Fig. 1.9 Hand's plot for the ternary diagram in Fig. (1.8) after Welch modification (1982). The data clearly do not have constant slope as required by Hand's plot (1930).

Chapter 2: Phase Split Calculations with Reduced Method

In this research, we extend Michelsen's approach (1986) for fluid characterizations when all the BIPs are nonzero without resorting to an eigenvalue approximation. The speed and robustness of Michelsen's approach (1986) is retained in our new method. Further, this model allows the temperature and pressure dependence without any additional calculations. The new model reduces to Michelsen's (1986) or Jensen and Fredenslund's (1987) models with proper simplification of the BIP matrix. We also extended the new method for the reduced phase-split calculations to three or more phases, giving the required objective functions and derivatives for the Jacobian matrix.

2.1 CONVENTIONAL TWO-PHASE SPLIT CALCULATIONS

For an equilibrium phase-split calculation, the pressure, temperature, and overall mole fractions are specified and the amounts of the phases and their compositions at equilibrium are calculated. An expression for the fugacities of each component in each phase is needed to calculate the phase equilibrium. At equilibrium,

$$\hat{f}_i^L = \hat{f}_i^V, \qquad i = 1,...,N_C \tag{2.1}$$

where $\hat{f}_i$ is the fugacity of a component, L and V are noted for liquid and vapor phases respectively, and N_C is the number of components. For a vapor-liquid equilibrium, Eqs. (2.1) can be rewritten in terms of the component fugacity coefficients $\hat{\phi}_i$ as,

$$x_i P\hat{\phi}_i^L = y_i P\hat{\phi}_i^V \quad i = 1, \ldots, N_C \tag{2.2}$$

where P is the reservoir pressure, x_i is the liquid equilibrium phase composition, and y_i is the vapor equilibrium phase composition.

The general procedure for a two-phase flash calculation is as follows:

Step 1: Perform a stability analysis. Michelsen's method (1982a) is often used to determine when a phase is stable based on minimizing the Gibbs free energy. Stability analysis could also be performed in reduced space (Pan and Firoozabadi, 2001; Firoozabadi and Pan, 2002; Hoteit and Firoozabadi, 2006). If the phase is found not stable, a phase-split calculation is performed. The method also gives an excellent initial guess of the *K*-values (or reduced parameters) for any subsequent flash calculation.

Step 2: Make an initial guess of the K-values, where $K_i = y_i / x_i$. The phase-split calculation will converge rapidly when the guess of the *K*-values is near the equilibrium solution. If the guess is not good, the procedure may not converge at all. Most EOS programs use some empirical correlation such as the Wilson equation (1969) to estimate the phase mole fractions based on *K*-values. One can also use other correlations (Varotsis, 1989) or the results from the stability analysis (Michelsen, 1982a) from step 1.

Step 3: Calculate x_i *and* y_i *using the Rachford-Rice procedure (1952).* Once the *K*-values for each component are specified, the Rachford-Rice procedure (1952) is used to estimate the phase mole fractions by determining the liquid mole fraction L. The procedure is based on solving a nonlinear equation by Newton-Raphson iteration, where convergence is achieved once the updated value of L is within a relative tolerance of say 10^{-8} as is used here.

Step 4: Calculate the cubic EOS parameters (e.g. a_m *and* b_m*).* This step is very straightforward and depends on the selected EOS and its associated mixing rules. The

critical temperatures, pressures, and acentric factors for each component are needed to calculate the EOS parameters.

For example, the general cubic EOS (Coats, 1985) is given by

$$P = \frac{RT}{\bar{V} - b} - \frac{a}{\left(\bar{V} + \delta_1 b\right)\left(\bar{V} + \delta_2 b\right)} \tag{2.3}$$

where R is the gas constant, T is the reservoir temperature, $\bar{V}$ is the molar volume, a is the attraction parameter, b is the repulsion parameter and δ_1 and δ_2 are EOS dependent constants. The EOS constants for the van der Waals (1873) EOS are $\delta_1 = \delta_2 = 0$, for Redlich-Kwong EOS (Redlich and Kwong, 1949; Soave, 1972; Turek *et al.*, 1984) $\delta_1 = 1,\ \delta_2 = 0$, and for Peng-Robinson (1977, 1978) EOS, $\delta_1 = 1 + \sqrt{2},\ \delta_2 = 1 - \sqrt{2}$.

With the conventional mixing rules, we have:

$$\begin{aligned} a_m &= \sum_i \sum_j x_i x_j a_{ij} \\ b_m &= \sum_i x_i b_i \end{aligned} \tag{2.4}$$

where $a_{ij} = \left(1 - k_{ij}\right)\sqrt{a_i a_j}$. The parameters a_i and b_i are the EOS parameters for component i as a pure fluid and k_{ij} is the BIP between component i and j. The pure component parameters depend on the reservoir temperature, critical temperatures and pressures, and the acentric factors. In dimensionless form, Eq. (2.4) can be expressed as:

$$\begin{aligned} A_m &= \sum_i \sum_j x_i x_j A_{ij} \\ B_m &= \sum_i x_i B_i \end{aligned} \tag{2.5}$$

where $A_i = a_i P/(RT)^2$, $B_i = b_i P/RT$ and $A_{ij} = (1-k_{ij})\sqrt{A_i A_j}$.

Step 5: Solve the cubic EOS for the phase molar volumes $\bar{V}$. This step requires determining the roots of the cubic EOS for each phase using a cubic solver. The middle root for each phase is discarded because that root leads to an unstable phase. The correct roots are chosen so that they minimize the total Gibbs energy of that phase.

Step 6: Calculate the component fugacities of each component in each phase per Eqs. (2.1). The selected cubic EOS is used to determine an expression for the fugacity of a component in a phase.

Step 7: Check to see if equilibrium has been reached. In this research, we use a relative tolerance in the fugacities of 10^{-10} for each component.

Step 8: Update the K-values if the criteria of Step 7 have not been satisfied. This step is very important. It affects both the rate of convergence and whether the iteration converges at all. One procedure that works well is successive substitution where the new *K*-values are determined from the old ones by the ratio of the fugacity coefficients. Once the new *K*-values are determined, steps 3 – 7 are repeated until convergence in step 7 is achieved. Convergence by successive substitutions, however, can be very slow near the critical region and other methods may be required. In this research we use Newton-Raphson iteration to update the *K*-values since it is very fast, and those results can be compared directly with the results from our proposed rapid flash calculation method.

The flow chart for conventional two-phase flash calculations is shown in Fig (2.1). The major difficulties in conventional phase-split calculations are caused by (1) the use of N_C non-linear fugacity functions; (2) the presence of the Rachford-Rice procedure (1952) explicitly within the main fugacity convergence loop; and (3) non-

linear Rachford-Rice (1952) iterations, which have multiple roots and may not converge at all.

2.2 REDUCED TWO-PHASE SPLIT CALCULATIONS

In this research, we propose a new phase-split calculation based on six reduced parameters. The new approach uses exactly the same EOS (Redlich and Kwong, 1949; Soave, 1972; Peng and Robinson, 1977; Coats, 1985) and mixing rules. The key to the proposed rapid flash calculation procedure is to decompose the BIPs into two parts using the following simple quadratic expression:

$$k_{ij} = \left(h_i - h_j\right)^2 g_i g_j \tag{2.6}$$

where h_i and g_i are parameters for component *i* that are tuned to match PVT data. Substitution of this specific form for the binary interaction parameters given by Eqs. (2.6) into the mixing rule for the attraction parameter in Eqs. (2.5) gives,

$$A_m = \sum_i \sum_j x_i x_j \left[1 - \left(h_i - h_j\right)^2 g_i g_j\right] \sqrt{A_i A_j} \tag{2.7}$$

where x_i is the composition of a phase, either liquid or vapor. All other equations in the EOS model remain the same.

The use of Eqs. (2.6) guarantees that the BIP matrix remains symmetric and that all the BIPs between the same components are zero, i.e. the diagonal elements of the BIP matrix are zero. Further, the new formula for the BIPs contains $2N_C - 1$ independent variables, which is likely sufficient to match the PVT behavior of most complex mixtures. The expression in Eq. (2.7) can be expanded to obtain

$$A_m = \sum_i \sum_j x_i x_j \sqrt{A_i A_j} + 2\sum_i \sum_j x_i x_j \sqrt{A_i A_j} h_i h_j g_i g_j - 2\sum_i \sum_j x_i x_j \sqrt{A_i A_j} h_i^2 g_i g_j \quad . \tag{2.8}$$

Recognizing that *i* and *j* are interchangeable yields the desired result,

$$A_m = \left(\sum_i x_i \sqrt{A_i} \right)^2 + 2\left(\sum_i x_i \sqrt{A_i} h_i g_i \right)^2 - 2\left(\sum_i x_i \sqrt{A_i} h_i^2 g_i \right)\left(\sum_i x_i \sqrt{A_i} g_i \right) \tag{2.9}$$

By doing so, we are able to define the reduced parameters in an analogous way as was done by Michelsen (1986). The attraction and repulsion parameters in Eqs. (2.5) for a single-phase mixture become,

$$\begin{aligned} A_m &= \Theta_1^2 + 2\Theta_2^2 - 2\Theta_3\Theta_4 \\ B_m &= \Theta_5 \end{aligned} \tag{2.10}$$

where for the liquid phase there are six independent reduced parameters given by

$$\begin{aligned} \Theta_1 &= \sum_i x_i \sqrt{A_i} \\ \Theta_2 &= \sum_i x_i \sqrt{A_i} h_i g_i \\ \Theta_3 &= \sum_i x_i \sqrt{A_i} h_i^2 g_i \\ \Theta_4 &= \sum_i x_i \sqrt{A_i} g_i \\ \Theta_5 &= \sum_i x_i B_i \\ \Theta_6 &= L \end{aligned} \quad . \tag{2.11}$$

Further, we can define the reduced parameters for the pure components as:

$$
\begin{aligned}
q_{1i} &= \sqrt{A_i} \\
q_{2i} &= \sqrt{A_i} h_i g_i \\
q_{3i} &= \sqrt{A_i} h_i^2 g_i \\
q_{4i} &= \sqrt{A_i} g_i \\
q_{5i} &= B_i
\end{aligned}
\quad . \tag{2.12}
$$

The reduced parameters can then be written as:

$$
\begin{aligned}
\Theta_j &= \sum_i x_i q_{ji} \qquad \text{for } j = 1,...,5 \\
\Theta_6 &= L
\end{aligned}
\quad . \tag{2.13}
$$

The sixth reduced parameter for the liquid phase, the liquid mole fraction, is the result of the mass balance for a two-phase mixture where the overall molar composition is given by:

$$
z_i = (1-L) y_i + L x_i \quad . \tag{2.14}
$$

When *K*-values and *L* are calculated, the equilibrium compositions can be evaluated as:

$$
\begin{aligned}
x_i &= \frac{z_i}{K_i + (1-K_i) L} \\
y_i &= K_i x_i \qquad\qquad \text{for } i = 1,...,N_C
\end{aligned}
\quad . \tag{2.15}
$$

When all the BIPs are zero ($h_i = 0$ or $g_i = 0$), Eqs. (2.9) reduce to the same three reduced parameters as given by Michelsen (1986). When there exist only the BIPs

between a single component and the other components, Eqs. (2.9) simplify to the same five reduced parameters given in Jensen and Fredenslund (1987).

Once all these reduced parameters are determined, one can evaluate EOS parameters of A_m and B_m immediately by Eq. (2.10). In addition, we can show that all parameters needed in flash calculations can be expressed in terms of these reduced parameters, regardless the number of pseudocomponents. Thus, the equilibrium flash calculation can be reduced in terms of these six reduced parameters instead of N_C variables, for example *K*-values in the conventional method.

2.3 DERIVATION FOR PHASE-SPLIT CALCULATIONS IN REDUCED SPACE

In the conventional method, we use the difference in the fugacity of each component as our objective function, and the equilibrium ratios K_i as the primary variables. That is:

$$\begin{aligned} e_i &= f_i^V\left(\vec{K}\right) - f_i^L\left(\vec{K}\right) \quad \text{for } i = 1,...,N_C \\ \vec{K} &= \begin{bmatrix} K_1 & K_2 & ... & K_{N_C} \end{bmatrix} \end{aligned} \quad . \tag{2.16}$$

However, this approach would require evaluation of a Jacobian matrix with size $N_C \times N_C$. We can use reduced parameters as the primary variables as discussed earlier to decrease the calculation time. To estimate the reduced parameters, we can perform a multi-parameter Newton-Raphson iteration (NR) with the objective functions:

$$\begin{aligned} e_i &= \Theta_i - \sum_k x_i q_{ik} = 0 \qquad \text{for } i = 1,...,5 \text{ and } k = 1,...,N_C \\ e_6 &= \sum_k \frac{(K_k - 1) z_k}{K_k + L(K_k - 1)} = 0 \end{aligned} \tag{2.17}$$

where the residuals, e_i, should be below a specified tolerance at the completion of the NR iterations. In this research, a relative tolerance in fugacity of 10^{-10} is used. Once the reduced parameters for a given phase are determined at the end of each NR iteration, the reduced parameters for the other phase are found by a simple material balance. That is, the mass balance equations of Eqs. (2.14) can be multiplied by the appropriate parameters and summed to yield for each reduced parameter *k*

$$\Theta_k^Z = (1-L)\Theta_k^V + L\Theta_k^L \qquad k = 1,\ldots,5 \quad . \tag{2.18}$$

As a result, we can express the reduced parameters for the vapor phase using:

$$\begin{aligned} \Theta_k^V &= \frac{\Theta_k^Z - L\Theta_k^L}{(1-L)\Theta_k^L} \qquad \text{for } k = 1,\ldots,5 \\ \Theta_6^V &= 1-L \end{aligned} \quad . \tag{2.19}$$

When we choose the reduced parameters of the liquid phase as primary variables, the Jacobian matrix can be calculated as:

$$J_{ij} = \begin{cases} \delta_{ij} - \sum_k q_{ik} \dfrac{\partial x_k}{\partial \Theta_j} & \text{for } i = 1,\ldots,5 \\ \sum_k (K_k - 1)\dfrac{\partial x_k}{\partial \Theta_j} + \sum_k x_k \dfrac{\partial K_k}{\partial \Theta_j} & \text{for } i = 6 \end{cases} \tag{2.20}$$

where δ_{ij} is the Kronecker delta function. Further, the derivative of composition with respect to reduced parameters can be obtained from Eqs. (2.15) as:

$$\frac{\partial x_k}{\partial \Theta_j} = -\frac{z_k\left[\left(1-K_k\right)\delta_{6k} + \left(1-L\right)\partial K_k / \partial \Theta_j\right]}{\left[L + K_k\left(1-L\right)\right]^2} \quad . \tag{2.21}$$

The derivative of K-values respect to reduced parameters can be expressed using the chain rule as:

$$\frac{\partial K_k}{\partial \Theta_j} = K_k\left(\frac{\partial \ln \phi_i^L}{\partial \Theta_j} - \frac{\partial \ln \phi_i^V}{\partial \Theta_j}\right) = K_k\left(\frac{\partial \ln \phi_i^L}{\partial \Theta_j} - \sum_m \frac{\partial \ln \phi_i^V}{\partial \Theta_m^V}\frac{\partial \Theta_m^V}{\partial \Theta_j}\right) \quad . \tag{2.22}$$

Form mass balance equation (2.14), we have for some of the partial derivatives:

$$\frac{\partial \Theta_m^V}{\partial \Theta_j^L} = \begin{cases} -L/\left(1-L\right) & \text{if } m = j \neq 6 \\ \dfrac{\Theta_m^z - \Theta_m^L}{\left(1-L\right)^2} & \text{if } m = 1,...,5 \text{ and } j = 6 \\ -1 & \text{if } m = j = 6 \\ 0 & \text{otherwise} \end{cases} \quad . \tag{2.23}$$

The derivatives $\partial \ln \phi_i^L / \partial \Theta_j^L$ and $\partial \ln \phi_i^V / \partial \Theta_j^V$ share the exactly same formula, except that they are using values of reduced parameters for a different phase. From now on, we only derive the formula for the liquid phase reduced parameters. For the partial derivative of the fugacity coefficients with respect to the first five liquid-phase reduced parameters, we have:

$$\frac{\partial \ln \phi_i}{\partial \Theta_j} = \frac{B_i}{B_m}\frac{\partial Z}{\partial \Theta_j} - \frac{B_i\left(Z-1\right)}{B_m^2}\frac{\partial B_m}{\partial \Theta_j} - \frac{\partial Z/\partial \Theta_j - \partial B_m/\partial \Theta_j}{Z - B_m}$$
$$- \frac{A_m}{\left(\delta_1-\delta_2\right)B_m}\left(\frac{2\sum_k x_k A_{ik}}{A_m} - \frac{B_i}{B_m}\right)\left(\frac{\partial Z/\partial \Theta_j + \delta_1 \partial B_m/\partial \Theta_j}{Z+\delta_1 B_m} - \frac{\partial Z/\partial \Theta_j + \delta_2 \partial B_m/\partial \Theta_j}{Z+\delta_2 B_m}\right) .$$
$$- \frac{1}{\left(\delta_1-\delta_2\right)}\left[\frac{2}{B_m}\frac{\partial \sum_k x_k A_{ik}}{\partial \Theta_j} + \left(\frac{B_i}{B_m^3} - \frac{2\sum_k x_k A_{ik}}{B_m^2}\right)\frac{\partial B_m}{\partial \Theta_j} + \frac{B_i}{B_m^2}\frac{\partial A_m}{\partial \Theta_j}\right]\ln\left(\frac{Z+\delta_1 B_m}{Z+\delta_2 B_m}\right)$$

(2.24)

Some of the derivatives in Eqs. (2.24) can be readily calculated:

$$\frac{\partial B_m}{\partial \Theta_j} = \begin{cases} 1 & \text{if } j = 5 \\ 0 & \text{otherwise} \end{cases}$$
$$\frac{\partial A_m}{\partial \Theta_j} = \begin{bmatrix} 2\Theta_1 & 4\Theta_2 & -2\Theta_4 & -2\Theta_3 & 0 & 0 \end{bmatrix} \quad . \tag{2.25}$$
$$\frac{\partial\left(\sum_k x_k A_{ik}\right)}{\partial \Theta_j} = \begin{bmatrix} q_{1i} & 2q_{2i} & -q_{4i} & -q_{3i} & 0 & 0 \end{bmatrix}$$

The derivative of the *Z*-factor with respect to each reduced parameter can be calculated if we re-write Eq. (2.3) in *Z*-factor form:

$$Z^3 + PZ^2 + QZ + R = 0 \tag{2.26}$$

with

$$P = \left(\delta_1 + \delta_2 - 1\right)B_m - 1$$
$$Q = A_m - \left(\delta_1+\delta_2\right)B_m - \left(\delta_1+\delta_2-\delta_1\delta_2\right)B_m^2 \quad . \tag{2.27}$$
$$R = -A_m B_m - \delta_1\delta_2 B_m^2\left(B_m+1\right)$$

The differentiation of Eqs (2.26) and (2.27) yields:

$$\frac{\partial Z}{\partial \Theta_j} = -\frac{Z^2 \partial P / \partial \Theta_j + Z \partial Q / \partial \Theta_j + \partial R / \partial \Theta_j}{3Z^2 + 2PZ + Q} \tag{2.28}$$

where

$$\begin{aligned}
\frac{\partial P}{\partial \Theta_j} &= \left(\delta_1 + \delta_2 - 1\right) \frac{\partial B_m}{\partial \Theta_j} \\
\frac{\partial Q}{\partial \Theta_j} &= \frac{\partial A_m}{\partial \Theta_j} - \left(\delta_1 + \delta_2\right) \frac{\partial B_m}{\partial \Theta_j} - 2\left(\delta_1 + \delta_2 - \delta_1 \delta_2\right) B_m \frac{\partial B_m}{\partial \Theta_j} \quad . \\
\frac{\partial R}{\partial \Theta_j} &= -\frac{\partial A_m}{\partial \Theta_j} B_m - A_m \frac{\partial B_m}{\partial \Theta_j} - \delta_1 \delta_2 \left(3B_m^2 + 2B_m\right) \frac{\partial B_m}{\partial \Theta_j}
\end{aligned} \tag{2.29}$$

The partial derivatives of $\partial A_m / \partial \Theta_i$ and $\partial B_m / \partial \Theta_i$ are given in Eqs. (2.25).

Because fugacity coefficients are only functions of the first five reduced variables, $\partial \ln \phi_i / \partial \Theta_6 = 0$.

Both the liquid and vapor reduced parameters are used to calculate the component fugacity coefficients at each iteration. The cubic EOS is first solved for the molar volume of each phase as is done in the conventional method, except that the mixing parameters for each phase are calculated with Eqs. (2.10). The *K*-values for each component can then be calculated from Eqs. (2.2), where $K_i = \hat{\phi}_i^L / \hat{\phi}_i^V$. Last, eqs. (2.15) are used to solve directly for the equilibrium phase compositions.

When the number of pseudocomponents is less than six, some reduced parameters are dependent on each other. In those cases, the number of the reduced variables to

determine is chosen equal to the number of the components. However, $\Theta_6 = L$ must always be selected.

2.4 RAPID PHASE-SPLIT CALCULATIONS FOR THREE OR MORE PHASES

Similar to rapid flash calculations for two phases, the number of primary variables in phase-split calculations for three or more phases can be greatly reduced as well, speeding up the three-phase calculations. In the conventional flash calculations, there are several differences compared with the two-phase flash calculations in that: (1) The equal-fugacity condition is extended to multiple phases as:

$$\hat{f}_i^j = \hat{f}_i^{ref}, \quad i = 1, \ldots, N_C; \quad j = 1, \ldots, N_P - 1 \quad . \tag{2.30}$$

where *ref* stands for the reference phase. The primary variables for the conventional case are the *K*-values for each phase, which are defined as the ratio of the equilibrium composition of component *i* in phase *j* and that in the reference phase: $K_i^j = x_i^j / x_i^{ref}$. Thus, there are $(N_P - 1)N_C$ primary variables, and the Jacobian matrix is of size $(N_P - 1)N_C$ by $(N_P - 1)N_C$. (2) Rachford-Rice (1952) iterations are also more complex and time-consuming. Assuming the phase fraction of each phase is α^j, and the one for the reference phase is $1 - \sum_{j=1}^{N_P - 1} \alpha^j$, and from the mass balance equation $z_i = \sum_{j=1}^{N_P} x_i^j \alpha^j$, and the *K*-values defined earlier, we have for each component:

$$\begin{aligned} x_i^{ref} &= \frac{z_i}{1 + \sum_{j=1}^{N_P - 1} \left(K_i^j - 1\right)\alpha^j} \quad . \\ x_i^j &= K_i^j x_i^{ref} \end{aligned} \tag{2.31}$$

As a result, the Rachford-Rice objective functions for three or more phases are:

$$0=\sum_{i=1}^{N_C}\left(x_i^j-x_i^{ref}\right)=\sum_{i=1}^{N_C}\frac{\left(K_i^j-1\right)z_i}{1+\sum_{k=1}^{N_P-1}\left(K_i^k-1\right)\alpha^k} \qquad \text{for } j=1,...,N_P-1 \quad . \tag{2.32}$$

Finding the correct roots in Eqs. (2.32) can be very difficult.

For the reduced method, the new objective functions are very similar as for the two-phase case:

$$\begin{aligned}
e_1^j &= \Theta_1^j-\sum_i x_i^j q_{1i}=0\\
e_2^j &= \Theta_2^j-\sum_i x_i^j q_{2i}=0\\
e_3^j &= \Theta_3^j-\sum_i x_i^j q_{3i}=0\\
e_4^j &= \Theta_4^j-\sum_i x_i^j q_{4i}=0\\
e_5^j &= \Theta_5^j-\sum_i x_i^j q_{5i}=0\\
e_6^j &= \sum_{i=1}^{N_C}\frac{\left(K_i^j-1\right)z_i}{1+\sum_{k=1}^{N_P-1}\left(K_i^k-1\right)\Theta_6^k}=0\ , \qquad j=1,...,N_P,\ j\neq \text{ref}
\end{aligned} \quad , \tag{2.33}$$

except that there are now $6\left(N_P-1\right)$ objective functions.

The partial derivatives used in the Jacobian matrix for the phase-split calculation with three or more phases are almost the same as those in the two-phase split calculations except for two items. First, the partial derivative of the compositions is different:

$$\frac{\partial x_i^k}{\partial \Theta_j^l} = -\frac{z_i \left\{ \frac{\partial K_i^k}{\partial \Theta_j^l} \left[1 + \sum_{k=1}^{N_P-1} \left(K_i^k - 1 \right) \Theta_6^k \right] - \left(K_i^k - 1 \right) \sum_{m=1}^{N_P-1} \left[\frac{\partial K_i^m}{\partial \Theta_j^l} \Theta_6^m + \left(K_i^m - 1 \right) \frac{\partial \Theta_6^m}{\partial \Theta_j^l} \right] \right\}}{\left[1 + \sum_{m=1}^{N_P-1} \left(K_i^m - 1 \right) \Theta_6^k \right]^2} \qquad (2.34)$$

A second difference lies in the partial derivatives of the reduced parameters with respect to other reduced parameters, which using the chain rule are:

$$\frac{\partial \Theta_i^{ref}}{\partial \Theta_j^m} = \begin{cases} -\Theta_6^m \Big/ \left(1 - \sum_{l=1}^{N_P-1} \Theta_6^i \right) & \text{if } i = j \neq 6 \\ \dfrac{\Theta_i^z - \left(1 - \sum_{l=1}^{N_P-1} \Theta_6^i \right) \Theta_i^m - \sum_{l=1}^{N_P-1} \Theta_6^l \Theta_i^l}{\left(1 - \sum_{l=1}^{N_P-1} \Theta_6^i \right)^2} & \text{if } i = 1,...,5,\ j = 6 \\ -1 & \text{if } i = j = 6 \\ 0 & \text{otherwise} \end{cases} . \qquad (2.35)$$

The other partial derivatives are exactly the same as those in two-phase flash calculation. We can directly use all derivatives to construct the Jacobian matrix.

2.5 EXAMPLE TWO-PHASE SPLIT CALCULATIONS.

This section presents several example calculations for synthetic and real fluid characterizations using the new rapid flash method. The results are compared with conventional flash calculations.

2.5.1 Improvement in Speed Using Oil A.

Consider first the computational time required for flash calculations for seven-component synthetic oil A at 480 ^{o}F where the overall composition is near and far from the critical point. The pressure for the overall composition near the critical locus is 1040 psia, while the pressure is decreased to 300 psia to a less volatile oil (further from a critical points). Table (2.1) gives the EOS input parameters for oil A including the BIPs that result from the specified h_i and g_i. The BIPs for the diagonal elements are always zero based on Eqs. (2.6).

To ensure a fair comparison, we use the same initial guesses of the equilibrium phase compositions for both the conventional and rapid flash calculations. The initial guesses for both methods were obtained by conventional flash calculations until the component fugacities are converged to within a relative error of 10^{-4}. The computational times reported, therefore, are the times to perform the remaining iterations so that all component fugacities are converged to within a relative error of 10^{-12}. Both methods use Newton-Raphson iterations to achieve convergence. The flash calculations are computed with a Pentium 4 CPU at 2.66 GHz and 512 MB RAM.

Figures (2.3) and (2.4) show the comparison of computational time required for convergence for both the reduced and conventional methods based on the number of pseudocomponents. Additional pseudocomponents are obtained by splitting the heavy fraction (that is equivalent of nC_{10} here) for the case of interest as many components as are needed, where the resulting components have the same EOS properties as nC_{10}. As is shown, the computational time with the new method is about 1.3 to 25 times faster than the conventional method depending on the number of components. The speedup increases greatly as the number of components are increased. The computational time with the rapid flash method increases modestly with the number of components. That is,

the computational time with the new method at 50 components is about as fast as the computation time with the conventional method at 12 components. Both methods slow down for flash calculations near the critical region (see Fig. (2.4)) because the Jacobian matrix is singular there. The speedup with the new method, however, is greater when the overall composition is nearer the critical locus. The speedup with the reduced method is good even through the reduced method takes one more iteration. One goal of future research should be to reduce the number of iterations.

2.5.2 Fluid Characterization.

Equations-of-state are used to predict the compositions and volumetric behavior when oil and gas mix in the reservoir. These EOS fluid characterizations must be tuned to match the PVT behavior of the original reservoir fluid. The process of tuning an EOS involves: (1) selection of the pseudocomponents; (2) determination of EOS properties for the pseudocomponents; and (3) adjustment of pseudocomponent EOS properties by regression to the PVT data.

Fluid characterizations that result from the lumping and tuning process are dependent on the method used and the experimental PVT data available (Egwuenu *et al.*, 2005). Often the tuning process involves iteration and subjectivity about which parameters to regress and the number of pseudocomponents to use. There are no established norms in the industry and therefore there is no unique way to perform such characterization, while accepting that only very few of the methods are self-consistent and honor boundary conditions. The usual approach is to first lump the original fluid analysis, which may be as many as 30 components, to as few as 12 to 15 components. The 12- to 15-component EOS model is typically tuned to match the available PVT data, and can be lumped into fewer pseudocomponents as needed.

The parameters to tune to match a set of PVT data are more of an art than an exact science. The best method is to match the PVT data by adjusting as few parameters as possible. Adjusting too many parameters could result in poor PVT predictions away from the range of the measured PVT data. Typically, the parameters associated with the heaviest pseudocomponents are adjusted more because these components have properties with the largest measurement uncertainties.

The new rapid flash method contains the same adjustable parameters as the conventional method, except that the BIPs are constrained by a maximum of $2N_C - 1$ fitting parameters, that is, h_i and g_i thru Eqs. (2.5). In practice, however, we would never require or want to adjust all these $2N_C - 1$ parameters. All other tuning parameters, for example critical temperature and pressure are obtained in the exactly same way as in the conventional method. Further, the use of Eqs. (2.5) in the tuning process is advantageous because it simplifies the adjustment process in that when one parameter, such as h_i is adjusted, the entire column or row of BIPs are adjusted. This should help to avoid poor predictions away from the range of the PVT data fitted by reducing the uncertainty about how to adjust the BIPs.

There are two possible ways to tune the new model to PVT data. The first method is to fit the new model to the PVT data by using Eqs. (2.5) directly. This is preferred because it should give the best fit possible to actual data. Tuning can be done by including Eqs. (2.5) directly into a nonlinear regression model. Another possibility is to use an existing tuning program that uses the conventional flash calculation and perform the tuning process as before, but adjusting the BIPs by hand. Eqs. (2.5) simply restricts the BIPs that can be entered into the existing code based on the values of h_i and g_i. The BIPs can be manually adjusted by inputting the parameters h_i and g_i into a spreadsheet that calculates the BIPs until a good match to the PVT data is obtained.

The second method is to decompose the BIPs from the conventional flash characterization into the h_i and g_i parameters in Eqs. (2.5). Although this is not preferred, it could save a significant amount of effort in fluid characterization, and at the least could result in an initial fluid characterization for subsequent tuning. For mixtures with many components, the conversion process is likely only approximate in that the BIPs from the conventional EOS characterization cannot be matched exactly. In those cases, the values for h_i and g_i are determined by a best fit to the original BIP matrix. One could also use these values as initial estimates for additional tuning to the PVT data. In this research, the best fit is obtained by minimizing the sum of the square of the errors between the original BIPs and the BIPs calculated from Eqs. (2.5). We did not use weighting factors, although one could use the overall compositions of the oil and gas as weighting factors. We give two examples of the conversion process below for two real fluid characterizations.

2.5.2.1 Example Gas Condensate B.

Consider first the conventional fluid characterization of a twelve-component gas condensate reported by Jutila *et al.* (2001) at reservoir temperature of 275°F. We generated standard PVT data based on their characterization using PVTSIM, a commercial software package (Calsep, 2005). We also determined the values for h_i and g_i that gave a reasonable fit to their original BIPs into Table (2.2). There are many ways to do the nonlinear regression of the BIP matrix. To generate the zero BIPs on the nondiagonal elements of the BIP matrix, the values for those components must have the same h_i. Thus, in this example, there are sixteen unknowns of h_i and g_i in the regression when we took this into account. We did not explore all of the possible solutions (or use of weighting factors) from nonlinear regression, because the new BIPs

shown in Table (2.2) were sufficient to represent the phase behavior for the gas condensate. Further, we made no adjustments in the critical properties or acentric factors for any component.

Figure (2.5) shows the phase envelope for gas condensate B using the new model based on Eqs. (2.5), the conventional EOS model, and the model with zero BIPs from Micheleson. As shown, the new model is able to match the saturation pressures well as a function of temperature. Figures (2.6) and (2.7) demonstrate that the new model is also able to reproduce accurately the solution gas-oil ratios and formation volume factors. As expected, Michelsen's model with zero BIPs is not adequate.

2.5.2.2 Example Oil C.

Next, we consider a fifteen-component oil described by Hearn and Whitson (1989). We repeated the same steps as described for oil B and obtained a sufficient match to the original BIPs using Eqs. (2.5). Table (2.3) gives the values for h_i and g_i used for the rapid flash calculations. Figures (2.8) – (2.10) show that the new method is able to reproduce well the saturation pressures, solution gas-oil ratios, and formation volume factors.

2.5.2.3 Example Oil D.

Last, we consider a seven-component synthetic oil to demonstrate that in some cases the BIPs from the conventional method can be exactly matched. In this case, there are only one column of the BIPs as shown in Table (2.4). Table (2.4) gives the values for h_i and g_i required to exactly match the BIPs for the rapid flash calculations. Because only one column has nonzero BIPs, the reduced parameters for these flash calculations are the same as those in Jenson and Fredenslund (1989).

2.5.3 Improvement in Convergence.

We performed a variety of flash calculations with oils A and C to test convergence of the new method as compared with the conventional method. The flash calculations were performed for 52 random overall compositions, temperatures, and pressures. Of those flashes, the rapid flash converged to the trivial solution (the overall compositions) for 8 cases. All 8 cases are single phase mixture as confirmed by stability analysis. Thus the reduced method always converges when two phases were present. The conventional method, however, failed to converge or converged to the trivial solution in these 8 cases, but also for addition 8 cases that are in two-phase region. While this is not an absolute test of robustness, this indicates that the rapid flash method is likely more robust than the conventional method, as has been discussed in more theoretical detail by Pan and Firoozabadi (2003).

2.6 CONCLUSIONS

We developed a practical new method that can significantly increase the calculation speed of flash calculations. For the cases studied, the new rapid flash method is about 30% faster than conventional flash calculations when seven components are used and about 25 times faster when 50 components are used. Computational times with the new method only increase modestly with the number of components. The new method can also accurately characterize complex phase behavior and is more robust in the near critical region than conventional flash calculations. Compositional simulations with the new reduced phase-split calculation method could include many more pseudocomponents than currently used, thereby increasing phase behavior accuracy. Alternatively, compositional simulations could be made with significantly more grid

blocks for the same number of components, thereby decreasing numerical dispersion in compositional simulation.

	T_C (^{o}F)	P_C (psia)	ω	z_i (mol%)
CO_2	87.89	1069.87	0.225	5.0
C_1	-116.59	667.20	0.008	10.0
C_2	90.05	708.35	0.098	12.0
C_3	205.97	615.76	0.152	12.0
nC_4	305.69	551.10	0.193	15.0
nC_5	385.61	489.38	0.251	17.0
nC_{10}	652.01	305.68	0.490	29.0

Table 2.1 Input EOS properties for synthetic oil A.

	CO_2	C_1	nC_{10}	h_i	g_i
CO_2	0.000			1.00	1.170
C_1	0.144	0.000		0.30	0.250
C_2	0.120	0.002	0.040	0.00	0.103
C_3	0.120	0.002	0.040	0.00	0.103
nC_4	0.120	0.002	0.040	0.00	0.103
nC_5	0.120	0.002	0.040	0.00	0.103
nC_{10}	0.114	0.071	0.000	2.00	0.098

Table 2.2 Binary interaction parameters for synthetic oil A. All the BIPs not shown are zero.

	h_i	g_i	N_2	CO_2	C_1	z_i (mol%)
N_2	0.761	1.544				0.57
CO_2	0.665	1.322	0.019			1.65
C_1	0.895	1.598	0.045	0.112		81.35
C_2	1.028	0.458	0.051	0.080	0.013	6.86
C_3	1.056	0.526	0.071	0.106	0.022	2.80
nC_4	1.062	0.516	0.073	0.108	0.023	1.49
nC_5	1.062	0.516	0.073	0.108	0.023	0.77
nC_6	1.062	0.516	0.073	0.108	0.023	0.54
PS1	1.262	0.259	0.101	0.122	0.056	1.09
PS2	1.414	0.164	0.108	0.122	0.071	1.58
PS3	1.719	0.085	0.121	0.125	0.092	1.00
PS4	2.387	0.033	0.136	0.130	0.118	0.30

Table 2.3 Values for h_i and g_i for gas condensate B (Jutila *et al.*, 2001) at 275°F that give a sufficient fit to the original BIPs. The new BIPs calculated with Eqs. (2.5) are shown. All BIPs not given are zero.

	h_i	g_i	N_2	CO_2	C_1	z_i (mol%)
N_2	2.761	0.329				0.70
CO_2	0.376	0.013	0.024			0.60
C_1	3.159	0.917	0.048	0.003		33.40
C_2	3.225	0.843	0.060	0.013	0.004	5.00
C_3	3.275	1.029	0.094	0.013	0.004	5.50
iC_4	3.278	1.029	0.090	0.013	0.004	2.10
nC_4	3.278	1.029	0.090	0.014	0.004	3.90
iC_5	3.282	1.042	0.093	0.017	0.004	2.00
nC_5	3.290	1.068	0.098	0.017	0.004	2.80
C_6	3.290	1.068	0.098	0.023	0.004	4.40
$C_{7+}(1)$	3.313	1.032	0.103	0.024	0.023	9.60
C_{7+} (2)	3.321	1.021	0.105	0.027	0.028	9.90
C_{7+} (3)	3.331	1.006	0.107	0.030	0.036	8.70
C_{7+} (4)	3.341	0.992	0.109	0.031	0.045	6.80
C_{7+} (5)	3.345	1.021	0.115	0.003	0.054	4.60

Table 2.4 Values for h_i and g_i for oil C (Hearn and Whitson, 1989) that give a good fit to the original BIPs. The new BIPs calculated with Eqs. (2.5) are shown. All BIPs not given are zero.

	z_i (mol%)	MW	T_C (^{o}F)	P_C (psia)	ω
CO_2	6.1	44.01	87.93	1070.6	0.231
C_1	30.2	16.04	-116.7	667.8	0.012
nC_4	16.4	58.12	305.6	550.7	0.193
C_{7+}(1)	10.2	107.0	566.5	410.3	0.320
C_{7+} (2)	9.5	140.0	680.2	350.6	0.410
C_{7+} (3)	12.3	201.0	850.4	275.4	0.560
C_{7+} (4)	15.3	305.2	1002.0	205.1	0.783

Table 2.5 Input EOS properties for oil D.

	CO_2	h_i	g_i
CO_2	0.0000	1	1.0000
C_1	0.0973	0	0.0973
nC_4	0.1474	0	0.1474
$C_{7+}(1)$	0.1377	0	0.1377
C_{7+} (2)	0.1377	0	0.1377
C_{7+} (3)	0.1377	0	0.1377
C_{7+} (4)	0.1377	0	0.1377

Table 2.6 Input binary interaction parameters for oil D. Values are given for h_i and g_i that give an exact fit to the original BIPs associated with CO_2. All BIPs not given are zero.

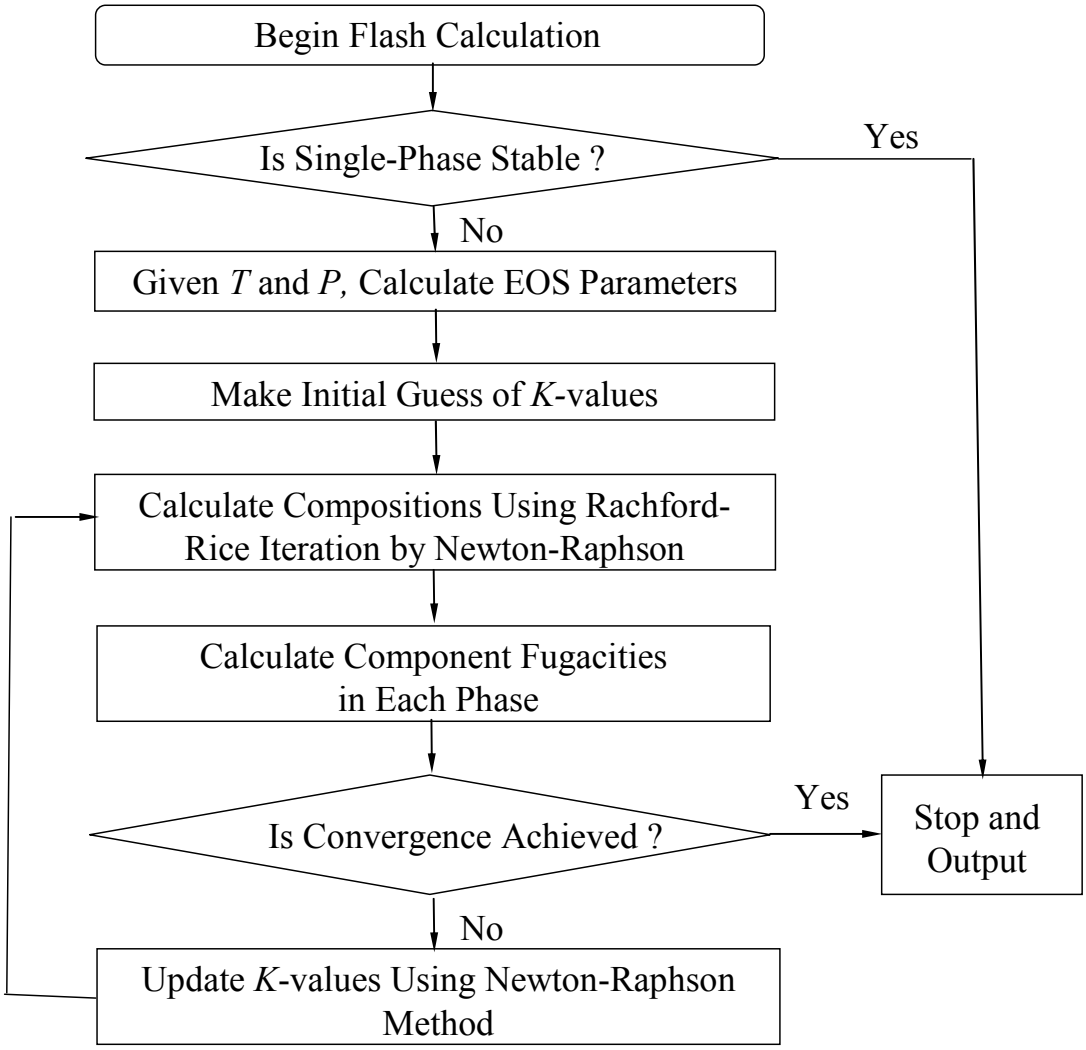

Fig. 2.1 Flow chart for conventional flash calculation.

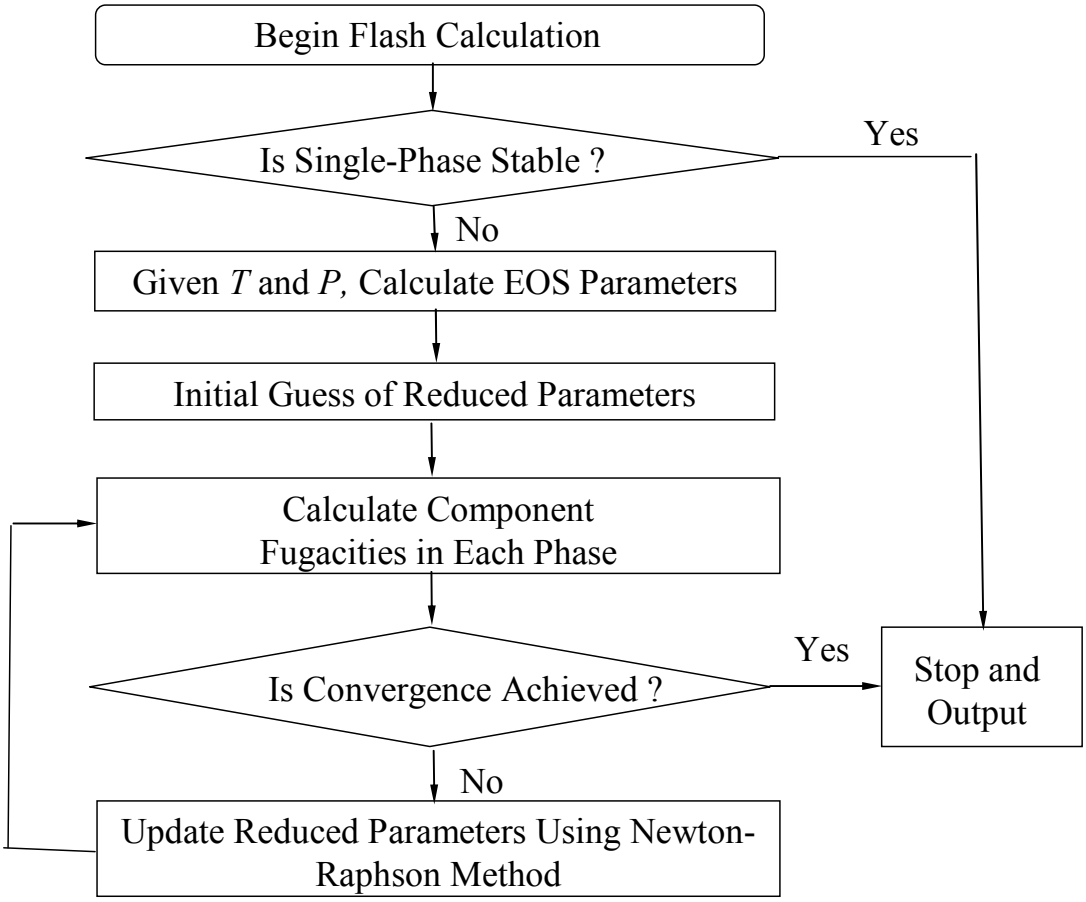

Fig 2.2 Flow chart for new rapid flash calculation.

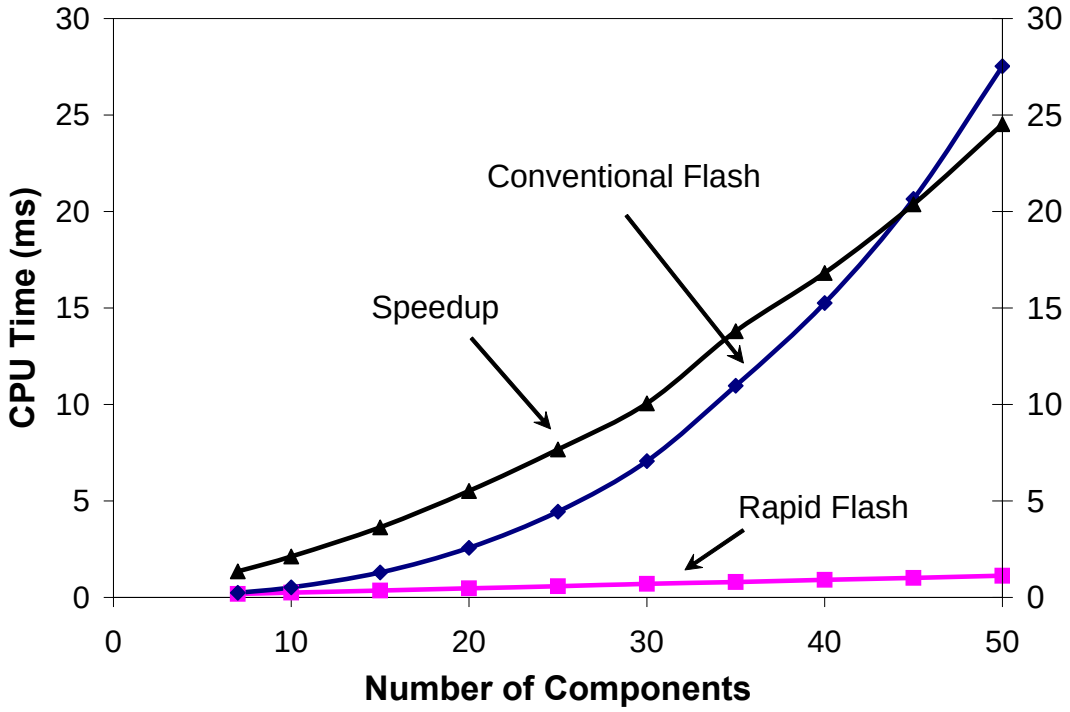

Fig 2.3 Speedup for oil A, where the overall composition is far from the critical locus.

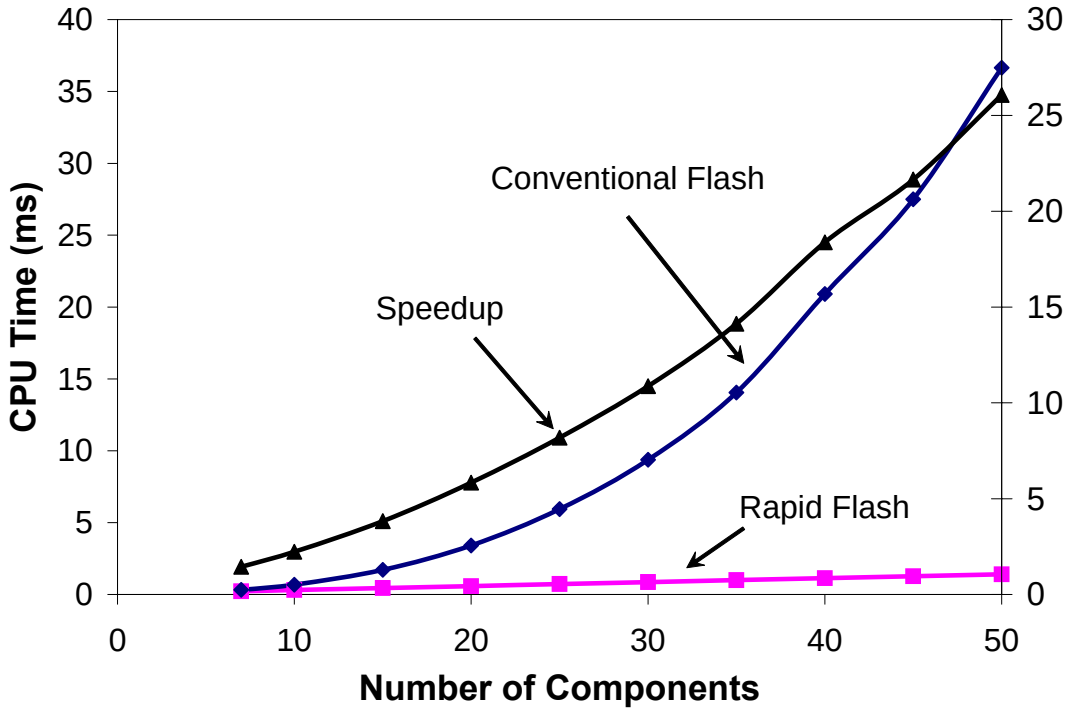

Fig 2.4 Speedup for oil A, where the overall composition is near the critical locus.

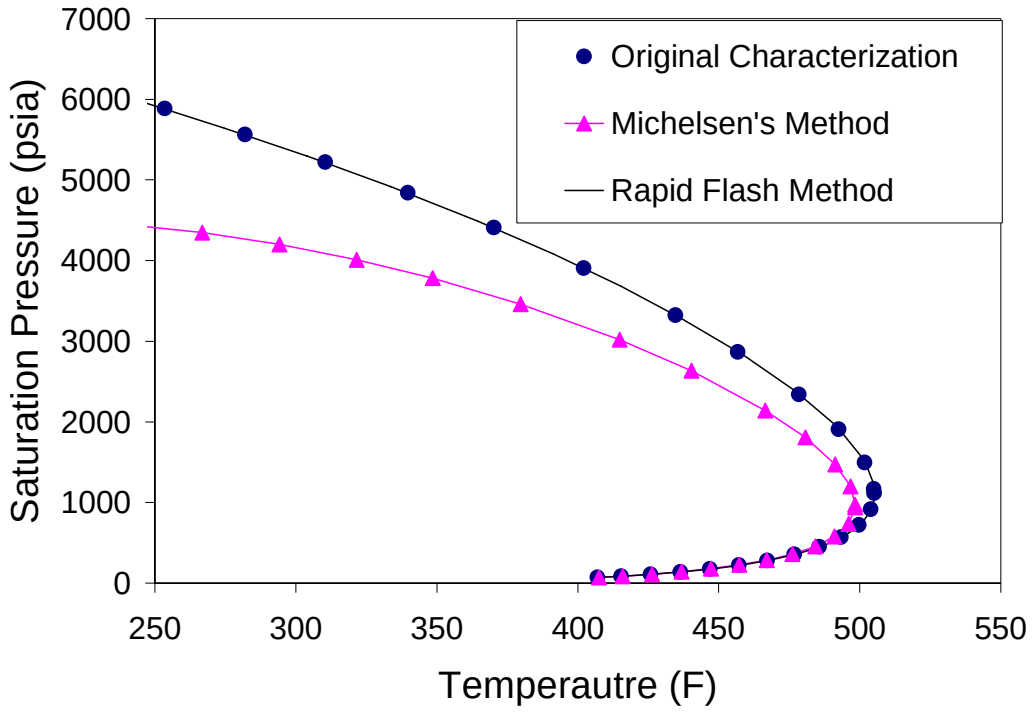

Fig 2.5 Comparison of calculated phase envelopes for gas condensate B (Jutila *et al*., 2001) to that generated by PVTSIM (Calsep, 2005). The new rapid flash method accurately reproduces the saturation pressures.

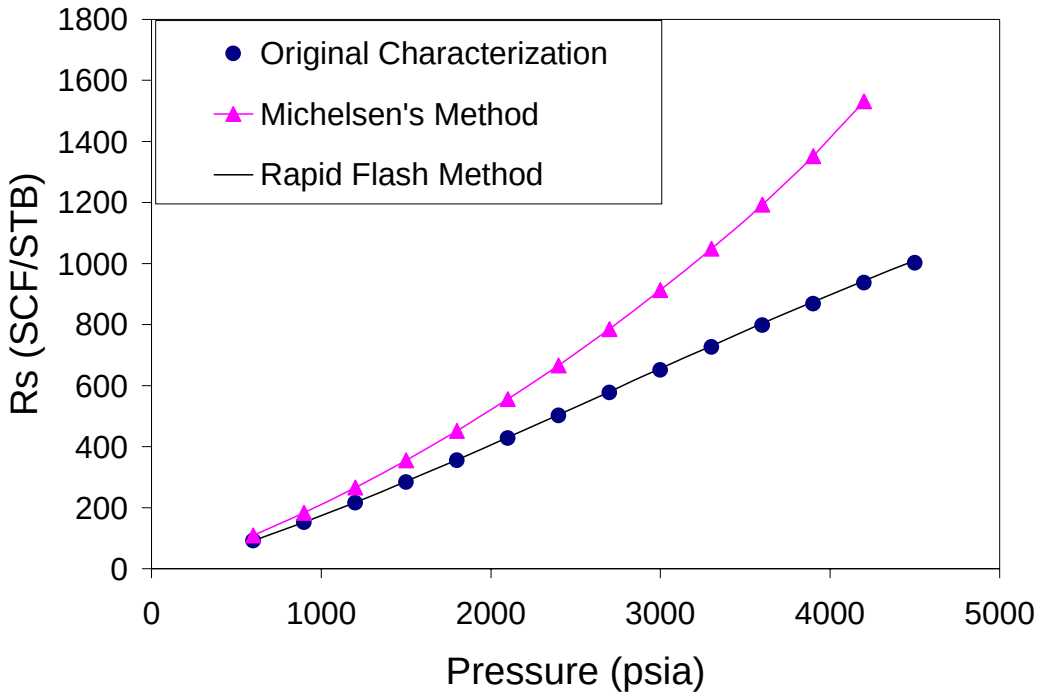

Fig 2.6 Comparison of calculated solution gas-oil ratios for gas condensate B (Jutila *et al*., 2001) at 275°F to that generated by PVTSIM (Calsep, 2005). The characterization with the new rapid flash method is very accurate.

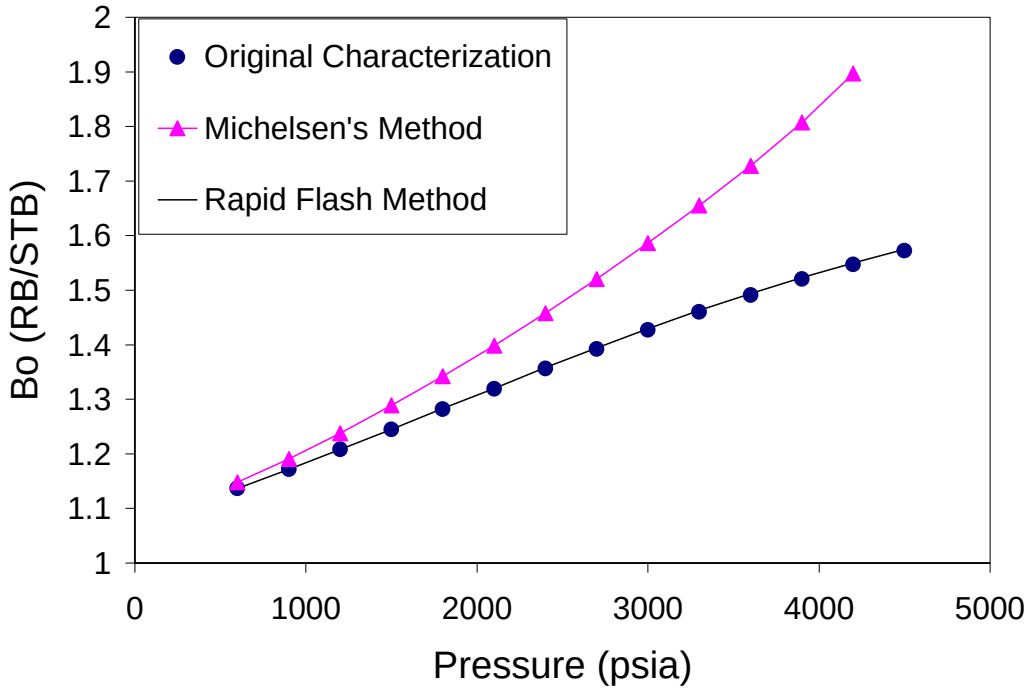

Fig 2.7 Comparison of calculated formation volume factors for gas condensate B (Jutila *et al*., 2001) at 275°F to that generated by PVTSIM (Calsep, 2005). The characterization with the new rapid flash method is very accurate.

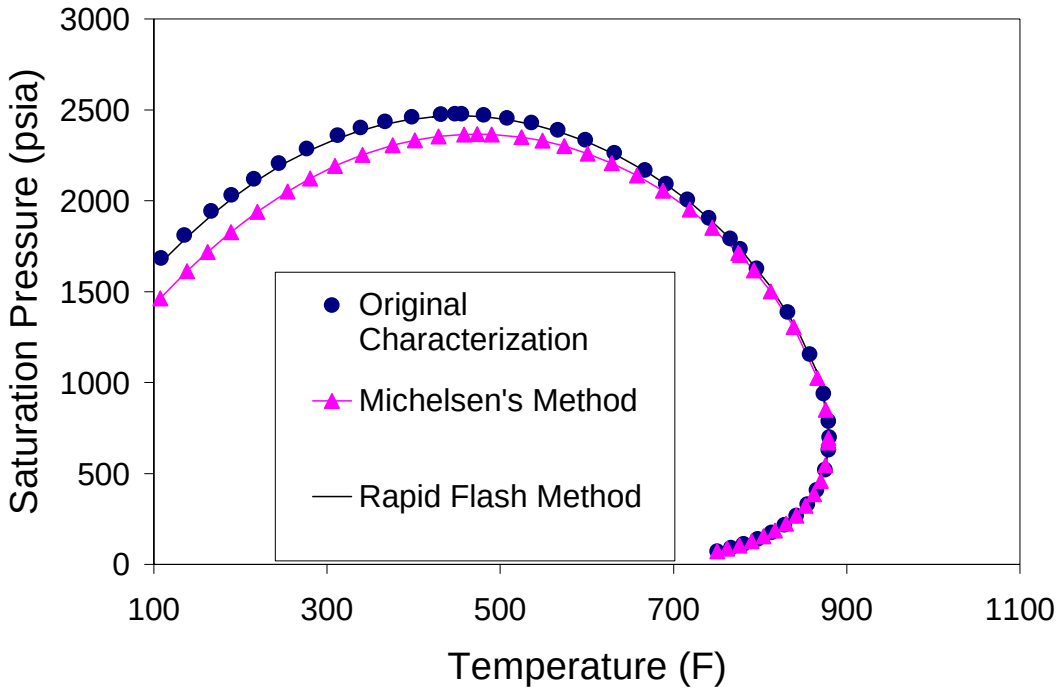

Fig 2.8 Comparison of calculated phase envelopes for oil C (Hearn and Whitson, 1995) to that generated by PVTSIM (Calsep, 2005). The characterization with the new rapid flash method accurately reproduces the saturation pressures.

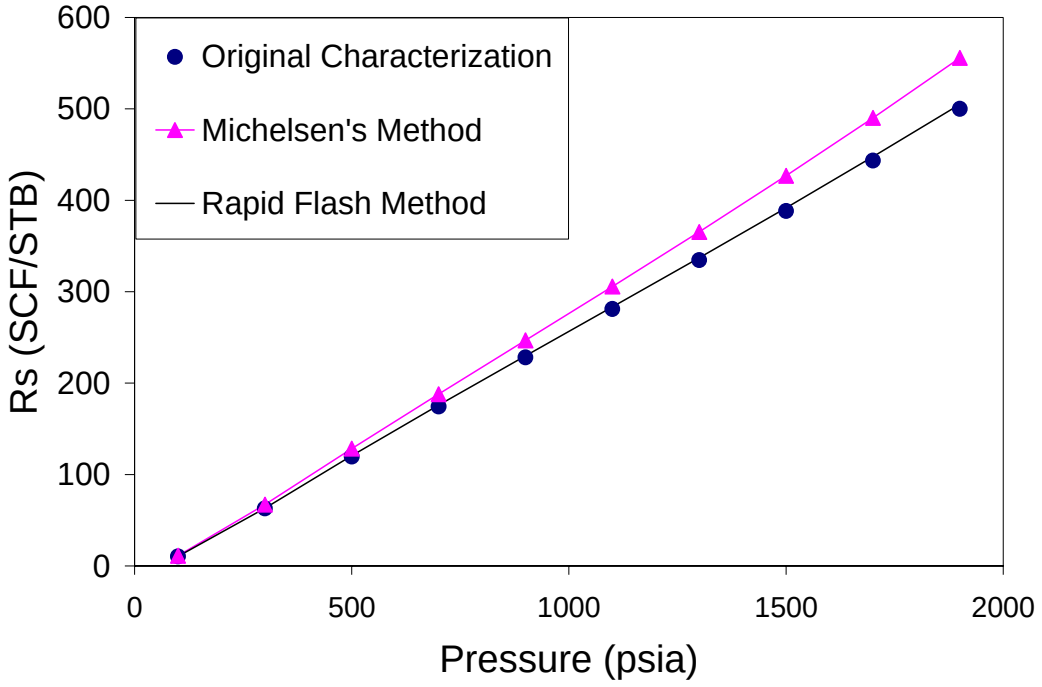

Fig 2.9 Comparison of calculated solution gas-oil ratios for oil C (Hearn and Whitson, 1995) at 212°F to that generated by PVTSIM (Calsep, 2005). The characterization with the new rapid flash method is very accurate.

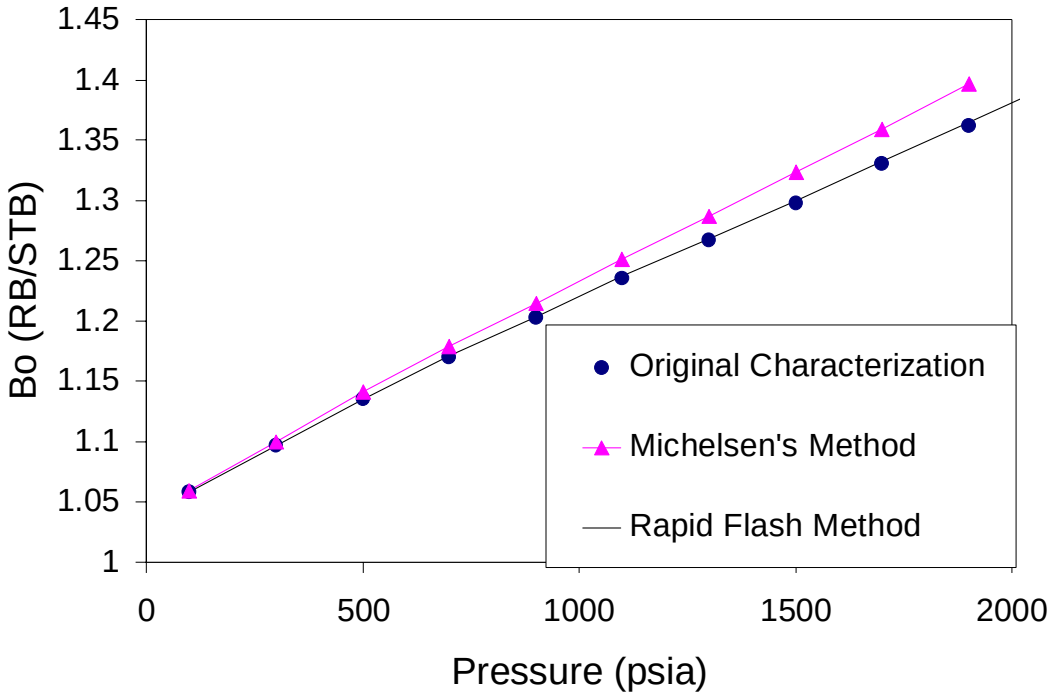

Fig 2.10 Comparison of calculated formation volume factors for oil C (Hearn and Whitson, 1995) at 212°F to that generated by PVTSIM (Calsep, 2005). The characterization with the new rapid flash method is very accurate.

Chapter 3: Stability Analysis in Reduced Space

In this chapter, stability analysis is done on a single-phase mixture to determine whether it forms multiple phases or not at a specified temperature and pressure. The stability analysis calculation is an integral part of the flash calculations. The stability analysis calculations can be performed for three or more phases simultaneously. However, this approach may require significant calculations, because the Jacobian matrix is much larger than that in the two-phase stability analysis calculations. In addition, two-phase stability tests can be used consequently in this case. For example, for a three-phase stability analysis, a two-phase flash calculation is first performed, then the phase stability analysis is applied on each of the pseudo-equilibrium compositions to check whether each of them is stable or not. It is also important to note that, besides the trivial solution of $x_i = z_i$, one may converge to the trivial pseudo-equilibrium compositions where $x_i = y_i$. A third solution must be found to confirm that the overall composition is unstable and will form three phases. A three-phase flash calculation is then carried out. The above procedure is repeated until each phase mixture is stable.

Conventional stability analysis is slow mainly because there are many primary variables, and the Jacobian matrix is of size $N_C \times N_C$. In addition, stability analysis calculations are needed in many grid blocks at a given time. There is a great need for a much faster and more robust stability analysis calculations.

In this research, we extend the reduced parameters using the proposed BIP model for an arbitrary number of components and non-zero BIPs matrix. In doing so, the stability analysis calculations are much faster and should be more robust than conventional methods.

3.1 CONVENTIONAL STABILITY ANALYSIS CALCULATIONS

The objective of stability analysis calculations is to find all stationary points of the tangent plane distance (TPD) function. In addition, the values of the TPD at these stationary points need to be evaluated. Consider an N_C-component mixture with overall composition of z_i at given reservoir temperature T and pressure P. For a trial phase composition y_i, the TPD can be expressed in dimensionless form as:

$$\begin{aligned} TPD(\vec{y}) &= \sum_{i=1}^{N_C} y_i \left[\mu_i(\vec{y}) - \mu_i(\vec{z}) \right] / RT \\ \vec{y} &= \begin{bmatrix} y_1 & y_2 & \dots & y_{N_C} \end{bmatrix} \\ \vec{z} &= \begin{bmatrix} z_1 & z_2 & \dots & z_{N_C} \end{bmatrix} \end{aligned} \quad . \tag{3.1}$$

where μ_i is the chemical potential for component *i*.

At the stationary points, the partial derivative of the TPD function with respect to y_i is zero. This condition for stationary points can be calculated combined with Gibbs-Duhem equation using the following:

$$\frac{\partial}{\partial y_i}(TPD) = \frac{\mu_i(\vec{y}) - \mu_i(\vec{z}) - \mu_{N_C}(\vec{y}) + \mu_{N_C}(\vec{z})}{RT} = 0 \quad . \tag{3.2}$$

Equations (3.2) can be re-written as:

$$\frac{\mu_i(\vec{y}) - \mu_i(\vec{z})}{RT} = \frac{\mu_{N_C}(\vec{y}) - \mu_{N_C}(\vec{z})}{RT} = k \tag{3.3}$$

where *k* must be constant.

Equations (3.3) show that the constant is independent of the component index *i*. The chemical potential μ_i is further written in terms of fugacity coefficients and compositions using $\mu_i(\vec{y})/RT = \ln\phi_i(\vec{y}) + \ln y_i$. Noting $\mu_i(\vec{z})/RT = d_i(\vec{z})$, Eqs. (3.3) can be written as:

$$\frac{\mu_{N_C}(\vec{y}) - \mu_{N_C}(\vec{z})}{RT} = k = \ln\phi_i(\vec{y}) + \ln y_i - d_i(\vec{z}) \quad . \tag{3.4}$$

A new set of primary variables are defined: $Y_i = y_i e^{-k}$. These new variables are substituted into Eqs (3.4), yielding:

$$e_i = \ln\phi_i(\vec{Y}) + \ln Y_i - d_i(\vec{z}) = 0, \qquad \vec{Y} = \begin{bmatrix} Y_1 & Y_2 & \dots & Y_{N_C} \end{bmatrix} \quad . \tag{3.5}$$

We solve Eqs. (3.5) using Newton-Raphson method with the Jacobian matrix:

$$J_{ij} = \frac{\partial e_i}{\partial Y_j} = \frac{\partial \ln\phi_i}{\partial Y_j} + \frac{1}{Y_j} = \frac{1}{Y_j} + \sum_k \frac{\partial \ln\phi_i}{\partial y_k}\frac{\partial y_k}{\partial Y_j} \quad . \tag{3.6}$$

The derivative $\partial \ln\phi_i / \partial y_k$ is the same as that in conventional phase-split calculations described in Chapter 2. The remaining partial derivatives can be calculated using:

$$\frac{\partial y_k}{\partial Y_j} = \frac{\delta_{kj}\sum_i Y_i - Y_k}{\left(\sum_i Y_i\right)^2} \quad . \tag{3.7}$$

When the overall composition is stable, the TPD function must be non-negative at all stationary points $\tilde{y}_i$. In other words, $k \geq 0$ is required for all solutions of the above N_C non-linear equations (see Eqs. (3.5)). From $Y_i = y_i e^{-k}$, we have for a stable phase:

$$\sum_{i=1}^{N_C} \tilde{Y}_i = \sum_{i=1}^{N_C} \tilde{y}_i e^{-k} = e^{-k} \leq 1 \quad \text{only if } k \geq 0 . \tag{3.8}$$

These non-linear equations (Eqs. (3.5)) can have the following possible solutions:

$$\begin{aligned} &\tilde{Y}_i = z_i \qquad \text{trivial solution} \\ &\sum_{i=1}^{N_C} \tilde{Y}_i > 1 \\ &\sum_{i=1}^{N_C} \tilde{Y}_i \leq 1 \quad \text{with } \tilde{Y}_i \neq z_i \end{aligned} \quad . \tag{3.9}$$

If all the roots to Eqs. (3.5) yield $\sum_{i=1}^{N_C} \tilde{Y}_i \leq 1$, the overall composition is stable, and the mixture will maintain a single phase; otherwise that phase must split in two phases. However, it would be costly to calculate all these roots without knowing *a priori* how many roots exist. Michelsen (1982a) suggested that it is often efficient enough to only test the initial guesses using compositions made up of either purely the most or the least volatile component in the mixture rather than test all the possible initial guesses. This approach is much easier and faster, and in most cases yields satisfactory results. Nevertheless, stability analysis calculations using the conventional approach require solving for stationary points using N_C variables.

3.2 STABILITY ANALYSIS CALCULATIONS IN REDUCED SPACE

Stability analysis can also be performed in reduced space where the number of the primary variables required to iterate on is much less. As a result, stability analysis calculations in reduced space have significant speedup compared with the conventional method. Further, the determination of stationary points of the TPD is more robust in reduced space since the global minimum of the TPD in theory should be easier to find.

As shown in the phase split calculation (see Chapter 2), the fugacity coefficients are only functions of the reduced parameters, so that:

$$\ln Y_i = d_i(z) - \ln \phi_i(\Theta), \text{ or } Y_i = \exp\left(d_i(z)\right)/\phi_i(\Theta) \quad . \tag{3.10}$$

From $1 = \sum_{i=1}^{N_C} y_i = \sum_{i=1}^{N_C} Y_i e^k = e^k \sum_{i=1}^{N_C} Y_i$, we have:

$$y_i = Y_i / \sum_{i=1}^{N_C} Y_i \quad . \tag{3.11}$$

Hoteit and Firoozabadi (2006) derived the objective function for the reduced method using dominant eigenvalue decomposition (Hendriks, 1988). From the definition of reduced parameters in Chapter 2, we have:

$$0 = \Theta_j - \sum_{i=1}^{N_C} y_i q_{ji} = \Theta_j - \sum_{i=1}^{N_C} Y_i q_{ji} \Big/ \sum_{i=1}^{N_C} Y_i \qquad \text{for } j = 1,...,5 \quad . \tag{3.12}$$

If $\sum_{i=1}^{N_C} Y_i$ is multiplied on both sides of Eqs (3.12), the following are obtained:

$$0 = \Theta_j \sum_{i=1}^{N_C} Y_i - \sum_{i=1}^{N_C} Y_i q_{ji} = \sum_{i=1}^{N_C} Y_i \left(\Theta_j - q_{ji} \right) \quad . \tag{3.13}$$

Substitution of Eqs (3.10) into Eqs (3.13), denoting $\exp\left(d_i\left(z\right)\right)$ as $D_i\left(z\right)$, yields the objective functions using reduced parameters as:

$$F_i = \sum_{k=1}^{N_C} \frac{\left(\Theta_i - q_{ik}\right) D_k}{\phi_k} = 0 \qquad \text{for } k = 1,...,5 \quad . \tag{3.14}$$

The Jacobian matrix for the objective functions in Eqs. (3.14) is evaluated as:

$$J_{ij} = \frac{\partial F_i}{\partial \Theta_j} = \sum_{k=1}^{N_C} \frac{\delta_{ij} - \left(\Theta_i - q_{ik}\right) \partial \phi_k / \partial \Theta_j}{\phi_k^2} D_k \quad . \tag{3.15}$$

The derivatives of the fugacity coefficients with respect to the reduced parameters are exactly the same as that in Chapter 2 for the phase-split calculations. In addition, each of the reduced parameters must fall into a hyperspace bounded by $q_{i\min} \le \Theta_i \le q_{i\max}$, where $q_{i\min}$ and $q_{i\max}$ are the smallest and largest values of the reduced parameter for all pure components. The procedure for stability analysis is as follows:

1. Evaluate the reduced parameters for the overall composition, and calculate the fugacity coefficients of the overall composition. Calculate the values of $D_i = z_i \phi_i\left(z\right)$, which are constant throughout the stability analysis;
2. Make an initial guess of the reduced parameters Θ for the trial phase. A possible approach is to use Θ that come from either the most or least volatile components, and use both initial guesses to initialize the NR iteration, as suggested by Michelsen (1982a). Another popular approach

uses the initial guesses of $\Theta_j = \sum_i q_{ji} K_i z_i$ and $\Theta_j = \sum_i q_{ji} z_i / K_i$, where the *K*-values come from Wilson correlations (1969). This dissertation uses the latter approach;

3. Calculate cubic EOS parameters (e.g. a_m and b_m). This step is very straightforward and depends on the selected EOS and its associated mixing rules. The cubic EOS for *Z*-factors is then solved for the trial phase. This step requires determining the roots of the cubic EOS for each phase using a cubic solver. The correct root is the one that gives the lowest Gibbs energy;
4. Calculate the fugacities of each component in the trial phase. The selected cubic EOS is used to determine an expression for the fugacity;
5. Check to see if convergence criteria are met. In this research, a tolerance of the objective function in Eqs. (3.14) of 10^{-10} is used;
6. Update the reduced parameters by Newton-Raphson iteration (for faster convergence) if the criteria of Step 5 have not been satisfied;
7. Evaluate Y_i by substitution of the converged solution of reduced variables into Eqs. (3.10);
8. If the NR iteration converges to a trivial solution or non-trivial solution where $\sum_{i=1}^{N_C} Y_i \le 1$, the other initial guess is used and steps 3-7 repeated. If the NR iterations converge to a non-trivial solution that gives $\sum_{i=1}^{N_C} Y_i > 1$, the phase-split calculations (see Chapter 2) can be performed immediately because the overall composition is unstable and forms two or more phases.

3.3 EXAMPLE CALCULATIONS

This section presents several example stability calculations with various fluid characterizations using the new reduced method to examine the efficiency of stability analysis calculations. The results are compared with the conventional method that iterates on Y_i. This section shows the advantages of the reduced method over the conventional method especially in speed.

3.3.1 IMPROVED SPEED

The most important advantages using reduced parameters over the conventional methods are significantly improved speed. We uses different oils at various temperatures and pressures to show: (1) how fast the stability analysis calculations are when the reduced method is compared with the conventional method; and (2) how fast the stability analysis calculations are compared with the phase-split calculations of the reduced method.

3.3.1.1 STABILITY ANALYSIS FOR OIL A FAR FROM CRITICAL POINT

First, we examine the synthetic seven-component oil A described in Section (2.5.1) at 260^{o}F and 300 psia. The computation time required for the stability analysis in the conventional method is determined. With the same initial guess of the trial phase compositions, the stability analysis calculations are performed in reduced space using the procedure outlined earlier. Even though the objective functions are different in these two methods, the final converged compositions are within an absolute tolerance of 10^{-10} in the composition to ensure that the same convergence criteria were met (Okuno, 2007).

Figure (3.1) compares the computation time required for convergence for both methods with a different number of pseudocomponents. Additional pseudocomponents are obtained by the same method detailed earlier (see Section (2.5.1)) that splits the least volatile component to a desired number of pseudocomponents. For the case studied, the computational time with the new method is about 1.9 times faster at seven components, and 23 times faster at thirty-five components than the conventional method. It is also shown that the stability analysis calculation using thirty-five components has a similar speed as that with ten components in the conventional method. Figure (3.2) shows the comparison of computation time per NR step. Stability analysis calculations using the reduced parameters are even faster per NR step, because less primary variables are required compared with the conventional stability analysis.

In addition, compared with Fig. (2.3), Fig. (3.1) also shows that the speedup in the stability analysis calculations is greater than that in the split calculation. This is mainly because: (1) the number of primary variables in the conventional method is the same in both subroutines (N_C); however, in the reduced method, the stability analysis requires five primary variables while the phase-spit calculation requires six; (2) the stability analysis in reduced space requires fewer iterations than phase-spit calculations in this study, which increases speedup.

The speedup in stability analysis calculations increases significantly with the number of components, as expected. The computation time for the reduced method approximately increases linearly only with the number of pseducomponents, whereas the conventional method increases on the order of 2.7. The following may explain why the reduced method is almost linearly dependent on the number of pseudocomponents while the conventional method increases at the power of 2.7:

1. In the reduced method, a five by five Jacobian matrix is used regardless of the number of pseudocomponents. The difference in computation time is mainly controlled by the evaluation of the objective functions and the Jacobian matrix. The evaluation is almost linearly correlated to the number of pseudocomponents;
2. In the conventional method, the speed of Gaussian elimination depends on approximately the third power of the number of pseudocomponents, the evaluation of Jacobian matrix approximately the second power, and the evaluation of the objective function is approximately linearly correlated to the number of pseducomponents. Normally, the Jacobian evaluation takes the largest portion of the computation time, followed by Gaussian elimination. The evaluation of the objective function is the least expensive. Therefore, in the conventional method, the computation time increases between the second and third power as a function of the number of pseudocomponents.

3.3.1.2 STABILITY ANALYSIS FOR OIL A NEAR CRITICAL POINT

Oil A is again examined at 485^{o}F and 1044 psia to illustrate the calculation near the critical points. The speed of the reduced method is compared with that of the conventional method. The total CPU time is plotted in Figs. (3.5) and (3.6).

Both reduced and conventional methods slow down stability analysis calculations near the critical point. The reduced method is over two times faster than the conventional method when seven components are used, compared to approximately 1.9 far from the critical locus. Similar results were obtained in the phase-split calculations.

That is, the reduced method has a larger speedup near the critical point than far from the critical point.

3.3.1.3 SPEED COMPARISON FOR STABILITY ANALYSIS AND PHASE-SPLIT CALCULATIONS

It is also of interest to compare the total computation time of stability analysis and phase-split calculations, to determine that whether stability analysis should be used or not. Many simulators apply stability analysis calculations before using phase-split calculations. This is to avoid the slow phase split calculations when the phase in the grid block in the previous time step is stable. This section compares the computation time of both stability analysis and phase-split calculations using the reduced method.

For the same oil A, the comparison of both calculations using the reduced method is shown in Fig. (3.3). In this figure, we did not use successive substitution in the phase-split calculations, which is different from the procedure in Chapter 2. Figure (3.3) indicates a mixed result. The stability analysis calculation is faster than the phase split calculation using the reduced method, by a factor approximately 2.5. This is mainly because the number of iterations required for the stability analysis calculation (three NR iterations) is significantly less than that for the phase-split calculations (seven NR iterations). In each NR step, the stability analysis calculation is only moderately faster than the phase-split calculation, as shown in Fig. (3.4). The reduction in speedup is mainly because the Jacobian matrix is smaller (six compared with five). Similar results were seen by Hoteit and Firoozabadi (2006).

The fact that stability analysis is substantially faster than phase-split calculations should be examined for more fluids. In the example calculations, the non-trivial solution is always found with the first initial guess of $Y_i = K_i z_i$. Stability analysis

calculations will slow down if a second initial guess is required. When both initial guesses are required, the CPU time for the phase-spit calculations is approximately 50% more than that for the stability analysis calculations. This is still a substantial savings of time if most of the grid blocks are in single phase. When a gas flood is operated at a low pressure, most grid blocks have two phases where the application of stability analysis may have little advantage.

3.3.2 IMPROVED ROBUSTNESS OF REDUCED METHOD

Previous research has shown that robustness in stability analysis is improved in reduced space mainly because of a smoother Gibbs free energy surface in the reduced space (Firoozabadi and Pan, 2002). In this research, we did not found a case where the conventional method failed to converge. This is because in stability analysis, there is always at least one solution, that is the trivial solution of $y_i = z_i$. In addition, because the Rachford-Rice or a similar method is not used in the stability analysis, there is no convergence problem owing to the iterative RR procedure. However, we did find that stability analysis in reduced space is relatively faster compared with the conventional method, especially when the overall composition is near a critical point. We compare the speedup in Figs. (3.1) and (3.5), and find out that the speedup in Fig. (3.5) is significantly greater than that in Fig. (3.1). This is mainly because the conventional method is relatively slower to converge. Because of the improved smoothness in reduced space, there is not much of a difference in convergence in both cases. Nevertheless, the reduced method converges significantly faster than the conventional method even when the overall composition is near critical. With fewer primary variables, we speculate that the reduced method should be more robust.

3.4 CONCLUSIONS

In this chapter, the reduced method was implemented to perform stability analysis calculations for two phases. Calculations based on direct solution of the tangent plane distance function were formulated. The example cases studied reveal the advantages of the new method over the conventional method as the following:

1. The number of primary variables in the direct solution of the TPD function is significantly reduced from N_C to a maximum of five, depending on binary interaction parameters;
2. The computation speed is significantly enhanced compared to the conventional method without sacrificing accuracy. The conventional method requires approximately 1.9 times the computation time than for the reduced method at seven components, and 23 times at 35 components;
3. The robustness of the rapid calculations is also slightly improved for compositions near the critical locus;
4. Compared to phase-split calculations in reduced space, stability analysis calculations in reduced space are faster by approximately 3 times independent of the number of components. However, if most of the grid blocks are two phases at the previous time step, it may not be efficient to apply the stability analysis calculations at all. Negative flash calculations with the reduced method may be all that is required.

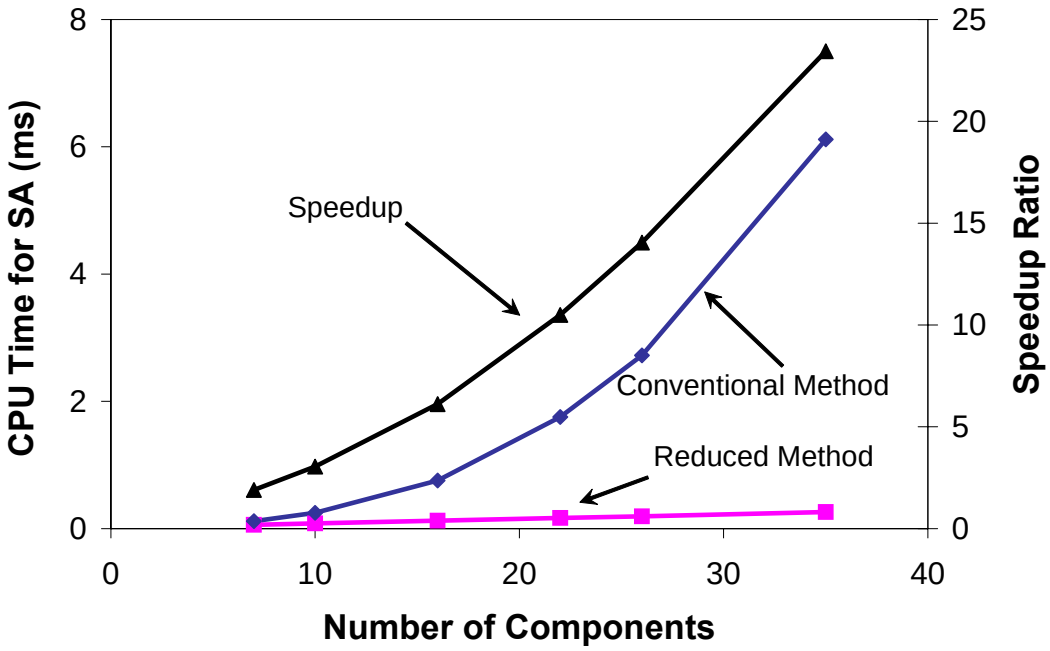

Fig. 3.1 Comparison of the total computation time for both the reduced method and the conventional method in stability analysis as a function of the number of pseudocomponents for oil A. For seven components, the speedup from the conventional method is approximately 1.9 and for 35 components, the speedup is 23 (Okuno, 2007).

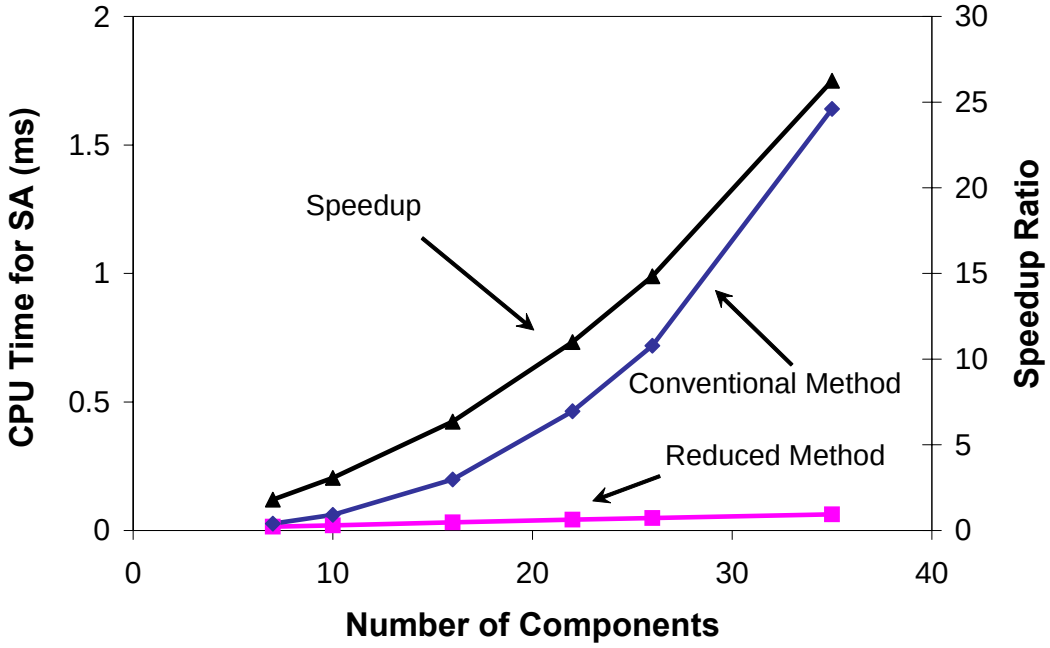

Fig. 3.2 Comparison of the computation time for stability analysis per NR iteration for oil A that is far from a critical point. Both the reduced and the conventional methods are tested. As shown, the reduced method is significantly faster (Okuno, 2007).

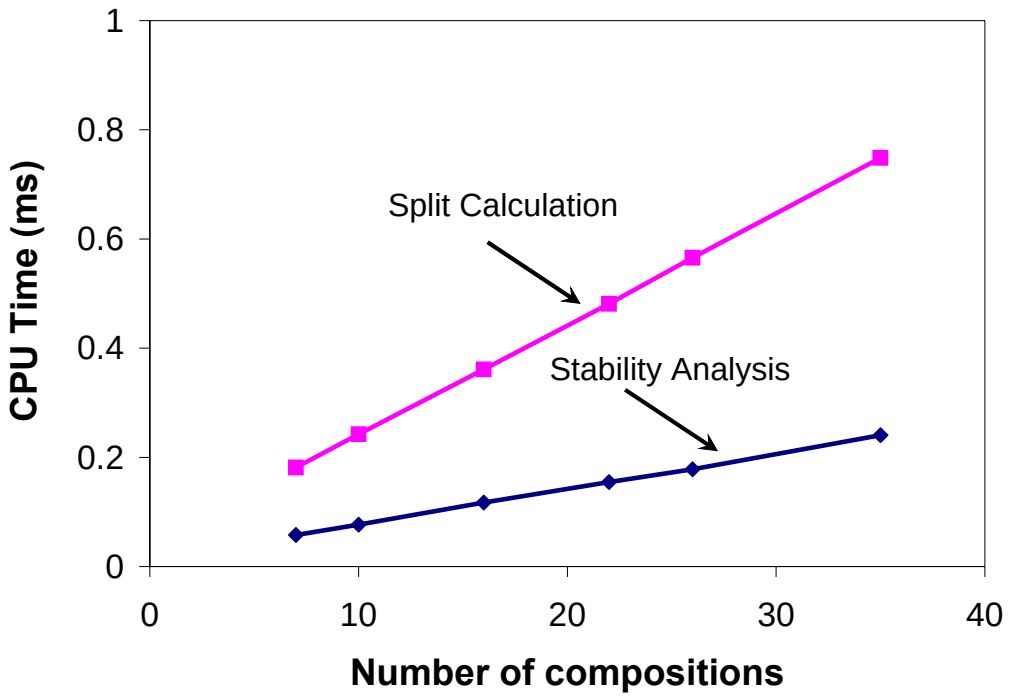

Fig. 3.3 Comparison of the total computation time for stability analysis and phase-split calculations using the reduced method for oil A. The stability analysis is approximately three times faster. In this case, the oil is far from a critical point (Okuno, 2007).

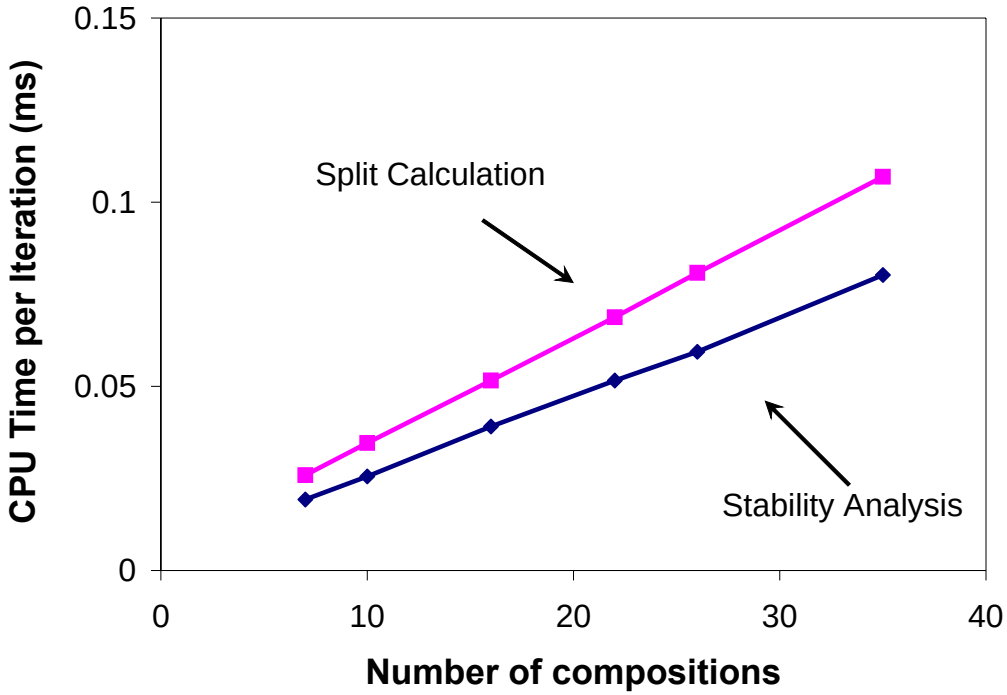

Fig. 3.4 Comparison of the computation time per iteration for stability analysis and phase-split calculations using the reduced method for oil A. The stability analysis in reduced space is moderately faster than the phase-split calculation in reduced space. In this case, the oil is far from a critical point (Okuno, 2007).

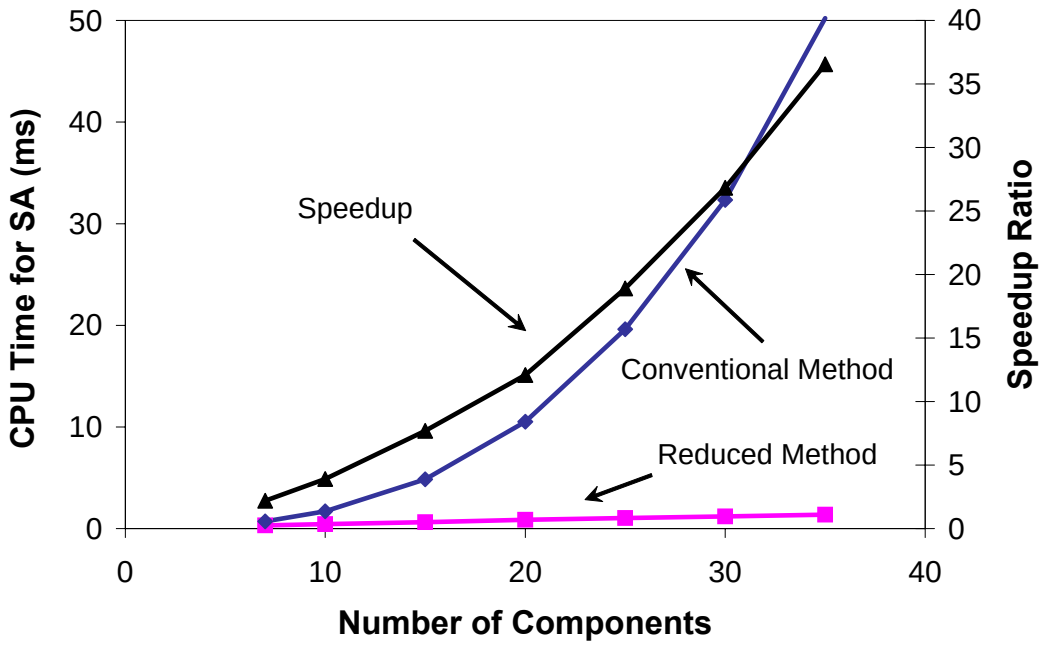

Fig. 3.5 Comparison of the total computation time for oil A near a critical point. Both the reduced and the conventional methods are used. The reduced method is much faster than the conventional one (Okuno, 2007).

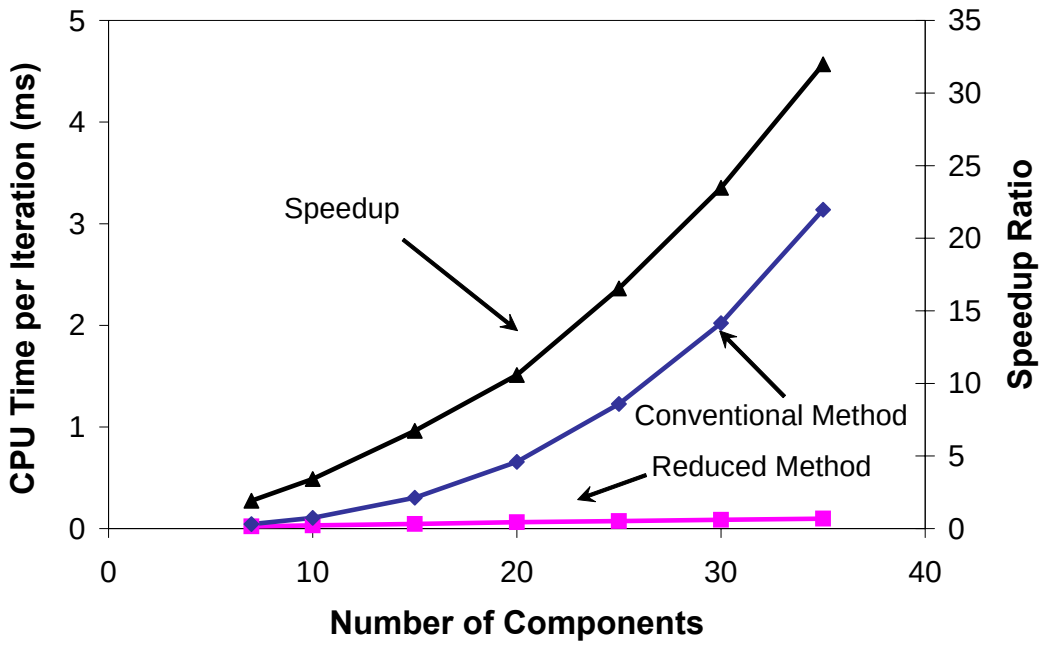

Fig. 3.6 Comparison of the computation time for stability analysis per NR iteration for oil A near a critical point. The reduced method is significantly faster and requires fewer iterations (Okuno, 2007).

Chapter 4: Two-Phase Flash Calculations with Constant K-values

Rachford-Rice (1952) iterations are widely used in equations-of-state (EOS) flash calculations to determine phase equilibrium compositions with constant equilibrium ratios (*K*-values). The method, however, can be slow to converge and in some cases may not converge at all.

In this chapter, we derive a new objective function in terms of one of the equilibrium liquid phase mole fractions. The new method also specifies a small window in which the physical roots must lie. The new objective function is continuous and nearly linear in this predetermined window. We first summarize conventional Rachford-Rice (1952) calculations, and then derive the new objective function and window. Several example calculations are performed and the results are compared with the Rachford-Rice (1952), Wang and Orr (1997, 1998), and Leibovici and Neoschil (1992) methods. The Peng-Robinson (1977, 1978) EOS is also used to demonstrate that the function can converge very near the critical region.

4.1 RACHFORD-RICE FLASH CALCULATIONS

Rachford-Rice (1952) iterations are typically used to determine the phase compositions and amounts as outlined in step 3 in Section (2.1). The objective function for this method is easily derived from the definition of *K*-values for two-phase equilibrium:

$$y_i = K_i x_i \qquad i = 1,...,N_C \quad . \tag{4.1}$$

where y_i and x_i are equilibrium compositions of the vapor and liquid phase respectively, K_i are the constant equilibrium ratios and N_C is the number of components. Furthermore, a mass balance on a given component gives,

$$z_i = Lx_i + Vy_i \qquad i = 1,...,N_C \tag{4.2}$$

where L is the molar fraction of the liquid phase, V is the molar fraction of the vapor phase, and z_i is the overall composition of the mixture. The phase compositions and amounts must sum to 1.0. Substitution of Eqs. (4.1) into Eqs. (4.2) together with $L+V=1$ gives,

$$x_i = \frac{z_i}{1+V\left(K_i-1\right)} \quad i = 1,...,N_C \quad . \tag{4.3}$$

The Rachford-Rice (1952) objective function is then defined by,

$$F\left(V\right) = \sum_{i=1}^{N_C} y_i - \sum_{i=1}^{N_C} x_i = \sum_{i=1}^{N_C} \frac{z_i\left(K_i-1\right)}{1+V\left(K_i-1\right)} = 0 \quad . \tag{4.4}$$

The roots of Eq. (4.4) in terms of the vapor molar fraction are often solved by Newton-Raphson method. Convergence is achieved once the updated value of V satisfies a relative tolerance of say 10^{-8}. Once V is determined, the equilibrium phase compositions are calculated from Eqs. (4.3) and (4.1).

Unfortunately, there are N_C+1 roots for V given by Eqs. (4.3) and the function can be highly nonlinear owing to N_C poles at $V=1/(1-K_i)$. Rachford and Rice (1952) initially constrained the value of V to lie within the range or window from [0, 1],

but this requires that the overall composition lies within the two-phase region of the current set of *K*-values. Whitson and Michelsen (1989) improved the robustness for overall compositions outside the two-phase region (negative flash calculations) by showing that the correct root of V can be defined from the poles corresponding to the largest and smallest volatile components, that is, within the window $1/(1-K_1) < V < 1/(1-K_{N_C})$. Even with this improvement, the Rachford-Rice (1952) function still suffers from the disadvantages described previously, and may not always converge for some special cases.

4.2 DERIVATION OF NEW METHOD

Similar to the approach of Whitson and Michelsen (1989), the derivation of our new objective function and window requires that the components are ordered based on *K*-values. We assume that $K_1 > 1 > K_{N_C}$.

The objective function is determined by transforming the original compositions so that equilibrium phase compositions of the intermediate components in the transformed compositional space are equal. For a ternary system this directly implies that all tie lines are parallel, including the limiting tie lines at critical points. Such a transform reduces the nonlinearity of the objective function.

The transform follows closely the procedure described by Hand (1930) for ternary diagrams, although he used transformation parameters independent of composition. We extend that approach here to a multicomponent system by introducing a set of transformation parameters, in which each one is a function of composition. The transformed intermediate compositions are given by

$$x_i^* = \frac{x_i}{(\alpha_i - 1)x_1 + 1} = y_i^* = \frac{y_i}{(\alpha_i - 1)y_1 + 1} = z_i^* = \frac{z_i}{(\alpha_i - 1)z_1 + 1} \quad \text{for } i = 2,...,N_C - 1 \tag{4.5}$$

where α_i is the transformation parameter. From Eq. (4.5), α_i can be evaluated by

$$\alpha_i = 1 + \frac{1}{x_1}\left(\frac{K_i - 1}{K_1 - K_i}\right) \qquad i = 2,...,N_C - 1 \ . \tag{4.6}$$

From Eqs (4.5) and (4.6), one can also show that for the liquid phase:

$$x_i = \frac{(K_1 - 1)z_i x_1}{(K_i - 1)z_1 + (K_1 - K_i)x_1} \quad i = 2,...,N_C - 1 \ . \tag{4.7}$$

Equations (4.7) can also be derived directly from Eqs. (4.3) by solving for *V*, but with loss of physical meaning. In addition to Eqs. (4.7), the phase compositions must sum to 1.0 so that

$$x_{N_C} = 1 - \sum_{i=1}^{N_C - 1} x_i \tag{4.8}$$

$$y_{N_C} = 1 - \sum_{i=1}^{N_C - 1} y_i \ . \tag{4.9}$$

If we substitute Eqs (4.8) and (4.3) into Eq (4.9), we have after some rearrangement:

$$1+\frac{\left(K_1-K_{N_C}\right)}{\left(K_{N_C}-1\right)}x_1+\sum_{i=2}^{N_C-1}\frac{\left(K_i-K_{N_C}\right)}{\left(K_{N_C}-1\right)}x_i=0 \quad . \tag{4.10}$$

Substitution of Eqs (4.7) into Eq (4.10) gives the new objective function as,

$$F\left(x_1\right)=1+\left(\frac{K_1-K_{N_C}}{K_{N_C}-1}\right)x_1+ \sum_{i=2}^{N_C-1}\frac{\left(K_i-K_{N_C}\right)}{\left(K_{N_C}-1\right)}\left[\frac{z_i\left(K_1-1\right)x_1}{\left(K_i-1\right)z_1+\left(K_1-K_i\right)x_1}\right]=0 \quad . \tag{4.12}$$

In addition, the derivative for NR iteration is given by:

$$\frac{dF}{dx_1}=\frac{K_1-K_{N_C}}{K_{N_C}-1}+\sum_{i=2}^{N_C-1}\frac{\left(K_i-K_{N_C}\right)\left(K_1-1\right)\left(K_i-1\right)z_1z_i}{\left(K_{N_C}-1\right)\left[\left(K_i-1\right)z_1+\left(K_1-K_i\right)x_1\right]^2}$$

The correct root(s) from the new objective function must lie within a small window. This window is developed by limiting all phase and overall compositions to be positive in Eqs. (4.7). The simplest expression for the window (although not the smallest possible) is given by

$$\left(\frac{1-K_{N_C}}{K_1-K_{N_C}}\right)z_1\le x_1\le\frac{1-K_{N_C}}{K_1-K_{N_C}} \quad . \tag{4.13}$$

The derivation of Eq. (4.13) along with a more complex, but even smaller window for x_1 can be found from Eqs (4.16) and (4.18) in Section (4.2.1). Because of its

simplicity, we only use Eq. (4.13) in the calculations made in this research. When at least one composition is negative, a new window is derived in Appendix.

The new objective function of Eq. (4.12) always converges to a physical root no matter the overall composition. The new method has significant advantages over the Rachford-Rice (1952; Whitson and Michelsen, 1989) or similar variations (Wang and Orr, 1997, 1998). First, $x_1 = 0$ is not a trivial root of the new objective function as it is for Wang and Orr (1997, 1998). Second, when multiple tie lines exist that go through the same composition, the new function can find all tie lines or physical roots from the negative flash. Third, the root(s) must lie within a very small window as defined by Eq. (4.13). Fourth, the function is often linear and continuous within that window. There are never poles within the window, as proved in Section (4.2.2). Fifth, the function is always positive at the lower limit of the window and negative at the upper limit so that bisection methods can be easily used if required (see Section (4.2.3.)). Last, the new objective function is properly scaled to reduce truncation error compared with that of Rachford-Rice (1952). These features can significantly reduce the number of iterations for convergence compared with Rachford-Rice (1952) and are discussed in the next section.

4.2.1 Initial Guess for Phase Mole Composition

A good initial guess for the equilibrium liquid phase mole fraction is important for convergence. In the derivations that follow we assume that all overall compositions are positive.

From Eq. (4.3), we have

$$V = \frac{z_i - x_i}{(K_i - 1)x_i} = \frac{1 - x_i/z_i}{1 - K_i} \quad \text{for } i = 1,\ldots,N_C \quad . \tag{4.14}$$

Considering only the lightest and heaviest components, Eq. (4.14) is

$$V = \frac{z_1 - x_1}{(K_1 - 1)x_1} = \frac{1 - z_{N_C}/x_{N_C}}{1 - K_{N_C}} \le \frac{1}{1 - K_{N_C}} \tag{4.15}$$

because $z_{N_C} / x_{N_C} \ge 0$. Thus, after rearrangement of Eq. (4.15), we obtain the left-hand side of Eq. (4.13) to be

$$x_{1\min} = \left(\frac{1 - K_{N_C}}{K_1 - K_{N_C}} \right) z_1 \quad . \tag{4.16}$$

To determine a maximum limit, we recognize that for all components $K_i x_i \ge K_{N_C} x_i$. Summation of this expression yields after some rearrangement:

$$\sum_{i=2}^{N_C} K_i x_i = 1 - y_1 = 1 - K_1 x_1 \ge \sum_{i=2}^{N_C} K_{N_C} x_i = K_{N_C} (1 - x_1). \tag{4.17}$$

From Eq. (4.17), we obtain the right-hand side of Eq. (4.13) as,

$$x_{1\max} = \frac{1 - K_{N_C}}{K_1 - K_{N_C}} \quad . \tag{4.18}$$

A more complex, but smaller window can be found recognizing that all equilibrium liquid phase compositions must be positive so that

$$\begin{aligned} 0 \le x_i \le \frac{1}{K_i} \quad & \text{if } K_i > 1 \\ 0 \le x_i \le 1 \quad & \text{if } K_i < 1 \end{aligned} \quad . \tag{4.19}$$

Substitution of Eqs. (4.7) into Eqs. (4.16) and (4.18) gives,

$$x_{1\min} = \max\left[\frac{(1-K_i)z_1}{(K_1-K_i)-z_i(K_1-1)}\right] \text{ for all } K_i < 1 \tag{4.20}$$

$$x_{1\max} = \min\left[\frac{(K_i-1)z_1}{K_i z_i(K_1-1)-(K_1-K_i)}, \frac{1-K_{N_C}}{K_1-K_{N_C}}\right] \quad \text{for all } K_i > 1 . \tag{4.21}$$

This smaller window compared with Eq. (4.13) can decrease the number of iterations slightly, especially when the number of components is greater than 10. For example, when $N_C = 12$ the smaller window is approximately 15% faster in computational time than when using the window given by Eq. (4.13). Equation (4.20) is identical to that used by Lebovici and Neoshil (1992), but the maximum limit given by Eq. (4.21) is new to this research.

The window given by Eqs. (4.20) and (4.21) can also be used to determine if a physical root exists. If $x_{1\min} = x_{1\max} = 0$ then no physical root exists. For reservoir simulation, however, this problem will not arise, but it might in other applications such as the MMP/MME determination from analytical methods (Jessen *et al*., 1998; Yuan and Johns, 2005).

4.2.2 Continuity of New Method

The objective function contains no poles within the window of Eq. (4.13). The poles of Eq. (4.12) are defined by

$$x_1 = \frac{(1-K_i)z_1}{(K_1-K_i)}, \qquad i = 2,...,N_C-1 \quad . \tag{4.22}$$

Because $(1-K_i)(K_1-K_{N_C}) < (1-K_{N_C})(K_1-K_i)$,

$$\frac{(1-K_i)z_1}{(K_1-K_i)} < \frac{(1-K_{N_C})z_1}{(K_1-K_{N_C})} = x_{1\min} \qquad . \tag{4.23}$$

Equation (4.23) shows that when $z_1 \neq 0$, all poles are to the left (towards negative x_1) of the window given by Eq. (4.13). Thus, the objective function will be continuous in the window. When $z_1 = 0$ the pole coincides with $x_{1\min}$ and there is a discontinuity in the objective function at $x_{1\min}$. As explained in Section (4.2.3) that discontinuity can be easily handled by selecting another variable to iterate on.

4.2.3 Finding All Possible Roots

More than one physical root is possible when one or more components are not present, for example at the apex or the base of a ternary diagram. It may also be possible with the new method that no root exists within the window when the lightest component is not present in the overall composition and $V > 0$. For some applications such as MMP/MME estimation (Jessen *et al*., 1998; Yuan and Johns, 2005), we want to find all tie lines that extend through the overall composition. An easy method to find all

tie lines is first to make the flash calculation with all N_C components. The flash is then repeated, but the number of components is reduced one by one by eliminating the missing component(s) from the objective function. This would continue until all components have *K*-values less than 1.0. Each flash will yield another tie-line solution.

A more formal way of writing this is to recognize that the selection of the component to calculate the liquid phase mole fraction is arbitrary. Thus, we can write Eq. (4.12) in a more general form as:

$$F\left(x_j\right)=1+\left(\frac{K_j-K_{ref}}{K_{ref}-1}\right)x_j+\sum_{i=1,i\neq j,i\neq ref}^{N_C}\frac{\left(K_i-K_{ref}\right)}{\left(K_{ref}-1\right)}\frac{z_i\left(K_j-1\right)x_j}{\left(K_i-1\right)z_j+\left(K_j-K_i\right)x_j}=0\,. \qquad (4.24)$$

where K_j is the selected component to use as the iteration variable and $K_j>1$ and $K_{ref}<1$. Typically, $K_{ref}=K_{N_C}$ and $K_j=K_i$.

The case when no root exists within the window can be identified prior to calculation. When $z_1=0$, no root is present when

$$1+\sum_{i=2}^{N_C-1}\left(\frac{K_1-K_{N_C}}{K_{N_C}-1}\right)z_i<0 \quad . \qquad (4.25)$$

Equation (4.25) is derived by finding when the objective function given by Eq. (4.12) is negative at $F(0+)$. For such cases there is a discontinuity at $x_1=0$.

Another possible complication for the new method and the Rachford-Rice (1952) is when the overall composition of the primary variable is very small, that is, $z_1<10^{-9}$. In such cases many iterations are often required to obtain convergence because of the nonlinearity that occurs near the root. This problem is more likely to occur with Rachford-Rice. For the new method, we can eliminate this problem by changing the

primary variable to the next lightest component. Based on experience we recommend to do this when $z_1 / K_1 \le 10^{-12}$. The variable to iterate with should be chosen so that $z_i / K_i \ge 10^{-12}$ when $K_i > 1$ or $z_i K_i \ge 10^{-12}$ for $K_i < 1$.

4.3 EXAMPLE CALCULATIONS

This section presents several example calculations using the new method. The robustness and speed with the new objective function are compared with that obtained with the iterative methods of Rachford-Rice (1952; Whitson and Michelsen, 1989), Wang and Orr (1997, 1998), and Leibovici and Neoschil (1992). To ensure a proper comparison, the convergence criteria for each method is always 10^{-8} for the relative error in V. For methods that iterate on x_1, we translated the value of x_1 to V so that the criteria for all methods were exactly the same.

4.3.1 Improved Robustness and Linearity of New Method.

We first consider a ternary system with constant K-values, where $K_1 = 5.0$, $K_2 = 2.0$ and $K_3 = 0.5$. Figure (4.1) shows the phase behavior for this set of K-values along with the overall compositions at points A, B, C, and D, all of which lie on the same tie line or its extension. We then examine convergence for phase behavior with K-values near 1.0 and also with a cubic EOS (Peng and Robinson, 1977, 1978).

4.3.1.1 Point A

This composition lies near the center of the two-phase region in Fig. (4.1). Figure (4.2) shows the Rachford-Rice (1952) objective function for this tie line along with the correct root (solution) that lies within the window given by Whitson and

Michelsen (1989). Figure (4.3) also shows a comparison of the objective functions of Wang and Orr (1997, 1998) and our new function plotted against the same parameter x_1. The window based on Eq. (4.13) is also shown in Fig. (4.3).

Because point A lies within the two-phase region all methods can converge to the same root. Wang and Orr's method (1997, 1998), which does not specify a window other than $0.0 \le x_1 \le 1.0$, could converge, however, to the trivial solution at $x_1 = 0$ depending on the initial guess. That trivial solution does not exist in our proposed objective function. The new function is also more linear than either Rachford-Rice (1952) or Wang and Orr (1997, 1998) so that fewer iterations are required for convergence. As shown in Fig. (4.4), the number of iterations using the new function is largely independent of the initial guess within the window of Eq. (4.13). For example, for an initial guess of V of about 2.0, Rachford-Rice (1952; Whitson and Michelsen, 1989) takes 12 iterations to converge compared with only 5 iterations for the new function. Both methods require about 4 iterations when the initial guess is closer to the actual root, although with the new function there is a small region very near the correct root of x_1 where three iterations are required compared with four in Rachford-Rice (1952). For the same initial guess, the number of iterations with the new function will always be less than or equal to the number of iterations with Rachford-Rice (1952).

4.3.1.2 Point B

Composition B is in the single phase region and lies on the same tie-line extension as A, but unlike A does not contain component 1. Thus, there is a second tie-line that extends though A along the base (2-3 axis) of the ternary diagram. Ideally, a negative flash at this composition could yield the root corresponding to either tie line.

Point B is problematic for both Rachford-Rice (1952) and Wang and Orr (1997, 1998). The Wang and Orr objective function (1997, 1998) cannot be calculated because z_1 is zero there and a divide by zero error occurs. The Rachford-Rice (1952) function (see Fig. (4.5)) does have the root corresponding to the tie line in the base of the ternary diagram, but this root is outside of the Whitson-Michelsen window (1989). Thus, the Rachford-Rice (1952) root is not bounded correctly and convergence is not guaranteed.

The window for the new function (see Fig. (4.6)), however, contains the correct root for the tie line that passes through point A. Furthermore, Section (4.2.3) describes an easy way to locate the second tie line in the base of the ternary diagram. Thus, both tie lines can be found with the new function with few iterations. The new function can also converge even when the overall composition is on any one of the three apexes of the ternary diagram.

4.3.1.3 Point C.

This overall composition is in the vapor region, but also lies on the tie-line extension through point A. Thus, like B this is a negative flash. Figure (4.7) gives the Rachford-Rice function (1952), whereas Fig. (4.8) compares the Wang and Orr function (1997, 1998) with our new function. Similar to point A, all methods converge to the correct solution, although the number of iterations with Rachford-Rice (1952) is similar to that shown previously in Fig. (4.4). Also, as for point A, the Wang and Orr function (1997, 1998) can converge to the trivial root depending on the initial guess.

4.3.1.4 Point D.

Composition D lies exactly on the 1-2 axis of the ternary diagram. This point is again problematic for Rachford-Rice (1952) as the correct root corresponding to the tie-line extension through point A is not present (see Fig. (4.9)). The root shown in Fig. (4.9) for Rachford-Rice (1952) corresponds to a tie line that is nonphysical, that is, one or more of the equilibrium phase compositions are negative. Wang and Orr's objective function (1997, 1998) also cannot converge to the correct root as only the trivial solution ($x_1 = 0$) is present (see Fig. (4.10)). The new method, however, has the correct root and will converge in a few iterations.

4.3.1.5 Point E - Near Critical

The new method also converges well for points very near the critical locus where all *K*-values are within numerical precision of 1.0. For example, Figure (4.11) shows the tiny two-phase region for *K*-values of $K_1 = 1 + 2\varepsilon$, $K_2 = 1 + \varepsilon$ and $K_3 = 1 - \varepsilon$ with $\varepsilon = 10^{-9}$. In that plot the bubble-point curve and dew-point curve nearly coincide with each other.

All methods converge to the correct root; although the Wang and Orr method could mistakenly converge to the trivial root at $x_1 = 0$ (see Figs. (4.12) and (4.13)). Similar to convergence at point A, the new function requires fewer iterations for convergence than Rachford-Rice (1952).

For very small values of ε, the Rachford-Rice method (1952) can also suffer from truncation error owing to addition or subtraction of a large number from a small one. The new function, which is better scaled, preserves all sixteen digit accuracy if double precision is used, whereas Rachford-Rice (1952) has thirteen digit accuracy. The scaling issue is apparent by considering the values of the objective functions. For

example, for an initial guess at the midpoint of Whitson-Michelsen window (1989), the value of the Rachford-Rice objective function (1952) is -2.35×10^{-10}, and its derivative is -1.59×10^{-18}, much small than the value of the objective function. The value of the new objective function at the midpoint of Eq. (4.13) is 0.076, and its derivative is -3.76.

4.3.1.6 Use of New Method with Equations of State

Michelsen (1993) showed that successive substitution for updating *K*-values is guaranteed to converge, although very slowly near critical points (convergence could be a trivial solution, however). Figure (4.14) shows a three-component phase behavior predicted using the Peng-Robinson (1977, 1978) EOS and our new function. Convergence in the flash calculations is always achieved as the critical point is approached to within the tolerance used for component fugacities. The advantages of the new function are twofold: (1) the number of iterations are generally reduced decreasing the time for the flash calculations near the critical point; and (2) convergence is slightly more accurate near the critical point than when Rachford-Rice (1952) is used.

4.3.2 Improved Speed of New Method.

There are two ways to examine the speedup of the new method compared with Rachford-Rice (1952; Whitson and Michelsen, 1989) and Leibovici and Neoschil (1992). The first approach is to perform compositional simulations and compare the average processor time. That approach is useful because it incorporates prior values as the initial guess for the next time step, but simulation may not cover all possible combinations of *K*-values and overall compositions. Another approach is to randomly vary the compositions and *K*-values within a realistic range to estimate the average overall

speedup. We have followed both approaches here to illustrate the improved overall performance of the new method. Wang and Orr's method (1997, 1998) is not tested here as those results are similar to Rachford-Rice (1952; Whitson and Michelsen, 1989) and could mistakenly converge to a trivial solution.

4.3.2.1 Average Performance Based on Random K-values

We conducted a total of 120 million different flash calculations for each of the three methods. That is, for each method, we randomly generated 20 million sets of *K*-values and overall compositions for six multicomponent systems with 3, 5, 7, 10, 12, and 15 components. The random *K*-values were obtained using a linear distribution of $\ln K_1$ between 0.0 and 8.0. We then randomly generated values for $\ln K_{N_C}$ between -16.0 and 0.0 and assigned linearly distributed values for all other *K*-values between $\ln K_1$ and $\ln K_{N_C}$. For overall compositions, we generated random values evenly distributed over the entire composition space.

The flash calculations were conducted with an initial guess at the midpoint of each window as specified by each method. For Rachford-Rice (1952), we used the Whitson and Michelsen window (1989), but for the new method the window defined by Eq. (4.13). The window for Leibovici-Neoschil (1992) is that described in their paper, which is smaller than the window of Rachford-Rice. A relative tolerance of 10^{-8} in terms of V is used for all methods. Bisection is done instead of NR when the next iteration value estimated from NR is outside the window. For such cases, the next guess of V (or x_1) is taken to be the midpoint of the current guess and the value at the proper limit of the window. After one step(s) of bisection NR iterations continue until convergence.

There is one exception to the use of bisection for our new function and that of Leibovici-Neoschil (1992). This exception is needed because the objective functions in rare cases can have a maximum for our function and a minimum for Leibovici-Neoschil (1992) within the window. We easily circumvent this problem by examining the derivative at the first NR iteration. When the derivative of the objective function is positive for our method, we use the average of the current guess of the primary variable and the maximum limit from the window as the new value for x_1.

The average CPU time of one flash calculation is in μs and the number of iterations as a function of the number of components are shown in Figs. (4.15) and (4.16) respectively. As shown, the new method is significantly faster than the other methods. For example, the average speedup with the new method compared with Rachford-Rice (1952) is 25% for three components and 40% with fifteen components. Thus, speedup is greater as the number of components increases. The increase in speedup occurs because the number of iterations required with the new method increases only slightly with an increase in components.

The Leibovici-Neoschil method (1992) is slightly slower than Rachford-Rice (1952; Whitson and Michelsen, 1989) until the number of components is greater than 7, but is always significantly slower than our new method. This is true even though the Leibovici-Neoschil (1992) requires about the same number of iterations as our new method (see Fig. (4.16)).

The new method is much faster than Leibovici-Neoschil (1992) per iteration (see Fig. (4.17)). Rachford-Rice (1952) is the fastest method per iteration, but requires many more iterations to achieve convergence.

4.3.2.2 Six-Component Example

We illustrate with a six-component example to show why the Rachford-Rice (1952; Whitson and Michelsen, 1989) requires more iterations compared with our new method. Leibovici and Neoschil (1992) point out that the Rachford-Rice function (1952) becomes highly nonlinear and slow to converge when the *K*-value of the heaviest component and its overall composition are small, especially for fluids with many components. This is also true they state when the lightest component has a very large *K*-value, but small composition. These conditions are more likely to exist when the fluid contains many components where the lightest and heaviest components will typically have smaller compositions. The Rachford-Rice function (1952) is also generally more nonlinear because the number of poles increases with the number of components.

We demonstrate here, however, why convergence with the Rachford-Rice function (1952) is also slow even when K_{N_C} is not small. As shown in Table (4.1), the *K*-values of all components in this example are near 1.0 including the heaviest component. For this case, the Rachford-Rice function (1952) is highly nonlinear and the root is close to a pole (see Fig. (4.18)). Thus, the Rachford-Rice method (1952) with an initial guess at the midpoint of the Whitson-Michelsen window (1989) takes 12 iterations to converge to the correct solution compared with 4 iterations with our new method. Our new objective function is not near a pole and is nearly linear in the window (see Fig. (4.19)).

Figures (4.20) and (4.21) also demonstrate that convergence with Rachford-Rice (1952; Whitson and Michelsen, 1989) is slow even when the lightest component has a large composition (see Table (4.2)). For this case the Rachford-Rice method (1952) takes eighteen iterations to converge compared with six with our function. This is true even though a pole is near the lower limit for x_1 given by Eq. (4.13).

We conclude that if z_1 / K_1 and/or $z_{N_C} K_{N_C}$ are small, Rachford-Rice (1952; Whitson and Michelsen, 1989) will require many iterations unless the initial guess is very close to the correct root. Our new method, however, can handle these difficult cases because of improved linearity. However, as pointed out in Section (4.2.3), the new method will require more iterations when x_1 / K_1 is extremely small. For that case, this problem can be circumvented by changing the primary variable to a different component.

4.3.3 Implementation in a Compositional Simulator

We also implemented the new objective function in GPAS, a fully implicit compositional simulator (Okuno, 2007). Some example simulations are performed, and the result is listed in Table (4.3). The number of iterations is moderately reduced by approximately 5% for all the cases studied. This is mainly because in the simulations the values of the previous time step are used as the initial guess. Thus, the initial guesses during simulation are typically nearer the correct solution than those in batch mode. As shown in Fig. (4.4), when the initial guess is better, the difference of the number of iterations between the two methods is small. Nevertheless, the new method still requires less number of iterations in all cases as expected. We would expect the time savings to be greater when an IMPEC simulator is used.

4.4 CONCLUSION

We developed a new rapid and robust objective function that replaces Rachford-Rice (1952) in conventional flash calculations. The main conclusions are

1. The new objective always converges to double precision accuracy no matter the overall compositions and *K*-values. The function is properly

scaled near critical points;

2. The root corresponding to the physical tie line must lie within a small window as specified by Eq. (4.13);
3. The new objective function is continuous within the window and is often nearly linear;
4. Because of improved linearity, the new method is significantly faster than Rachford-Rice (1952) and always requires an equal or fewer number of iterations when starting at the same initial guess. On average, speed up compared with Rachford-Rice (1952) is 25% for three-component fluids and 40% for fifteen-component fluids based on random *K*-values;
5. The new method is easily incorporated into flash calculations using any cubic EOS (Coats, 1985);
6. Simulation results showed that the new method requires less number of iterations compared with the conventional Rachford-Rice method. Speedup using the new method is about 5% of the total simulation time.

	K-values	Compositions
1	1.00003	0.770
2	1.00002	0.200
3	1.00001	0.010
4	0.99999	0.010
5	0.99998	0.005
6	0.99997	0.005

Table 4.1 *K*-values and overall compositions for a six-component fluid that is near a critical point.

	K-values	Compositions
1	161.59	0.44
2	6.90	0.55
3	0.15	3.88E-3
4	1.28E-3	2.99E-3
5	5.86E-6	2.36E-3
6	2.32E-8	1.95E-3

Table 4.2. K-values and overall compositions for a six-component fluid far from a critical point.

Grid Blocks #	N_C	Total # of Iteration in RR	Total # of Iteration in LJ
7 by 7 by 3	6	104,318	97,920
18 by 18 by 3	6	731,321	698,898
18 by 18 by 3	4	593,370	571,067
14 by 14 by 1	12	257,791	244,406

Table 4.3 Comparison of the number of iterations by the Rachford-Rice method (1952) and the new objective function in simulations with GPAS (Okuno, 2007).

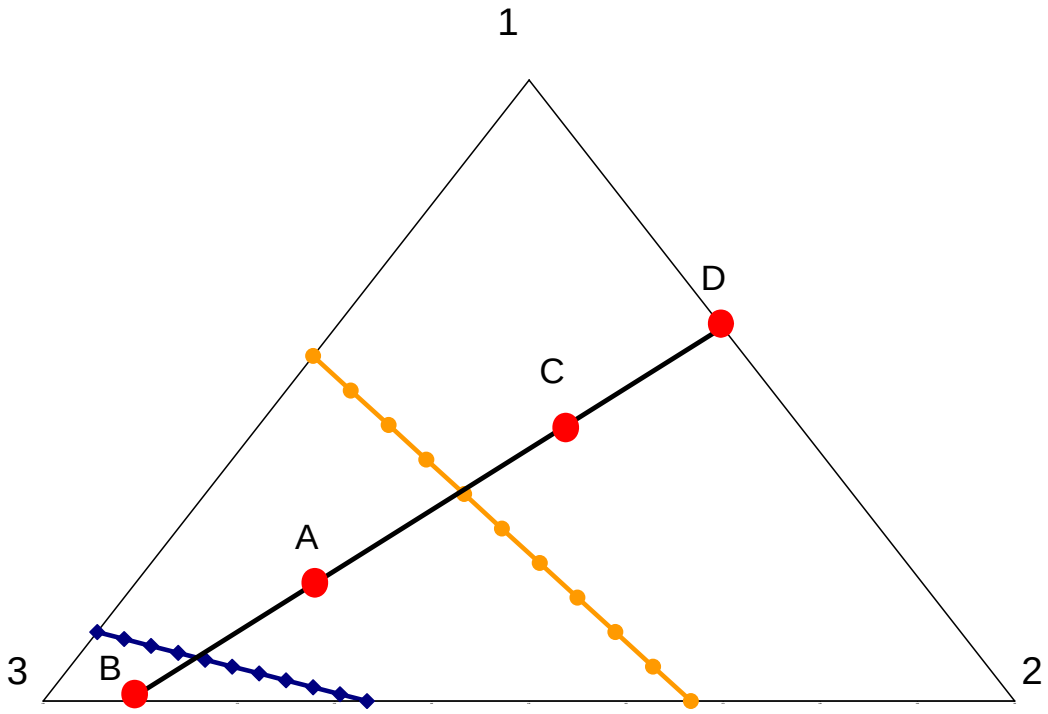

Fig. 4.1 Ternary diagram with K_1 =5.0 , K_2 =2.0 , and K_3 =0.5 . The four compositions shown all lie on the same tie line and its extension.

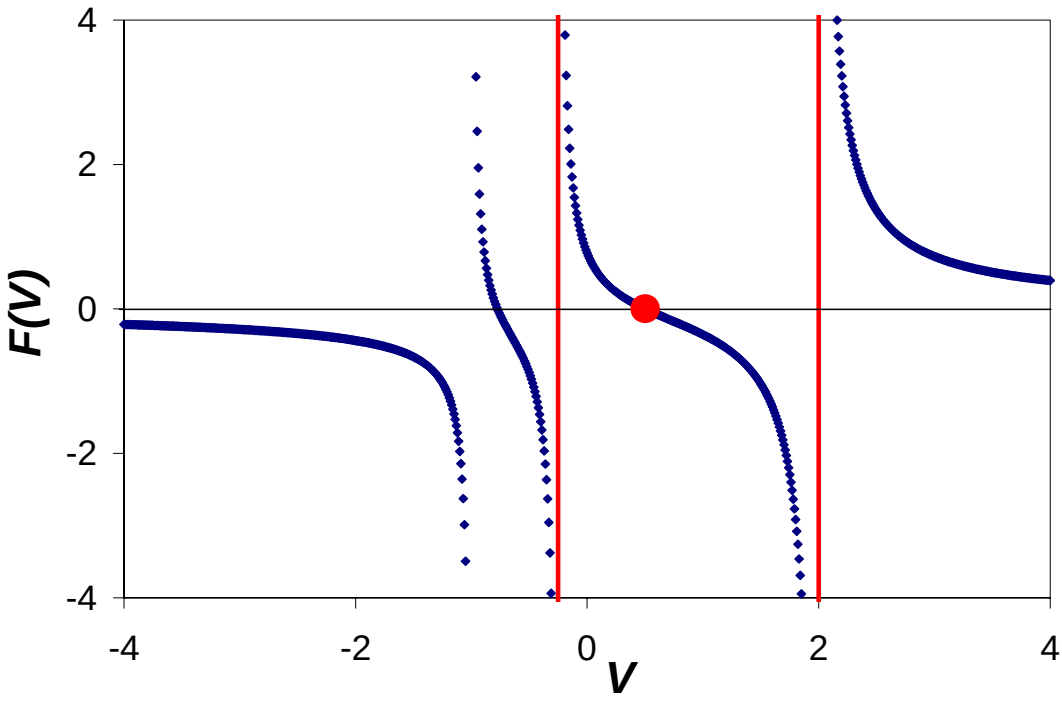

Fig. 4.2 Rachford-Rice function (1952) for point A in Fig. (4.1). The red vertical lines are the limits of the window given by Whitson and Michelsen.(1989) The correct root within that window is shown by the solid dot. There are three poles.

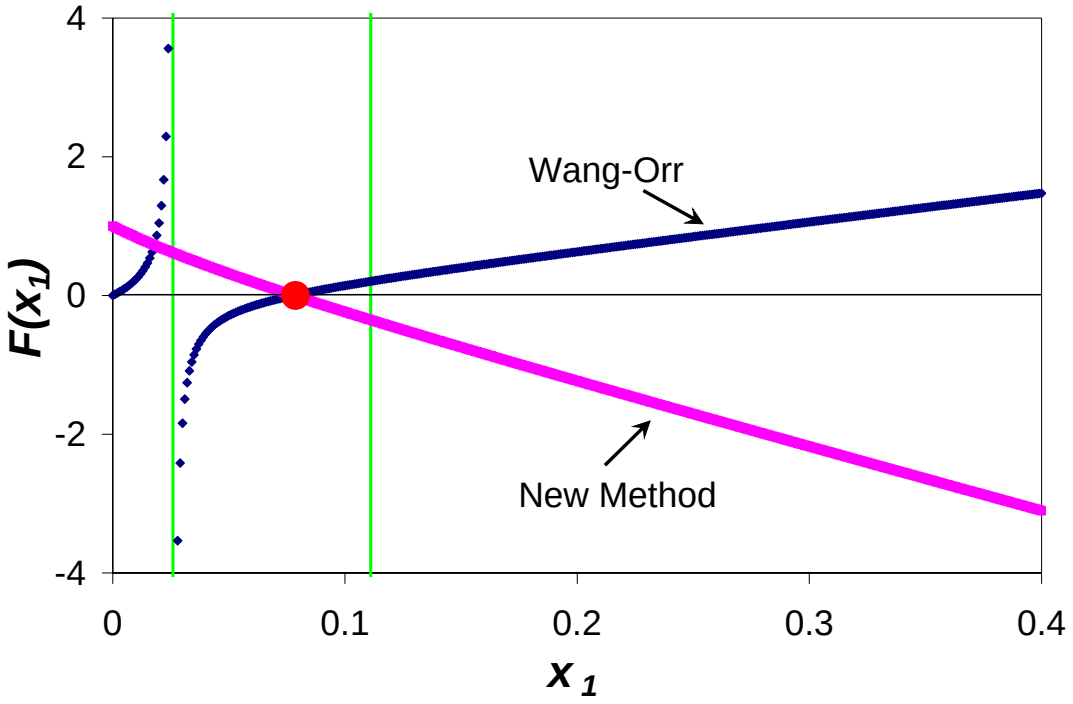

Fig. 4.3 Objective functions for point A based on our new method and that given by Wang and Orr. (1997, 1998) The correct root lies within the window given by Eq. (4.13). The new objective function is highly linear.

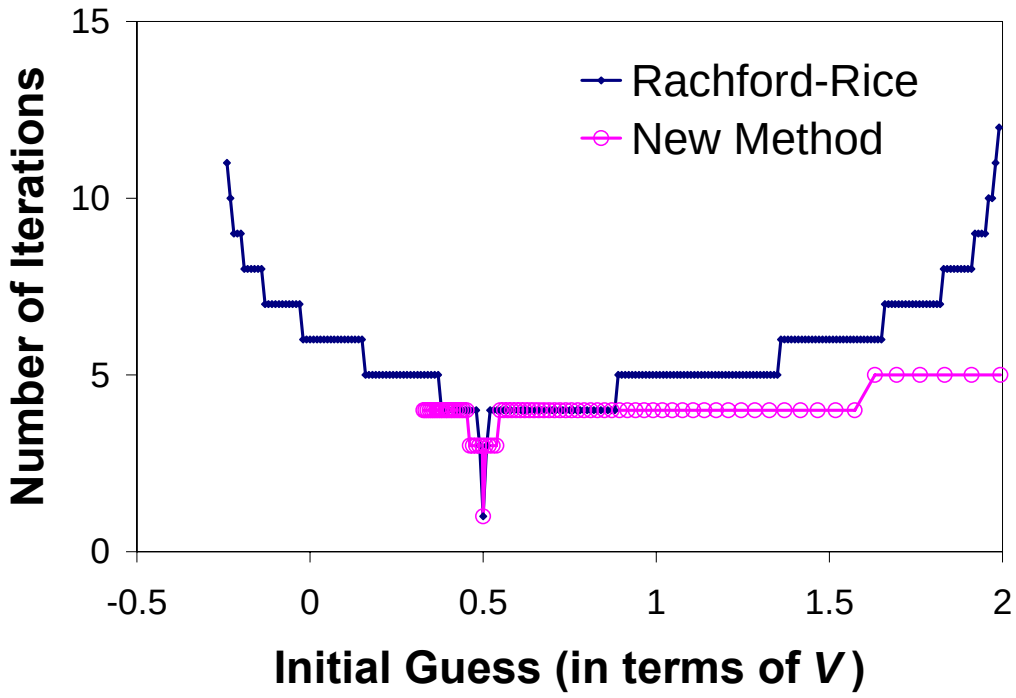

Fig. 4.4 Comparison of the number of iterations for convergence as a function of the initial guess for both Rachford-Rice (1952) and the new function in Eq. (4.12). The values of V shown for the new function lie in the window of Eq. (4.13).

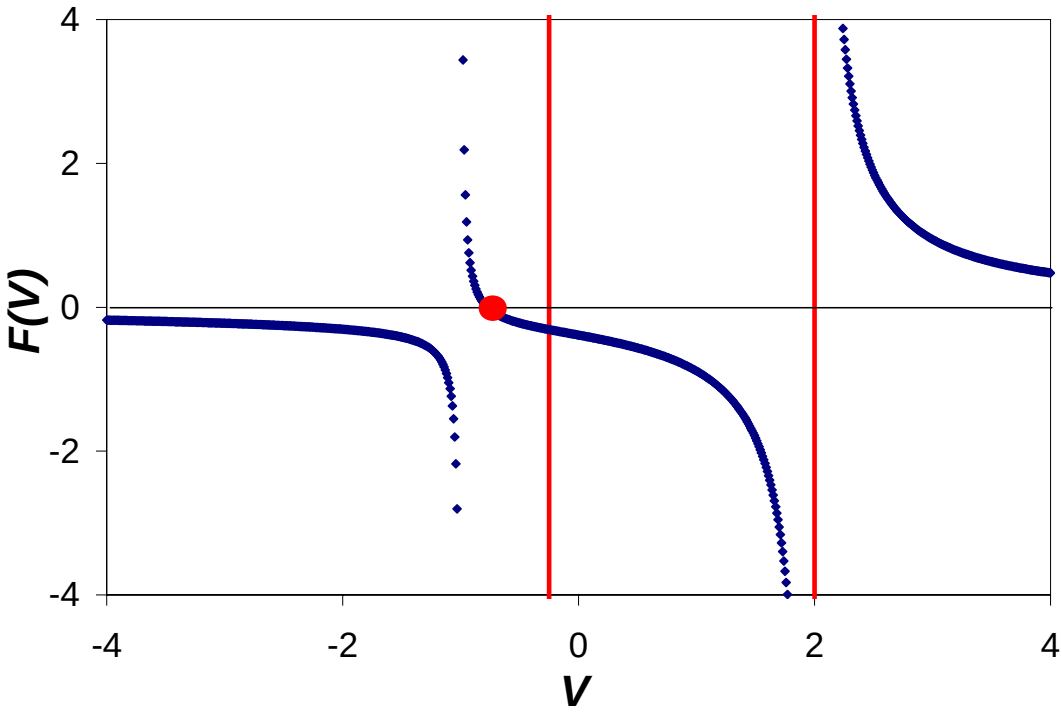

Fig. 4.5 Rachford-Rice function (1952) for point B in Fig. (4.1). The root shown is for the tie line at the base of the ternary diagram, but it does not lie within the Whitson-Michelsen (1989) window. Thus, convergence is not guaranteed.

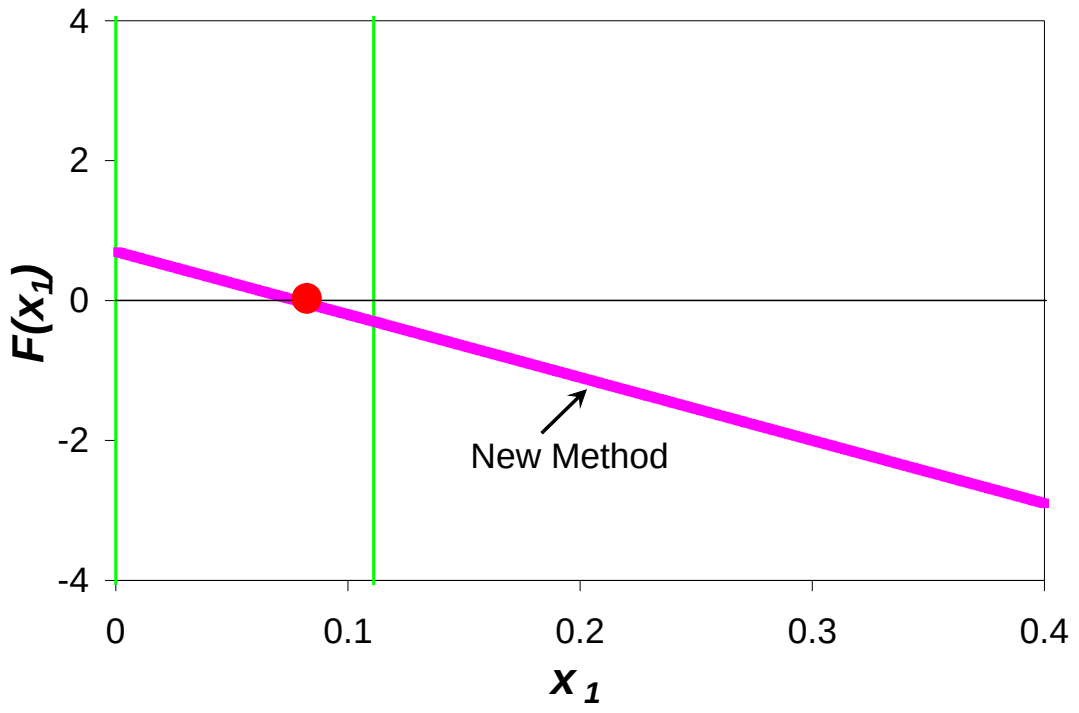

Fig. 4.6 Objective function for point B based on our new method. The function by Wang and Orr (1997, 1998) cannot be plotted because z_1 is 0.0. Our function, however, gives the correct root for the tie line through point A. The window of Eq. (4.13) is also shown.

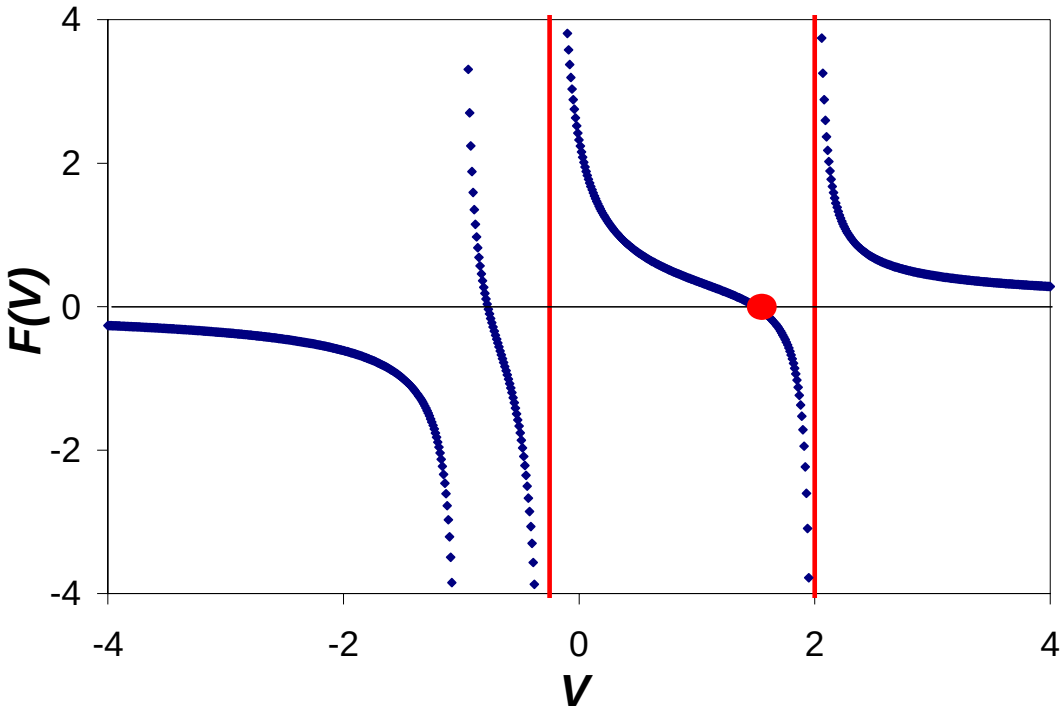

Fig. 4.7 Rachford-Rice (1952) function for point C in Fig. (4.1). The root shown lies within the Whitson-Michelsen window (1989). The solution is greater than 1.0 because it is outside the two phase region where only vapor exists.

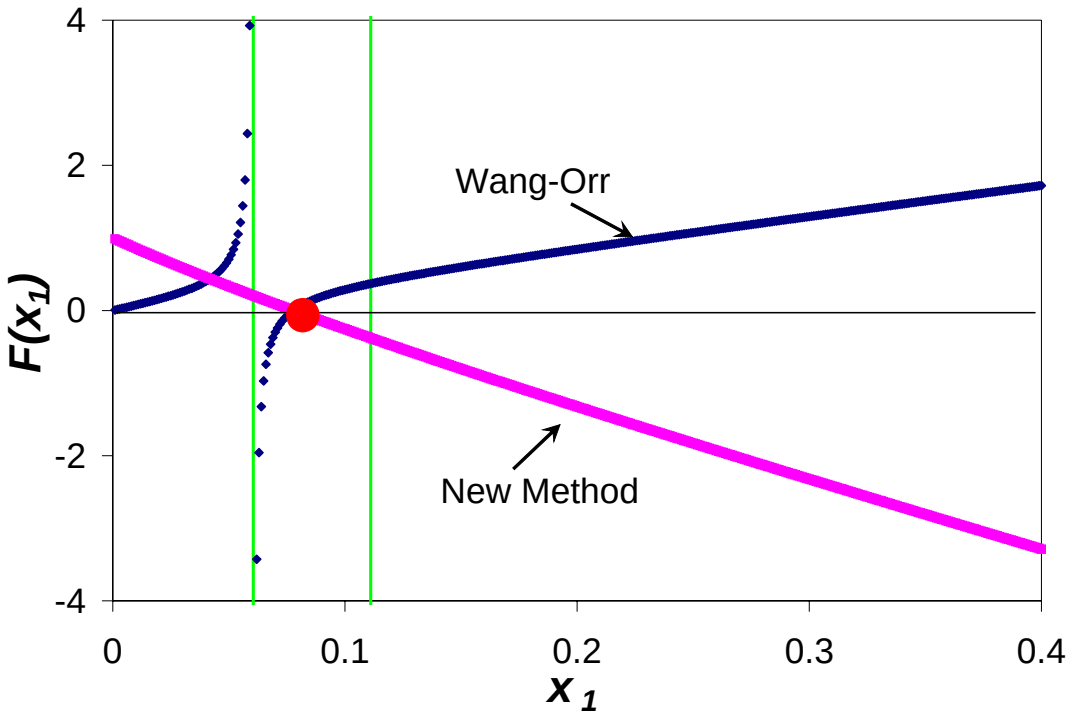

Fig. 4.8 Objective functions for point C based on our new method and that given by Wang and Orr (1997, 1998). The correct root lies within the window given by Eq. (4.13).

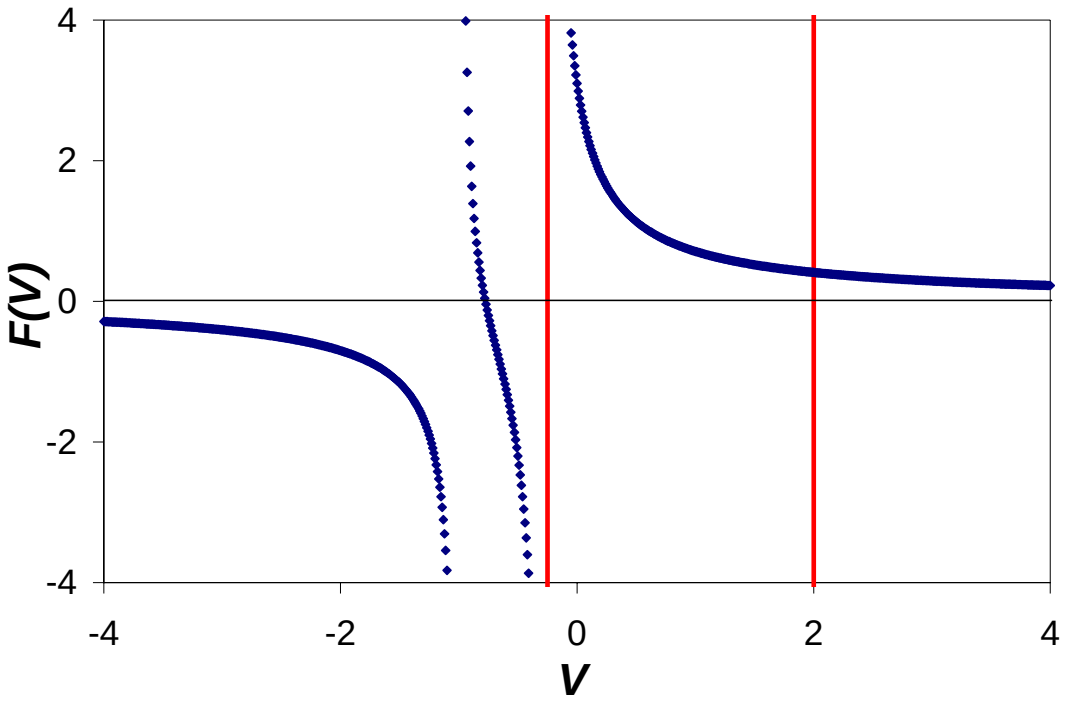

Fig. 4.9 Rachford-Rice (1952) function for point D in Fig. (4.1). There is no root within the Whitson-Michelsen (1989) window. Outside the window, there is a root, but it is nonphysical, i.e. one equilibrium phase composition is negative.

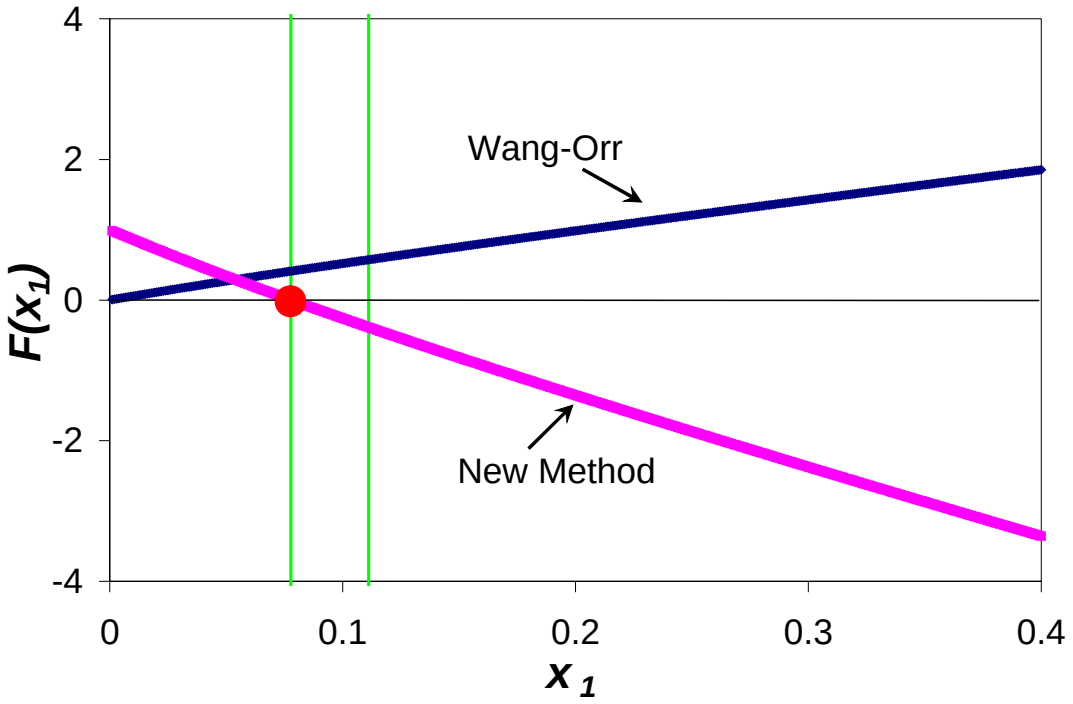

Fig. 4.10 Objective functions for point D based on our new method and that given by Wang and Orr (1997, 1998). The correct root lies just within the window given by Eq. (4.13), while only the trivial root exists for Wang and Orr (1997, 1998).

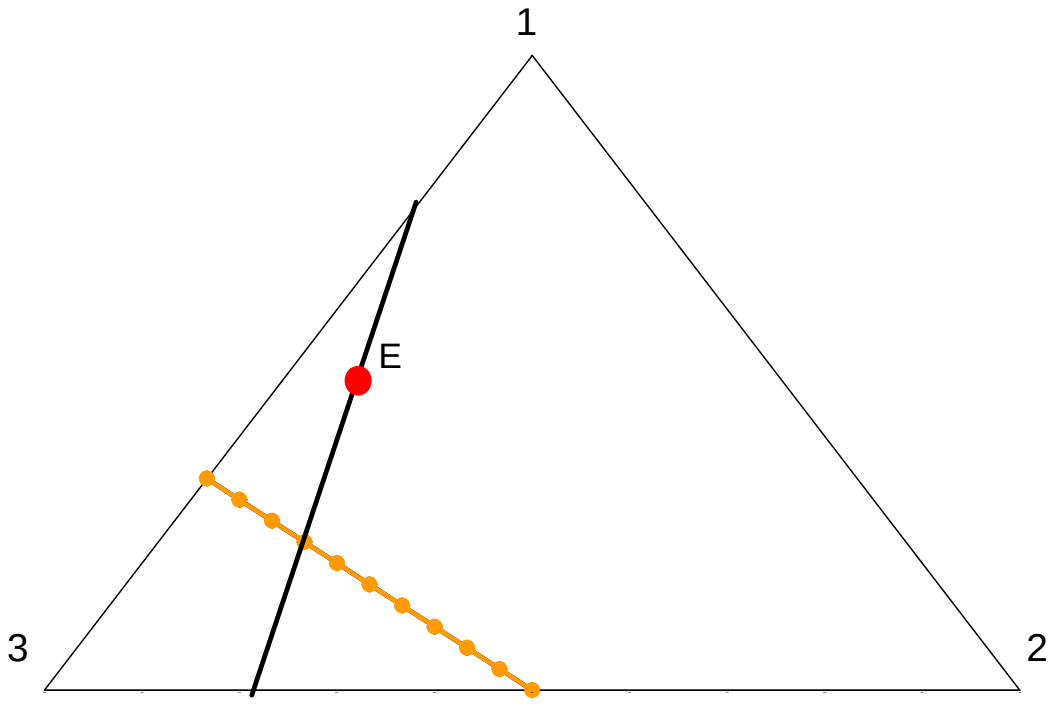

Fig. 4.11 Ternary phase behavior with $K_1 = 1.0+2\varepsilon$, $K_2 = 1.0+\varepsilon$, *and* $K_3 = 1-\varepsilon$ and $\varepsilon=10^{-9}$. The two phase region shown is very small and appears as a line in this diagram. The solid line is the tie-line extension through E.

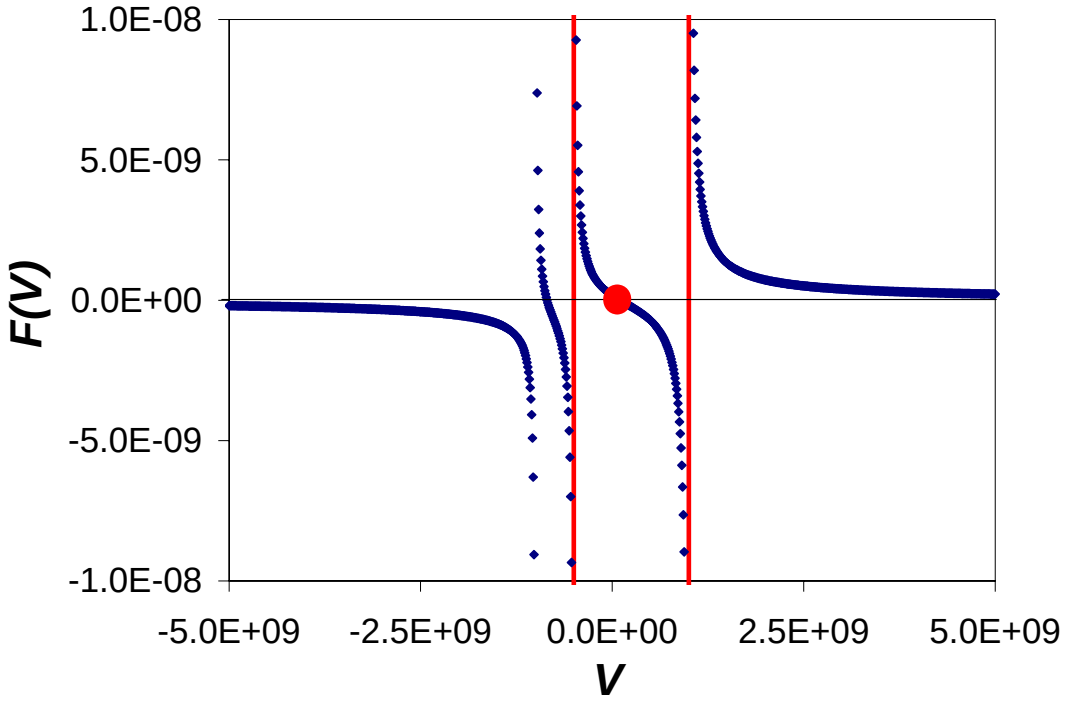

Fig. 4.12 Rachford-Rice (1952) function for point E in Fig. (4.11). The correct root lies within the Whitson-Michelsen (1989) window.

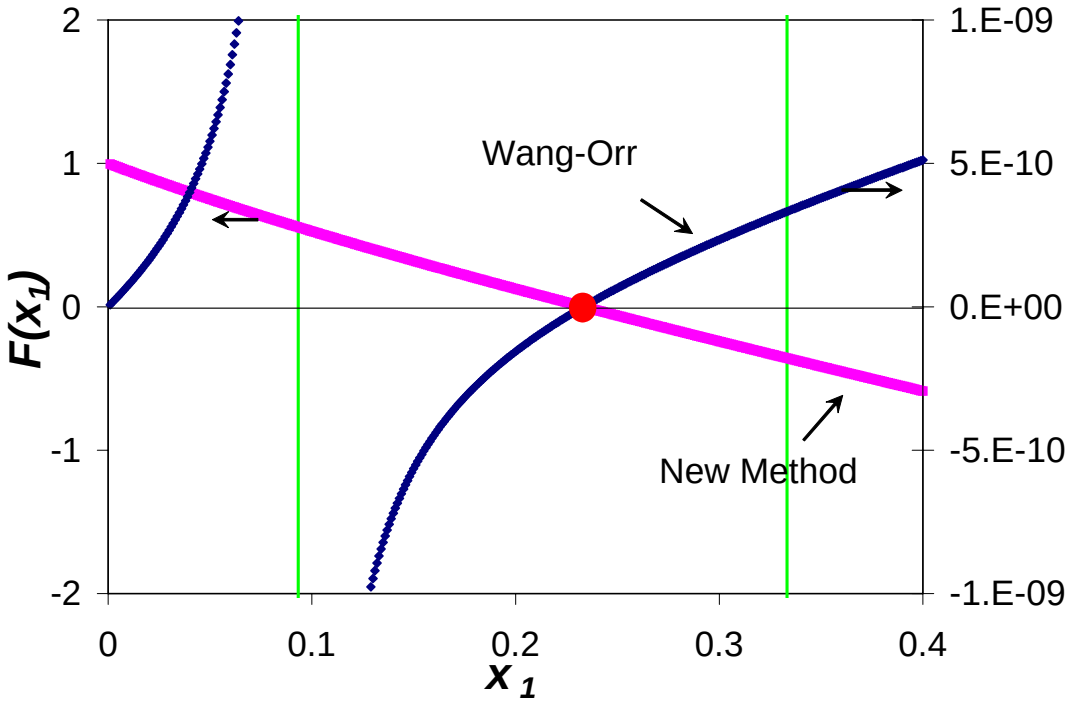

Fig. 4.13 Objective functions for point E based on our new method and that given by Wang and Orr (1997, 1998). The correct root lies within the window given by Eq. (4.13). Wang and Orr's method (1997, 1998) could mistakenly converge to the trivial root.

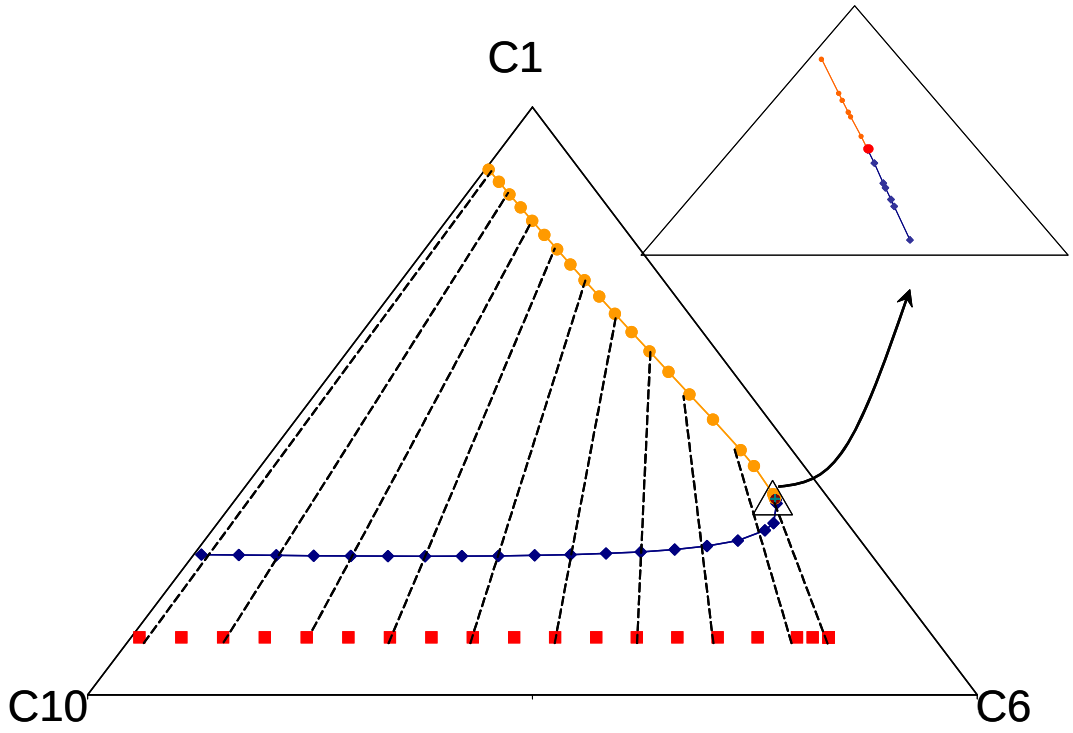

Fig. 4.14 Ternary diagram at 1015 psia and 440 ^{o}F for C_1-C_6-C_{10} system. Flash calculations with Peng-Robinson EOS (1977, 1978) converge to overall compositions within double precision values of the critical point (see triangular region).

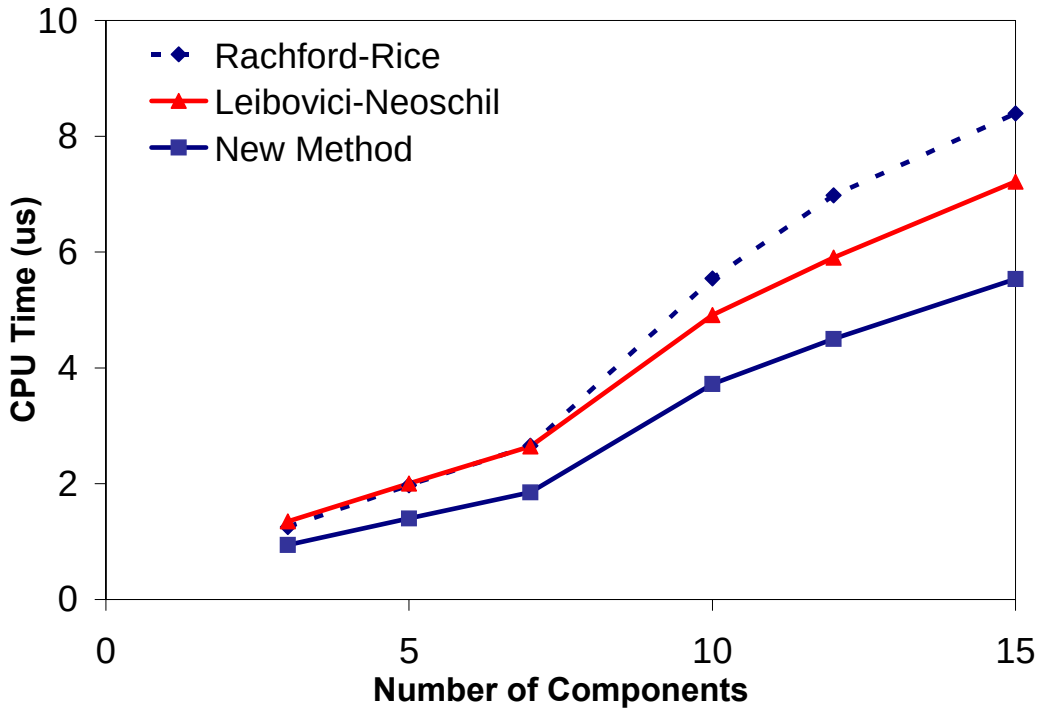

Fig. 4.15 Comparison of the average CPU time for one flash calculation as a function of the number of components in the fluid. The new method is significantly faster than both Rachford-Rice (1952; Whitson and Michelsen, 1989) and Leibovici-Neoschil (1992).

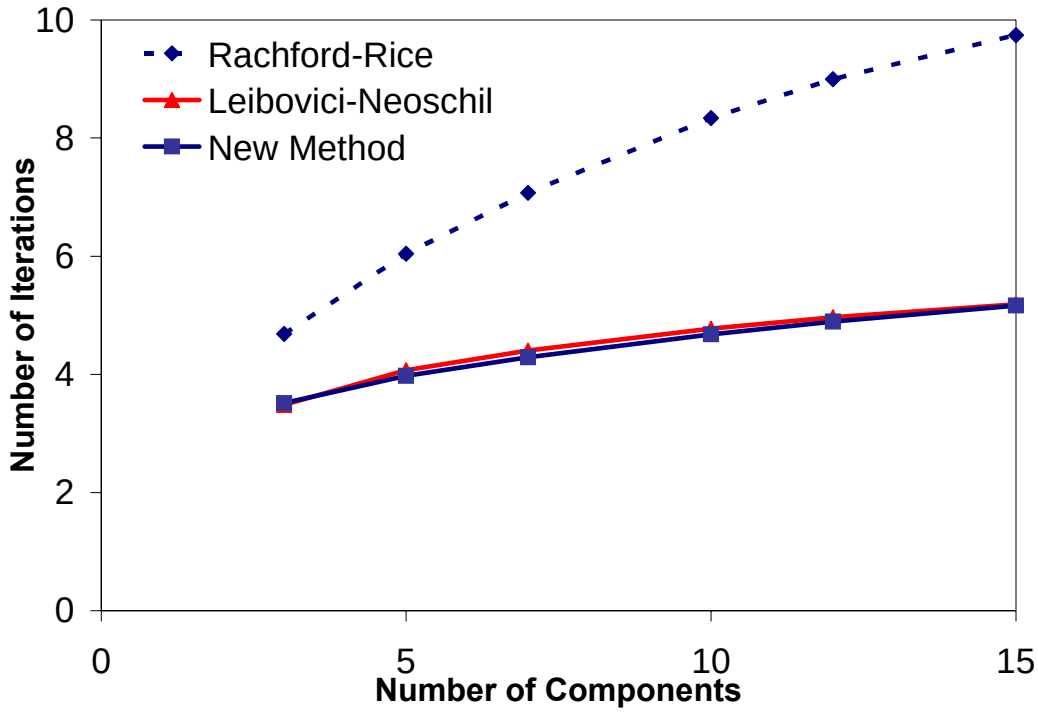

Fig. 4.16 Comparison of the average number of iterations required for convergence for each method as a function of the number of components. Leibovici-Neoschil (1992) and the new method give about the same number of iterations.

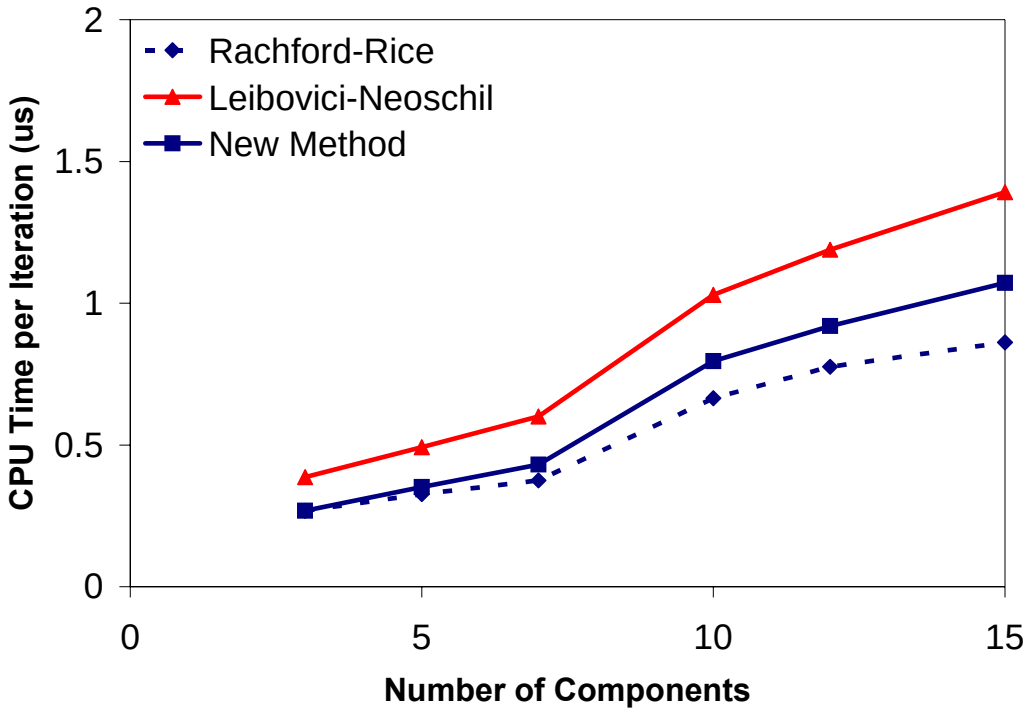

Fig. 4.17 Comparison of the average CPU time per iteration for each method as a function of the number of components. The new method is much faster than Leibovici-Neoschil (1992), but slower than Rachford-Rice (1952; Whitson and Michelsen, 1989).

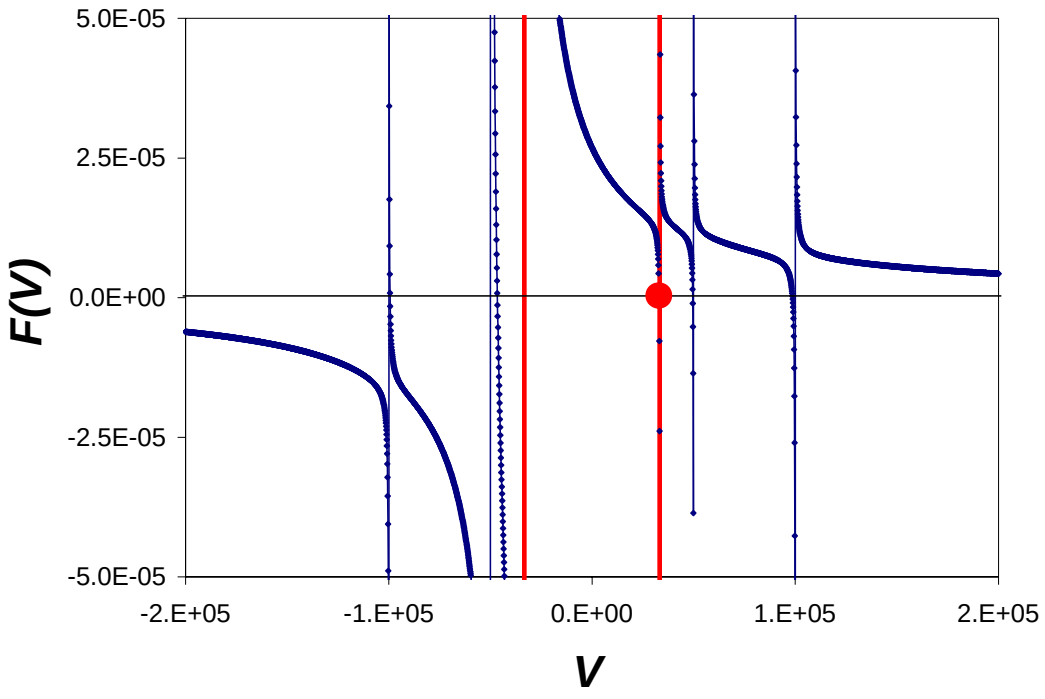

Fig. 4.18 Rachford-Rice (1952) function for the *K*-values and overall composition given in Table (4.1). The function is highly nonlinear and the root lies just within the Whitson-Michelsen (1989) window (red vertical lines) near the pole.

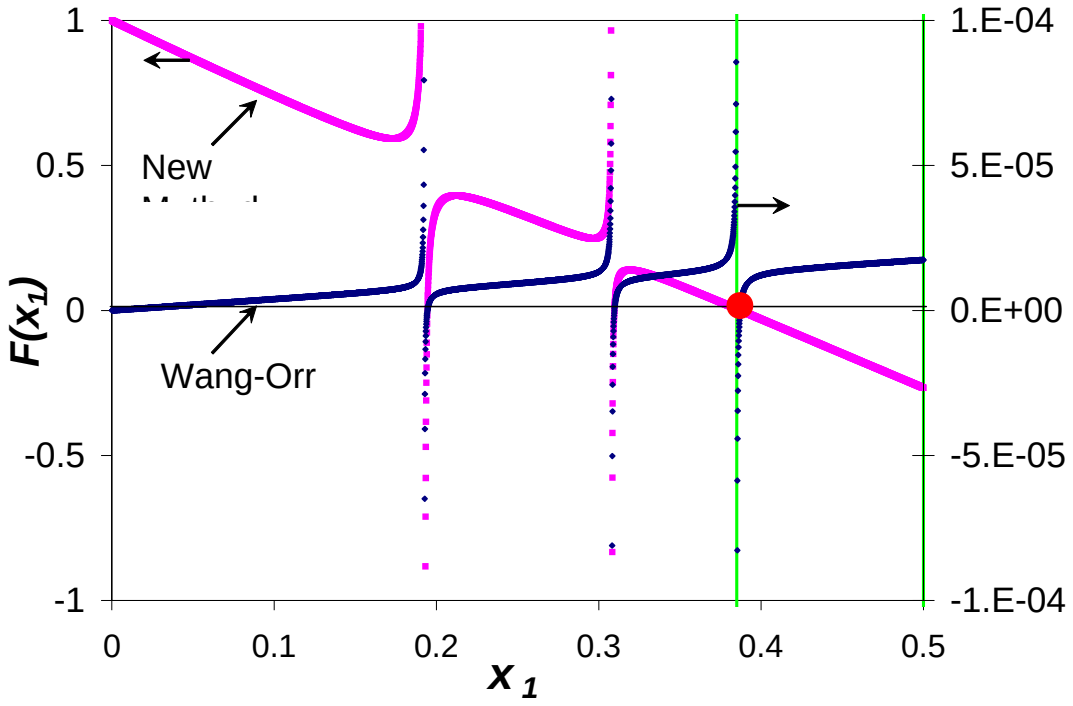

Fig. 4.19 Objective functions for the fluid given by Table (4.1) based on our new method and that given by Wang and Orr (1997, 1998). The correct root lies just within the window given by Eq. (4.13). Wang and Orr's method (1997, 1998), however, could converge to the trivial root.

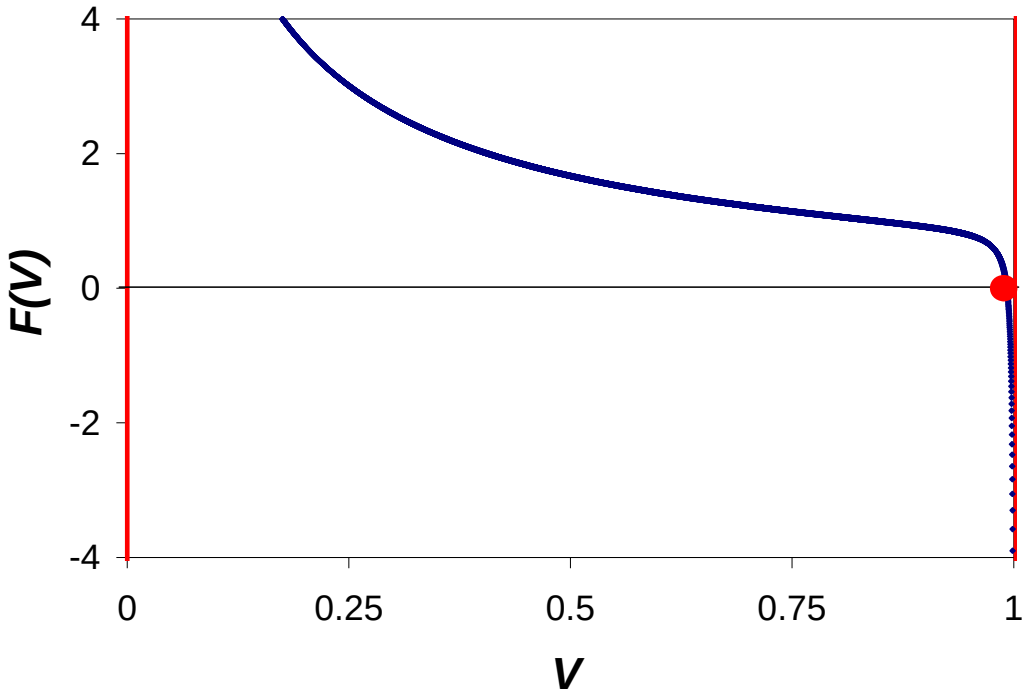

Fig.4.20 Rachford-Rice (1952) function for fluid given by Table (4.2). Convergence for V requires 18 iterations from an initial guess of 0.5. Convergence is difficult because the function is nonlinear and the root is near the right window limit.

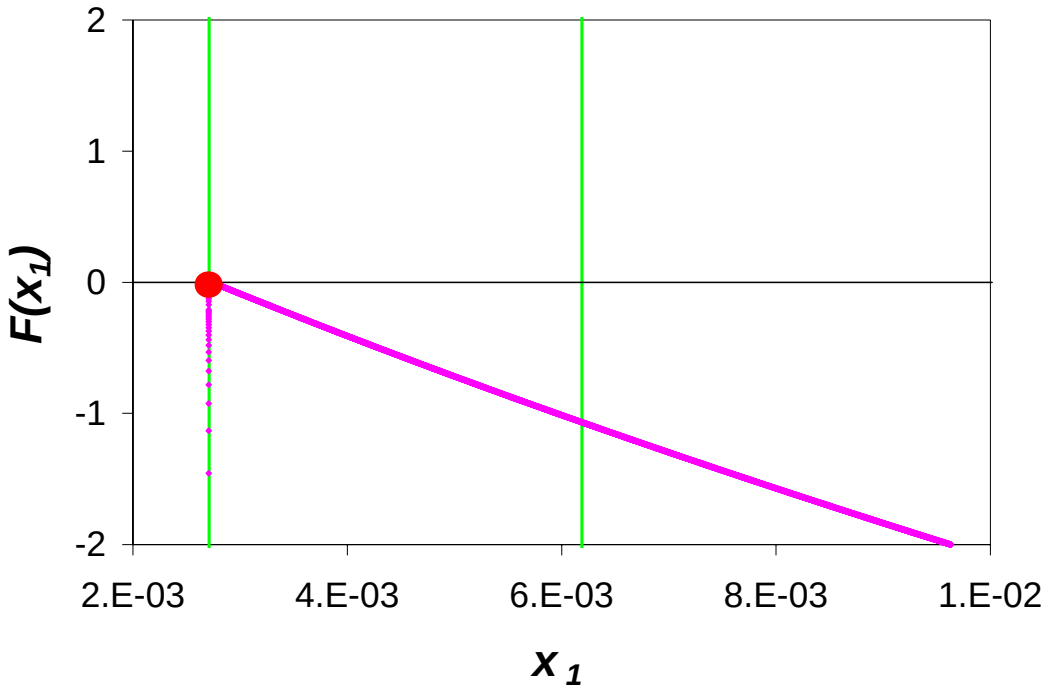

Fig. 4.21 The objective function for the new method based on the fluid in Table (4.2). Convergence is achieved in 6 iterations even though the root is near a pole. The pole is just outside the window given by Eq. (4.13).

Chapter 5: Phase Behavior for Limited Compositional Simulators

Another approach to speed up compositional simulation is to implement non-iterative flash calculations. Such an approach designed to be nearly as fast as black-oil models while achieving improved accuracy in modeling miscible floods. As a result, more grid blocks could be used than in standard compositional models at the expense of modeling many components. This approach also has potential use in modeling chemical floods.

In this chapter, a new phase behavior model for ternary systems is developed, and then applied to several gas and surfactant flooding examples to illustrate its accuracy and efficiency. Equation-of-state calculations are used only to generate the required parameters for the limited compositional model. This approach is implemented in UTCOMP and the results are compared to standard compositional simulation.

5.1 SIMPLIFIED PHASE BEHAVIOR MODEL

In this section, a simplified phase behavior model is presented using transformation factors. First, we demonstrate the use of transformation factors for a single composition. This transformation is then applied to tie lines in a ternary system, such that all tie lines become parallel on ternary diagrams. Last, the non-iterative flash calculation procedure is outlined using several simplified functions that describe the proposed transformation factors.

5.1.1 Transforming a Composition

For a given composition z_i in a ternary system, the following transformation using a constant α can be made (Hand, 1930). First, we multiply z_i by a constant factor, which we name the transformation factor α. Thus,

$$Z_1 = \alpha z_1,\ Z_2 = z_2,\ Z_3 = z_3 \quad .$$

We then normalize the resulting composition so that it sums to 1.0. That is, the transformed composition Z^* becomes:

$$\begin{aligned} Z_1^* &= \frac{\alpha z_1}{\alpha z_1 + z_2 + z_3} = \frac{\alpha z_1}{(\alpha - 1) z_1 + 1} \\ Z_2^* &= \frac{z_2}{(\alpha - 1) z_1 + 1} \\ Z_3^* &= \frac{z_3}{(\alpha - 1) z_1 + 1} \end{aligned} \quad . \tag{5.1}$$

There is one-to-one correspondent between Z^* and z for a given transformation factor α. Thus, the inverse is unique and the corresponding actual compositions are calculated from the transformed composition by:

$$\begin{aligned} z_1 &= \frac{Z_1^*}{\alpha - (\alpha - 1) Z_1^*} \\ z_2 &= Z_2^* \left[(\alpha - 1) z_1 + 1 \right] \\ z_3 &= Z_3^* \left[(\alpha - 1) z_1 + 1 \right] \end{aligned} \quad . \tag{5.2}$$

The physical meaning of the transformation space is to stretch or shorten one of the apex's of the ternary diagram.

5.1.2 Transforming a Tie Line

The above transformation for an overall composition yields no simplification in phase behavior. However, the same idea is applicable to a tie line. Given a tie line with equilibrium compositions of x_i and y_i in a ternary system, the same transformation factor is used for all the compositions along that tie line. The value of the transformation factor is determined so that the tie line is parallel to one of the axis of the ternary diagram, in this case the 1-3 axes. The objective of this transformation is to simplify the phase behavior in such a way that flash calculations of the equilibrium compositions would require no iteration. As shown before, the idea came from Hand (1930), but he assumed that all tie lines were parallel in real compositional space so that only one value of α is needed. In this research, however, the transformation factors are dependent on compositions (each tie line has a different value of α) so that real phase behavior can be modeled.

One practical way to achieve non-iterative flash calculations is to make tie lines parallel in transformed space by applying different transformation factor to each tie line. For a ternary system, the transformed intermediate composition should be the same along the same tie line, that is,

$$X_2^* = \frac{x_2}{(\alpha - 1)x_1 + 1} = Y_2^* = \frac{y_2}{(\alpha - 1)y_1 + 1} = Z_2^* \quad . \tag{5.3}$$

Thus, we can solve for α as:

$$\alpha = 1 + \frac{1 - K_2}{\left(K_2 - K_1\right) x_1} \quad . \tag{5.4}$$

The transformation factor is related to the tie-line slope through *K*-values and binodal curves through x_1. The combination of a proper value for the transformation factors and good models for the binodal curves in transformed space can yield equilibrium compositions without iterations. This process is described in the following section.

5.1.3 Flash Calculations Using Transformation Factors

In this section, the approach for non-iterative flash calculations is outlined. We assume that the values of the transformation factors are evaluated so that all tie lines are parallel to the 1-3 ternary base. For an arbitrary overall composition z_i with a transformation factor α, the intermediate composition in the transformed space can be calculated using:

$$X_2^* = Y_2^* = Z_2^* = \frac{z_2}{\left(\alpha - 1\right) z_1 + 1} \quad . \tag{5.5}$$

To do flash calculations, the binodal curves in the transformed space are modeled using any arbitrary functions $X_1^* = X_1^*\left(X_2^*\right)$ and $Y_1^* = Y_1^*\left(Y_2^*\right)$. There is no restrictions on the type of functions used, the functions could be a polynomial of any degree. Once the functions are specified we can solve for X_1^* and Y_1^*. From Eqs. (5.2), equilibrium compositions can then be transformed back to the actual compositional space using:

$$
\begin{aligned}
x_1 &= \frac{X_1^*}{\alpha-(\alpha-1)X_1^*} \\
x_2 &= \left[(\alpha-1)x_1+1\right]X_2^* \\
x_3 &= 1-x_1-x_2
\end{aligned}
\tag{5.6}
$$

and

$$
\begin{aligned}
y_1 &= \frac{Y_1^*}{\alpha-(\alpha-1)Y_1^*} \\
y_2 &= \left[(\alpha-1)y_1+1\right]Y_2^* \quad . \\
y_3 &= 1-y_1-y_2
\end{aligned}
\tag{5.7}
$$

The equilibrium compositions are exact if the transformation factors are calculated accurately and the binodal curves are modeled exactly. In practice, the binodal curves and the transformation factors are not modeled exactly, leading to a small error in the calculated equilibrium compositions. Examining the definition of the transformation factor in Eq. (5.3), we have:

$$
X_2^* = \frac{x_2}{(\alpha-1)x_1+1} = \frac{x_2(x_1)}{(\alpha-1)x_1+1} \tag{5.8}
$$

which shows a relationship between α and X_2^*. In addition, the critical point in transformed space is always at the maximum of the transformed intermediate composition on the α vs. X_2^* plot. Experimental data or cubic EOS are first used to calculate the transformation factor of a tie line using Eq. (5.4). The transformed intermediate compositions are then calculated using Eq. (5.8). We describe that relationship using simple functions as follows.

5.1.3.1 Linear Model for Transformation Factors

The simplest model that can be used to model the α and X_2^* relationship is the linear model,

$$X_2^* = A + B(\alpha - 1) \quad , \tag{5.9}$$

where A and B are determined by regression of the data to the linear function of Eq. (5.9). From Eq. (5.5), where $X_2^* = Z_2^*$, the following must be met:

$$\frac{z_2}{(\alpha - 1) z_1 + 1} = A + B(\alpha - 1) \quad . \tag{5.10}$$

Re-arrangement of Eq. (5.10) gives a quadratic function:

$$(\alpha - 1)^2 B z_1 + (\alpha - 1)[A z_1 + B] + (A - z_2) = 0 \quad , \tag{5.11}$$

which yields the following two possible solutions:

$$\alpha = 1 + \frac{-(A z_1 + B) \pm \sqrt{(A z_1 + B)^2 - 4 B z_1 (A - z_2)}}{2 B z_1} \quad . \tag{5.12}$$

There are two solutions of Eq. (5.12) either real or imaginary. Only the real solutions are considered. As mentioned earlier, the critical point in transformed space is always at the maximum of the transformed intermediate composition on the α vs. X_2^* plot. Thus, the transformation factors must be within a pre-determined range from that of the critical tie line to the base tie line (the tie line that lies on the 1-3 axis). The

transformation factor for the base tie line is determined in the limit as the base tie line is approached. The transformation factor for the critical tie line can be evaluated when the slopes of the binodal curves at the critical point are specified. The range in which the correct solution of α must lie is temperature and pressure dependent. The calculated real solutions for α using Eq. (5.12) are then compared with the pre-determined range. There are several possibilities:

1. Only one real solution is within that range. The overall composition is along a tie line or its extension. If this is the case, the equilibrium compositions in the transformed space can be non-iteratively calculated using the procedure outlined earlier;
2. Both real solutions are within that range. This case indicates that the overall composition is on two tie lines, and thus in the single phase region. This is because two tie lines cannot intersect in the two-phase region. Both tie lines are found using the different α's;
3. None of the solutions are within the appropriate range, or there are no real solutions to Eq. (5.11). This means that the overall composition is beyond the critical point in the single-phase region and outside the region of tie-line extensions.

5.1.3.2 Quadratic Model

Quadratic models can be used to improve the accuracy of the fit to the α and X_2^* relationship. That is:

$$X_2^* = A + B(\alpha - 1) + C(\alpha - 1)^2 \quad , \tag{5.13}$$

where A, B and C are determined using the same procedure in Section (5.1.3.1). A cubic equation results in terms of α :

$$CZ_1(\alpha-1)^3+(C+BZ_1)(\alpha-1)^2+(B+AZ_1)(\alpha-1)+(A-Z_2)=0 \quad . \qquad (5.14)$$

A cubic solver is needed for the solution of Eq. (5.14). There are three solutions of α possible, and only real roots are considered. The approach to determine the correct α used here is slightly different from that in Section (5.1.3.1). There are several possibilities:

1. Only one real solution is within the range of maximum and minimum of α. The overall composition is along a tie line or its extension. As a result, the equilibrium compositions in the transformed space are non-iteratively calculated using the procedure outlined earlier;
2. There are two or three real roots. This case indicates that the overall composition is on the extensions of two tie lines, and thus in the single phase region. This is because two tie lines cannot intersect in the two-phase region. Both tie lines are found using the different α 's;
3. None of the solutions are within the appropriate range. This means that the overall composition is beyond the critical point in the single-phase region and outside the region of tie-line extensions.

5.1.3.3 Reverse Cubic Function

A four-parameter function can also be used to model the X_2^* and α relationship if more accuracy is desired:

$$X_2^* = 1/\left[A + B(\alpha - 1) + C(\alpha - 1)^2 + D(\alpha - 1)^3 \right] \quad . \tag{5.15}$$

Equation (5.15) results in the following cubic equation,

$$DZ_2(\alpha - 1)^3 + CZ_2(\alpha - 1)^2 + (BZ_2 - Z_1)(\alpha - 1) + (AZ_2 - 1) = 0 \quad . \tag{5.16}$$

A cubic solver is again required to determine the solution to Eq. (5.16). A similar approach to determine the correct α is used here as in Section (5.1.3.2)

5.1.4 Reference Component in Transformation Method

In the above derivation, we apply transformation factors to the most volatile component. However, we can also apply the same method using the least volatile component. We assume that in both cases, the X_2^* and α relationship can be accurately modeled. Even though the transformation factors for a particular tie line has a different value using either the most or the least volatile components as reference, the calculated equilibrium compositions are exactly the same regardless of the reference component used.

5.1.5 Calculation Procedure

The calculation procedure using the transformation method is as the following:

1. Calculate equilibrium compositions using EOS or obtain from experimental data. Calculate transformation factor using Eq.(5.4), and the transformed intermediate composition by Eq. (5.3) for each tie line;

2. Regress transformation factors and transformed intermediate compositions using one of the functions in Section (5.1.3) or some other simple equations. Extrapolate the transformation factor at the base tie-line and evaluate that at the critical tie-line;
3. Evaluate the coefficients of the equilibrium compositions for the binodal curves in the transformed space as functions of pressure and temperature if needed. Any accurate function is workable;
4. Solve the polynomial equations in step 2, and obtain the correct one based on the analysis in Section (5.1.3) when multiple solutions exist;
5. Calculate the equilibrium compositions on the binodal curves in the transformed space using the functions in step 3;
6. Translate the equilibrium compositions back into the conventional space using Eqs.(5.6) and (5.7).

5.2 STABILITY ANALYSIS IN TRANSFORMATION MODEL

In EOS flash calculations, we use stability analysis to find whether a phase-split calculation is needed or not. Stability analysis calculations are iterative as well. In this new method, we do not need to perform a stability analysis by finding the stationary points of the TPD function. We can determine whether the overall composition is stable or not using the transformation method. The overall composition is in the two-phase region, only when (1) one real solution for the transformation factor in that range; and (2) the overall composition lies between the equilibrium compositions in transformed space. In any other cases, the overall composition is stable and in the single-phase region. Thus, the transformation method effectively eliminates the stability analysis calculations.

5.3 EXAMPLE FLASH CALCULATIONS

We illustrate the new method first for a ternary synthetic oil. A surfactant flooding example is then presented using the transformation method. Phase behavior calculations at different pressures are carried out. We also demonstrate the use of the method when very little experimental data is available, i.e., only two tie lines are available. The transformation method is also applied to a partial miscible case where there is no critical point. The transformation method is last implemented in UTCOMP to illustrate the accuracy and speed for a ternary case with varying pressures.

5.3.1 A C_2-nC_4-nC_{10} Ternary Synthetic Oil

Consider first a synthetic oil of C_2-nC_4-nC_{10} at 498.03 K and 6.125 MPa. Figure (5.1) gives the ternary diagram using the Peng-Robinson EOS (1978) for this oil. Table (5.1) lists the critical properties for the Peng-Robinson EOS (1978). All the BIPs are zero. The tie lines and binodal curves are shown in Fig. (5.2) after the transformation method is applied to the C_2 component. The transformation causes all tie lines to be parallel to the base tie line (where nC_4 composition is zero) as shown in Fig. (5.2). The critical point occurs at the maximum value of nC_4 in the transformed space. The X_2^* and α relationship is illustrated in Fig. (5.3), and then regressed using a quadratic function. Table (5.2) compares some calculated equilibrium compositions by Peng-Robinson EOS (1978) with those by the new transformation method. For a given overall composition, the X_2^* value as a function of the transformation factor is shown in Fig. (5.4) where the solid line is from the fitted quadratic curve and the dash line uses Eq. (5.2). The transformation factor at that overall composition can thus be calculated by finding the root when we equate both functions. Figure (5.5) shows that the equilibrium compositions by the new method are very accurate. The maximum relative error in

calculated equilibrium compositions of this simple method compared to Peng-Robinson EOS (1978) is less than 4%, with an average error less than 0.5%.

The transformation method could also be expressed based on the nC_{10} component. The transformed binodal curves are shown in Fig. (5.6), and the X_2^* and α relationship in Fig. (5.7). The flash calculations are still reasonably accurate as is shown in Fig. (5.8). The average relative error of the transformation method is less than 1% with the maximum less than 5%. The accuracy is increased slightly when C_2 is used because in this example the dew point curve is less accurately modeled than the bubble point curve in the transformed space.

The new method is remarkably faster than conventional flash calculations with three components. The equilibrium calculation for one overall composition requires approximately 50 micro-second in the conventional EOS method, but less that 0.5 micro-second in the transformation method. This is approximately 100 times improvement in speed using the new method. Although not shown here, it is likely that the speedup will increase significantly if more components were modeled. Also, because no iterations are used in the transformation method, convergence is always achieved in flash calculations. For the cases studied, the speed and robustness is substantially enhanced without significant sacrifice of accuracy.

5.3.2 Surfactant Flooding

This model can also be applied to surfactant flooding to replace the iterative Hand's model (1930). For example, at a particular salinity the equilibrium compositions for the excess and microemulsion phases is shown in Fig. (5.9) The calculated α and transformed compositions are given in Fig. (5.10). For this case, the X_2^* and α relationship can be accurately expressed using a reverse quadratic function:

$$C^*_{surf} = 1/\left[0.0611(\alpha-1)^2 + 7.7161(\alpha-1) - 32.511\right] \quad . \tag{5.17}$$

This problem can be accurately solved using the non-iterative method. Compared with the original experimental data, this approach gives very accurate results without iteration as is illustrated in Fig. (5.11).

We also compare our new transformation method to Hand's plot. Hand's plot for this case is shown in Fig. (5.12). This figure clearly indicates that Hand's approximation (1930) is reasonable (this is not always the case). However, in Hand's model, the bubble-point curve and dew-point curve must lie on the same line while in this example they fall on slightly different lines. Calculations using Hand's method are complex and take significant time, mainly due to required iterations. Figure (5.13) compares the computation result for the phase compositions using Hand's method (1930) and that from the original experimental data. Comparison of Figs. (5.13) and (5.11) shows that Hand's method (1930) is less accurate than the transformation method. It is also approximately 10 times slower than the proposed transformation method.

5.3.3 Phase Behavior at Multiple Pressures

In reservoir simulations, the reservoir pressure can vary spatially and with time. Temperature is assumed constant. Thus the constants in the transformation method must be pressure dependent to account for the change in phase behavior with pressures. In this example, a ternary system composed of C_1, nC_4 and nC_{10} are examined at different pressures. The binodal curves are shown in Fig. (5.14) at pressures of 2000, 2500, 3000, 3500 and 4000 psia. The temperature is constant at 150^{o}F. The tie lines are not plotted

in this figure; however, they are used to calculate the corresponding transformation factors.

At each pressure, the transformation is applied, and the required coefficients as functions of pressure are calculated using regression. The transformation factors and the intermediate composition are illustrated in Fig. (5.15). The figure clearly demonstrates that the critical tie line always has the largest transformed intermediate composition. The base tie line always has zero nC_4 composition. In addition, the transformed nC_4 composition at the critical tie line decreases as pressure increases. That satisfies the same feature in the phase envelope curves in Fig. (5.14), where at the critical points the intermediate composition decreases with an increasing pressure. All the coefficients are regressed using the following quadratic equations for this ternary system at 150°F:

$$\begin{aligned} nC_4^* &= A(\alpha-1)^2 + B(\alpha-1) + C \\ A &= -2.686\times10^{-5}\ P^2 + 4.337\times10^{-2}\ P - 58.66 \\ B &= -1.116\times10^{-5}\ P^2 + 1.467\times10^{-2}\ P - 24.24 \\ C &= -1.607\times10^{-5}\ P^2 + 3.020\times10^{-2}\ P - 34.97 \end{aligned} \quad . \qquad (5.18)$$

It is also important to locate the highest and lowest values of the transformation factor to determine how many phases are present. The end points of the transformation factors vary with pressure and have these forms (see Fig. (5.16)):

$$\begin{aligned} (\alpha-1)_{\min} &= -1.461\times10^{-8}\ P^2 + 1.412\times10^{-4}\ P - 1.206 \\ (\alpha-1)_{\max} &= -2.422\times10^{-9}\ P^2 + 1.181\times10^{-5}\ P - 0.8495 \end{aligned} \quad . \qquad (5.19)$$

All information needed to calculate the transformation factor and the transformed intermediate composition is now known. In the next step, the binodal curves are

transformed to the new compositional space. The transformed bubble-point curve is plotted in Fig. (5.17) (nC_{10}^* as a function of nC_4^*), and dew-point curve in Fig. (5.18) (C_1^* as a function of nC_4^*). One can interpolate the binodal curves accurately or use any other appropriate functions to model them. In this example, a quadratic function is used to model the binodal curves.

The calculated equilibrium compositions using the transformation procedure are compared with the calculations using Peng-Robinson EOS (1977, 1978) at a pressure of 3000 psia. The only difference from the example of Section (5.2.1) is that all required coefficients are now pressure-dependent functions instead of constant values. Figure (5.19) shows that the transformation method accurately captures both the binodal curves and the tie lines at this pressure. More important, the new method requires less than 0.5 micro-second in computational time, while the Peng-Robinson EOS (1977, 1978) requires 150 times more time.

5.3.4 Flash Calculations with Limited Data

The transformation method can be applied reasonably well as long as at least two tie lines are available. In this research, we use the method when only the base and critical tie lines are available. Linear interpolation of α is then used since there is no information on tie lines in between.

In this example, we use the same ternary system as in Fig. (5.14) with this simplification. The transformation factor relationship is re-plotted to show their linear dependence in the transformation space in Fig. (5.20). The dependence of the coefficients on the pressure is still non-linear and can be interpolated accurately using the following quadratic equations:

$$
\begin{aligned}
&nC_4^* = A(\alpha - 1) + B \\
&A = -7.207\times10^{-7}\ P^2\ -\ 7.493\times10^{-4}\ P\ -\ 3.420 \quad . \\
&B = -5.806\times10^{-7}\ P^2\ -\ 8.484\times10^{-4}\ P\ -\ 2.703
\end{aligned}
\tag{5.20}
$$

The minimum and maximum of the transformation factors are unchanged as in Eqs. (5.20). In addition, the binodal curves are straight lines in the transformed space rather in the actual compositional space. Figure (5.21) shows for the bubble point curve and Fig. (5.22) for the dew point curve from the base tie line to the critical tie line. The simplified transformation method is then implemented to calculate the equilibrium compositions at 3000 psia. The result is compared with the original equilibrium compositions by Peng-Robinson (1977, 1978) EOS in Fig. (5.23). Figure (5.23) demonstrates the accuracy of this simplified model that is based on only these two tie lines. Although speedup is slightly greater using this approach, the benefit is minimal.

5.3.5 Implementation with Real Fluid Experimental Data

This section compares the results of the transformation method to experimental results. Table (5.4) shows an experimental data of equilibrium compositions of nC_4-CO_2-nC_{10} system (Metcalfe and Yarborough, 1978). In this example, we use the method in Section (5.3.4) that only two tie lines are used at each pressure of 1000 and 1400 psia. The four tie lines used to initialize the calculation is highlighted in grey in Table (5.4). In addition, we assume that the simplified linear correlation exists for X_2^* and α relationship for the four tie lines. The values of transformation factor and intermediate composition are shown in Fig. (5.24). The maximum and minimum of the

transformation factors are assumed linearly dependent on reservoir pressure. The binodal curves (Fig. (5.25)) are straight lines in transformed space.

Figure (5.26) compares the equilibrium compositions by the transformed method with the experimental data at pressures of 1000 and 1400 psia. In Fig. (5.27), the equilibrium compositions at 1500 psia are calculated and compared with the experimental data. The compositions calculated are less accurate than that in Fig. (5.26), but can be improved by using a non-linear equation to estimate the maximum and minimum of α, given that more experimental data are used. Errors also result because the experimental data often have noise compared with EOS calculations. However, it is still reasonably accurate considering that only four tie lines in total are used (two tie lines each at the pressures of 1000 and 1400 psia).

5.3.6 Flash Calculations with Constant K-values

The new method can also be implemented to calculate the equilibrium compositions when *K*-values are constant. Compared with constant *K*-value flash calculations in Chapter 4 which are iterative, the new method is non-iterative. Because *K*-values are constant, only two tie lines are required to exactly model this example.

In this example, the following *K*-values are used: $K_1 = 5.0$, $K_1 = 2.0$ and $K_3 = 0.5$. The phase behavior is illustrated in Fig. (4.1). The X_2^* and α relationship is plotted in Fig. (5.29), and can be exactly expressed as:

$$C_2^* = -0.75/(\alpha - 1) + 0.25 \quad . \tag{5.21}$$

The binodal curves are also exactly described using the following linear functions:

$$x_1^* = \left(1 - C_2^*\right)/3$$
$$y_1^* = \frac{5}{6}\left(1 - C_2^*\right) \quad . \tag{5.22}$$

The binodal curves are straight lines in compositional space when the *K*-values are constant. This is also true in transformed space. The determined binodal curves from the simplified transformation method, compared with that from constant *K*-value flash calculations is illustrated in Fig. (5.29), which shows an exact match. The new method, however, is approximately 10 times faster than the constant *K*-value flash calculations and is robust because no iterations are required.

5.3.7 Simulation Comparison

We also implemented the new transformation method into UTCOMP, an IMPEC reservoir simulator using the same ternary system as in Section (5.3.3). The reservoir is 100 ft by 25 ft by 25 ft, with constant porosity of 16% and homogeneous permeability of 25 mD. The injection and initial fluid compositions are listed in Table (5.5). The reservoir temperature is constant at 150^{o}F and the initial reservoir pressure is 3000 psia. The injection well BHP is fixed at 4000 pisa and the production well pressure at 2000 psia. The 1-D simulations used a constant time step of 0.005 days. Phase densities are still calculated using the EOS while phase viscosities are calculated using the Lohrenz-Bray-Clark correlation (1964). The phase densities and viscosities, however, could be regressed in transformation space.

Figures (5.30) – (5.32) show the nC_{10} component recovery, average reservoir pressure and compositions at the production well as a function of simulation time using

standard flash calculations and the transformation method. The new method is nearly identical to standard compositional simulations.

The pressure profiles at 20 and 40 days (corresponding to approximately 0.15 and 0.33 pore volume injected) are shown in Figs. (5.33) and (5.34). The overall composition profiles at these time steps are also plotted in Figs. (5.35) and (5.36). All figures showed that the new transformation method has similar accuracy as using standard UTCOMP simulations.

We also tested the speed for a varying number of grid blocks using a 1.3 GHz CPU with 1.5G RAM. The CPU time used for flash calculations alone (including stability analysis) is shown in Fig. (5.39) for 10, 20 and 40 grid blocks in the x-direction. The CPU time required for the entire simulation, flash calculations and density calculations is given in Table (5.6). The total CPU time for the simulation using the new transformation method is approximately twice faster than the standard method, mainly because the flash calculation in this example is about 50% of total simulation time. The new transformation method is approximately 10 to 11 times faster than standard UTCOMP in the flash calculations (including stability analysis and density calculation). This is much less than the speedup in the batch calculations, mainly because: (1) densities are calculated from *Z*-factors using EOS; and (2) standard flash calculations in the simulation uses the values from the previous time step. The computation time for the equilibrium compositions using the transformation method is approximately 50 times faster than EOS flash calculations. If phase densities and viscosities are regressed in the transformed space, the simulation time using the transformation method would be less.

5.4 CONCLUSIONS

In this chapter, a new non-iterative transformation method is developed to calculate the equilibrium compositions for ternary systems. The new method is much faster than EOS flash calculations because the transformation method is non-iterative. The new method is robust since there is no iteration and will always converge. This method is also very accurate when compared to an EOS model. Moreover, stability analysis calculations are eliminated because the direct solution determines whether one or two phases are present.

Simulation results confirm the speed and accuracy of this new model. The flash calculation is approximately six to ten times faster than the conventional method. The accuracy of the simulation is nearly perfect and is more realistic than if a black-oil model had been used. This method may be useful for large-scale, fine-grid miscible flooding simulations.

	T_C (^{o}F)	P_C (psia)	ω
C_2	90.05	708.35	0.098
nC_4	305.69	551.10	0.193
nC_{10}	652.01	305.68	0.490

Table 5.1 Input EOS critical properties for the ternary system in Fig. (5.1).

	Bubble Point Curve			Dew Point Curve		
	C_2	nC_4	nC_{10}	C_2	nC_4	nC_{10}
EOS	38.59	4.84	56.57	80.53	5.58	13.90
TM	38.57	4.84	56.58	80.51	5.58	13.92
EOS	36.78	9.69	53.54	74.86	11.14	13.99
TM	36.74	9.68	35.70	74.92	11.15	13.93
EOS	34.96	14.52	50.51	69.22	16.68	14.10
TM	34.96	14.52	50.52	69.33	16.69	13.98
EOS	33.14	19.37	47.50	63.60	22.18	14.22
TM	33.16	19.37	47.48	63.73	22.19	14.08
EOS	31.30	24.21	44.49	58.03	27.61	14.36
TM	31.33	24.21	44.46	58.14	27.63	14.23
EOS	29.46	29.07	41.47	52.52	32.96	14.53
TM	29.47	29.06	41.47	52.59	32.97	14.44
EOS	27.62	33.93	38.45	47.08	38.19	14.73
TM	27.59	33.93	38.48	47.07	38.19	14.73
EOS	25.79	38.82	35.39	41.72	43.28	15.00
TM	25.73	38.81	35.46	41.63	43.24	15.12
EOS	23.98	43.75	32.28	36.46	48.17	15.34
TM	23.93	43.75	32.32	36.27	48.10	15.63
EOS	22.20	48.80	29.00	31.30	52.80	15.90
TM	22.26	48.79	28.95	31.02	52.68	16.31
EOS	20.63	53.94	25.43	26.10	57.00	16.80
TM	20.79	54.04	25.17	25.88	56.90	17.21
EOS	20.03	58.68	21.29	21.50	59.60	18.90
TM	19.83	58.54	21.63	21.87	59.94	18.20

Table 5.2 Comparison of the phase envelope in Fig. (5.1) by Peng-Robinson EOS (1977, 1978) with the new method. With the transformation method, the relatively difference is usually less than 1% of the EOS equilibrium compositions, with the maximum less than 4%. TM indicates "Transformation Method".

	T_C (°F)	P_C (psia)	ω
C_1	-116.59	667.20	0.008
nC_4	305.69	551.10	0.193
nC_{10}	652.01	305.68	0.490

Table 5.3 Input EOS critical properties for the ternary system in Fig. (5.8).

	Bubble Point Curve			Dew Point Curve		
	CO_2	nC_4	nC_{10}	C_2	nC_4	nC_{10}
1000 psia	47.87	18.41	33.73	94.54	5.23	0.23
	48.37	10.46	41.17	97.06	2.77	0.17
	47.94	26.44	25.62	91.97	7.58	0.18
	49.21	37.24	13.56	87.23	12.60	0.94
1400 psia	68.02	8.29	23.69	96.75	2.89	0.37
	68.52	12.80	18.68	94.87	4.39	0.75
	67.87	13.97	18.16	94.14	5.30	0.57
	70.96	17.90	11.14	90.61	8.71	0.68
	76.28	20.30	3.42	86.06	12.97	0.97
1250 psia	60.90	9.27	29.83	96.91	2.80	0.29
	60.23	15.93	23.84	94.34	5.28	0.38
	62.31	21.91	15.78	91.58	8.06	0.37
	65.20	27.45	7.35	87.47	12.08	0.45
	67.27	29.43	3.30	84.69	14.97	0.34
1500 psia	71.41	7.22	21.37	96.18	3.13	0.69
	73.16	10.57	16.28	94.78	4.45	0.78
	73.25	12.42	14.33	93.06	6.00	0.95
	76.30	13.94	9.76	91.73	7.29	0.99
	79.92	15.10	4.98	89.04	9.94	1.02

Table 5.4 Experimental data used in the transformation method in section (5.3.5). Four tie lines (in grey) are used to initialize the calculation. All other data are used to illustrate the accuracy of the non-iterative transformation method.

Injection Gas Composition			Initial Oil Composition		
C_1	nC_4	nC_{10}	C_1	nC_4	nC_{10}
0.95	0.05	0.0	0.0	0.6	0.4

Table 5.5 Initial oil composition and injection gas composition in the UTCOMP simulation for a ternary system.

# of Grid Blocks	CPU Time in second by UTCOMP		CPU Time in second Using TM			Speedup		
	Total	Flash	Total	Flash	Comp.	Total	Flash	Comp.
10	21.69	9.22	12.31	0.93	0.23	1.76	9.9	40.1
20	33.08	17.02	16.78	1.51	0.38	1.97	11.3	44.8
40	57.20	31.58	28.12	2.85	0.62	2.03	11.1	50.9

Table 5.6 Comparison of CPU time using standard UTCOMP with the transformation method. The simulation using the transformation method is much faster. TM means "Transformation Method."

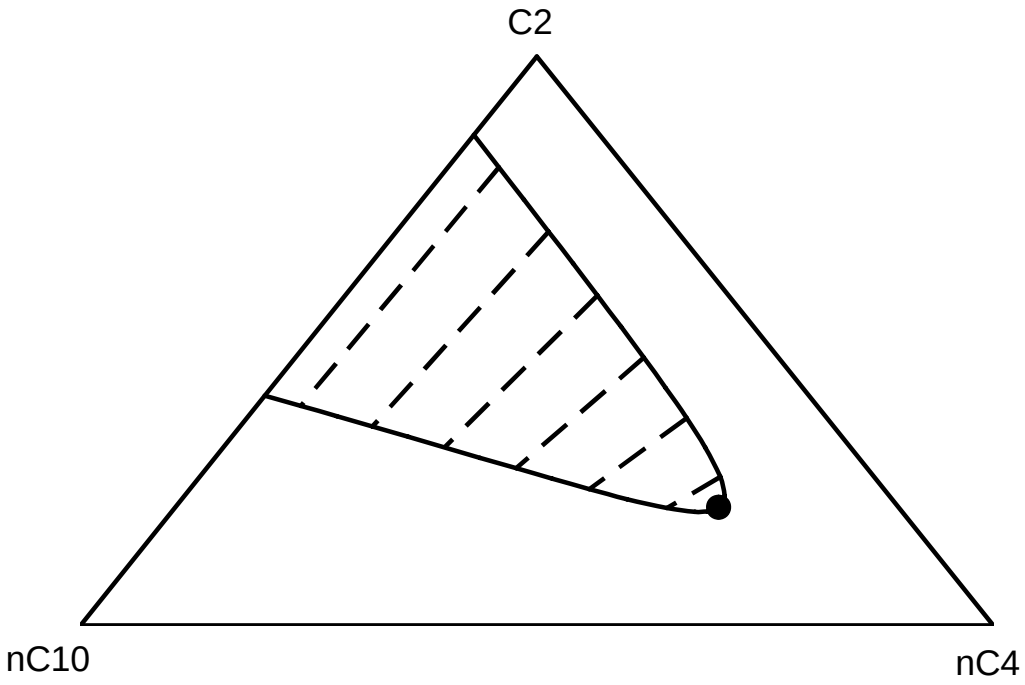

Fig. 5.1 Ternary diagram for C_2-nC_4-nC_{10} system at 498.03 K and 6.125 MPa. The equilibrium compositions are calculated using the Peng-Robinson EOS (1977, 1978).

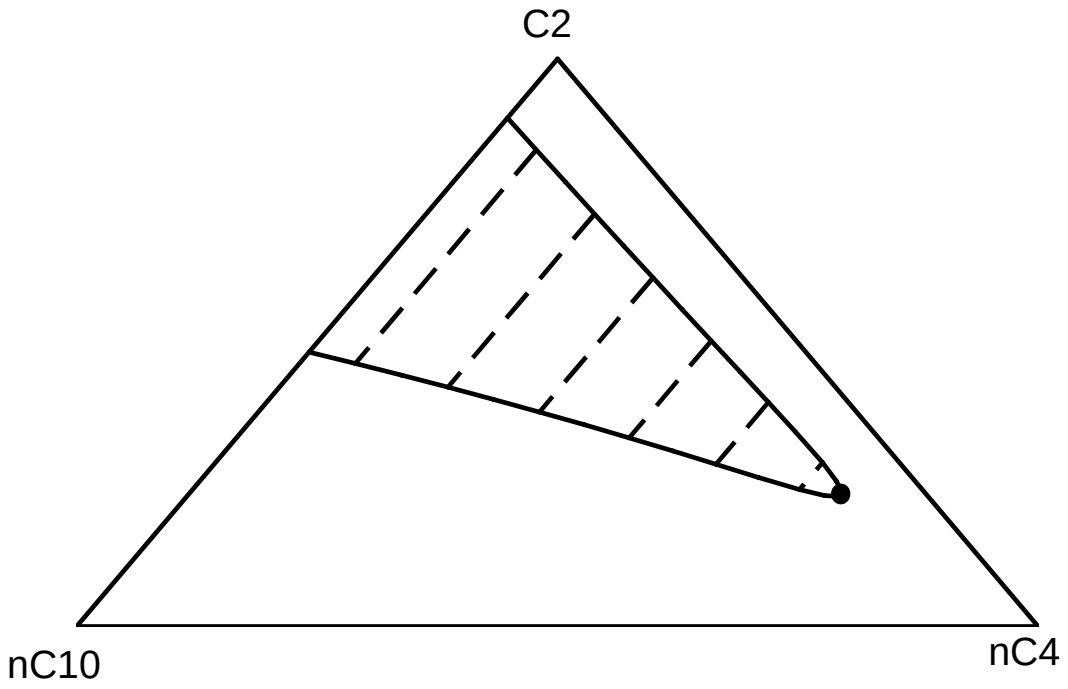

Fig. 5.2 Ternary diagram for C_2-nC_4-nC_{10} system in the transformed space at 498.03 K and 6.125 MPa. The transformation factor is applied to the C_2 component. In the transformed space, all tie lines are parallel, and the critical point occurs when nC_4^* is a maximum.

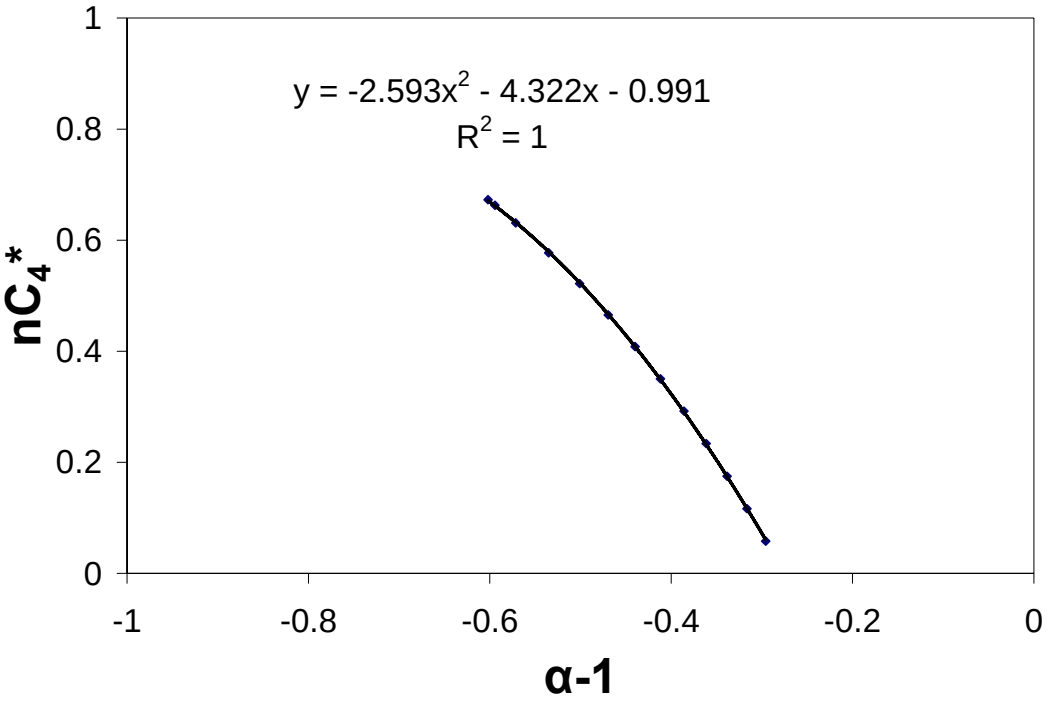

Fig. 5.3 Transformation factors for C_2-nC_4-nC_{10} ternary system in Fig. (5.1). A quadratic function is very accurate to describe the curve.

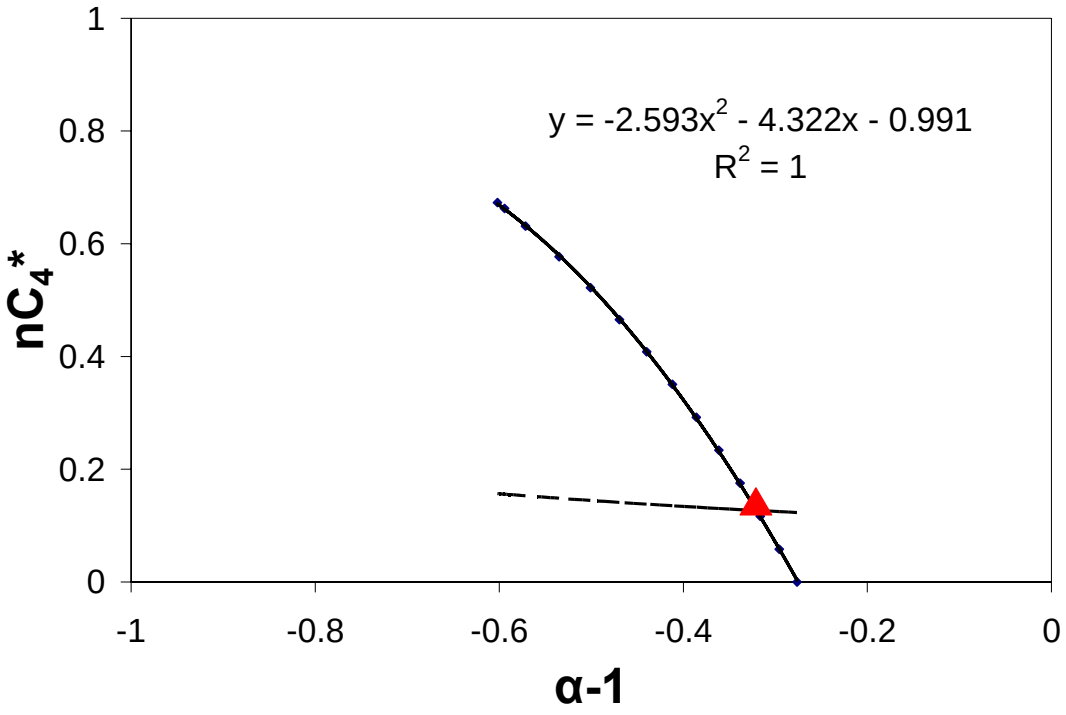

Fig. 5.4 Transformation factors for C_2-nC_4-nC_{10} ternary system in Fig. (5.1). The solid line uses the quadratic function, the dash line is that from Eq. (5.2) for an overall composition. The triangle is the correct transformation factor for the tie line passing through the overall composition.

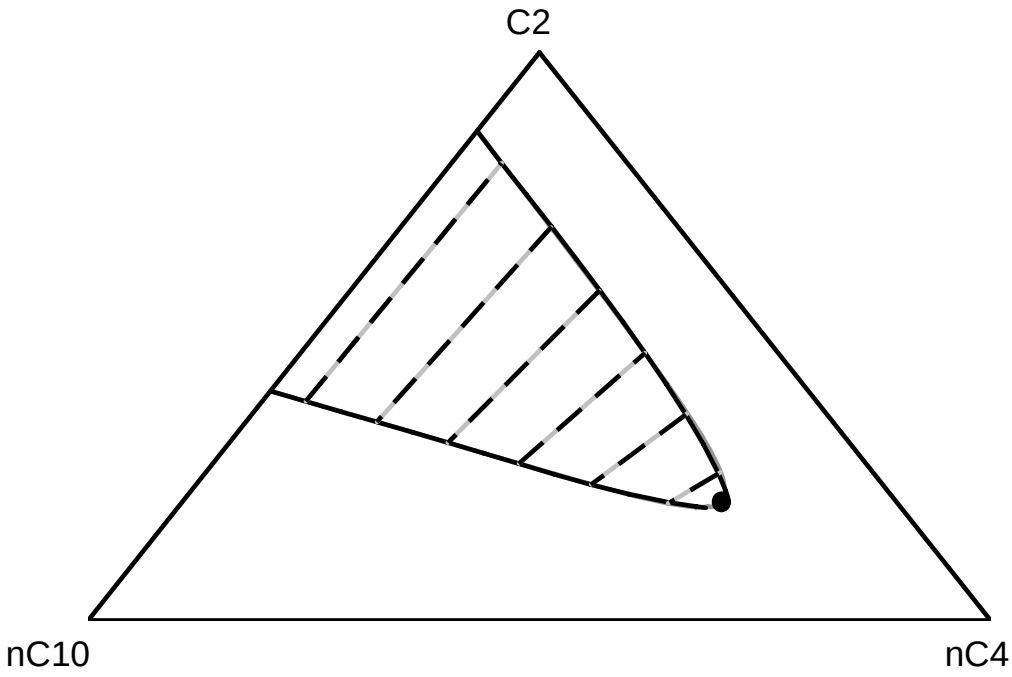

Fig. 5.5 Comparison of the equilibrium compositions for C_2-nC_4-nC_{10} system at 498.03 K and 6.125 MPa. The calculated values are in black, and the original data are in grey. The new non-iterative method yields almost identical results.

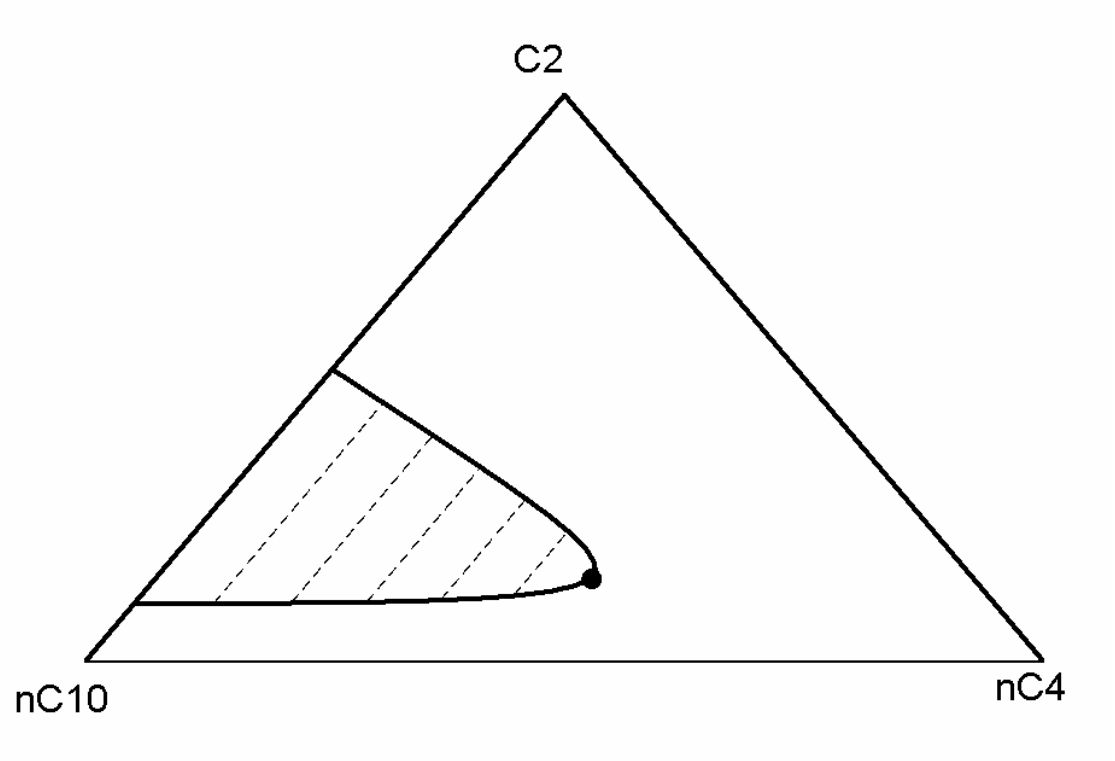

Fig. 5.6 Ternary diagram in the transformed space for C_2-nC_4-nC_{10} system. The transformation factor is applied to the nC_{10} component. The critical point occurs at the largest nC_4^* composition.

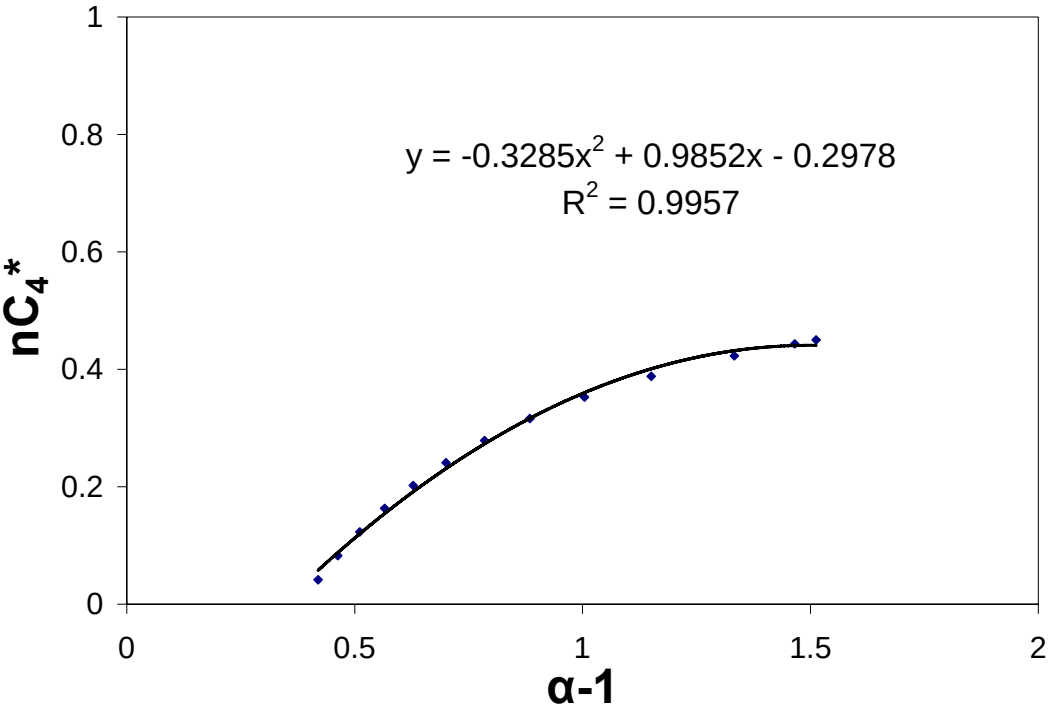

Fig. 5.7 Transformed nC_4 composition as a function of the transformation factor for the ternary system in Fig. (5.6). The transformation factors are applied to the nC_{10} component. An accurate quadratic curve is used in this case.

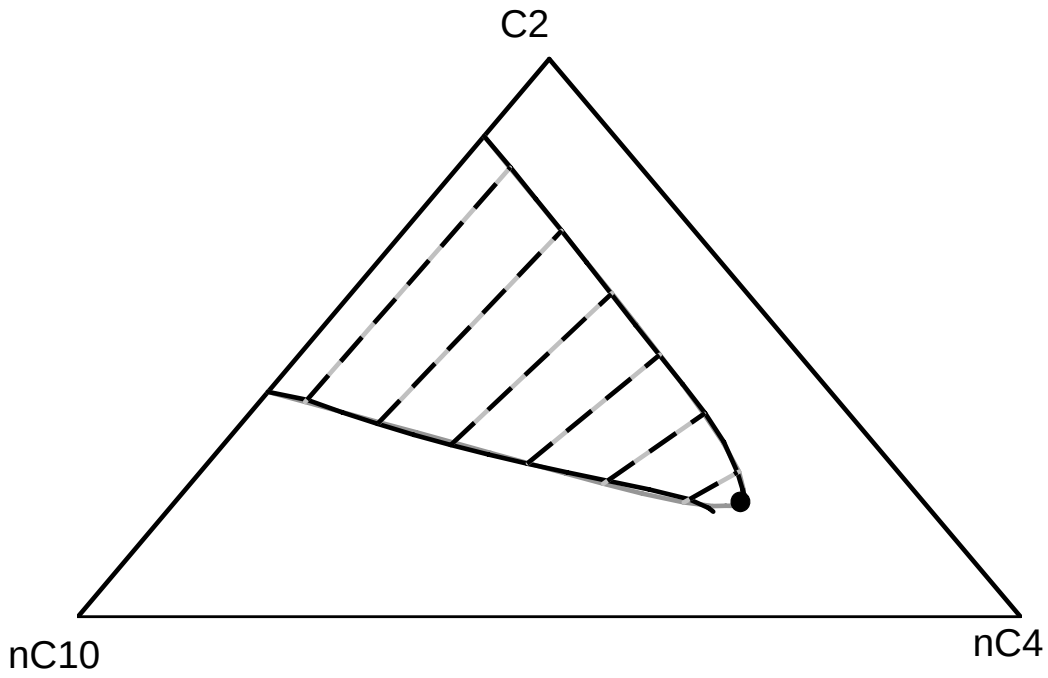

Fig. 5.8 Equilibrium compositions computed by the transformation method when the transformation factors are applied to nC_{10} component. The original data (gray) are from the Peng-Robinson EOS (1977, 1978). The non-iterative transformation method yields accurate phase behavior (black).

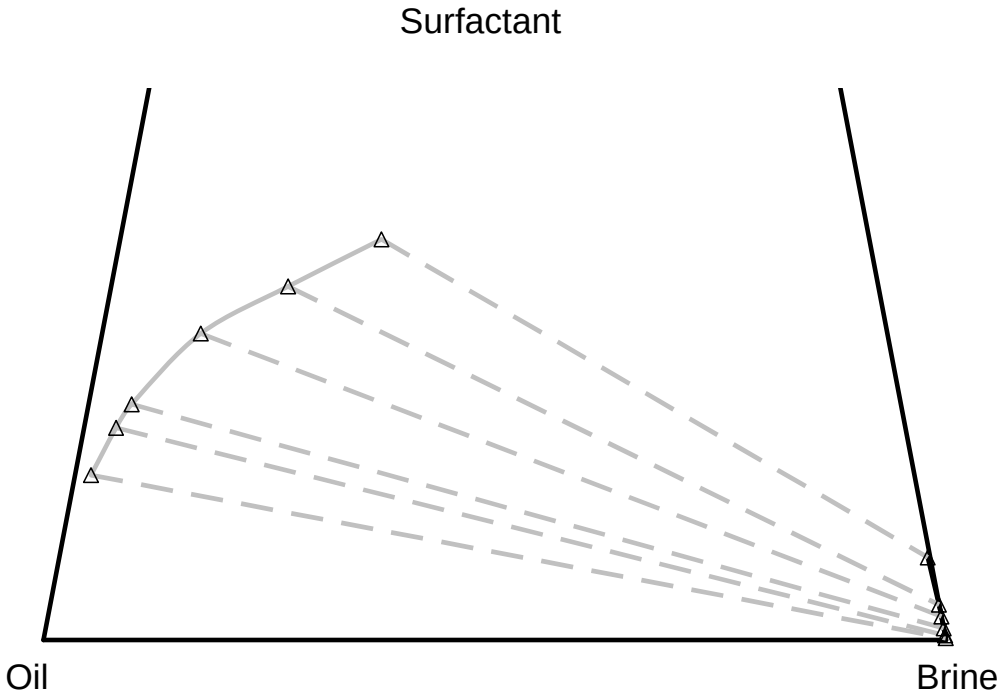

Fig. 5.9 Ternary diagram for a brine-oil-surfactant ternary system with co-surfactant injected (Pope, *et al.* 1982). The tie lines are in dash lines and the original data are in triangles.

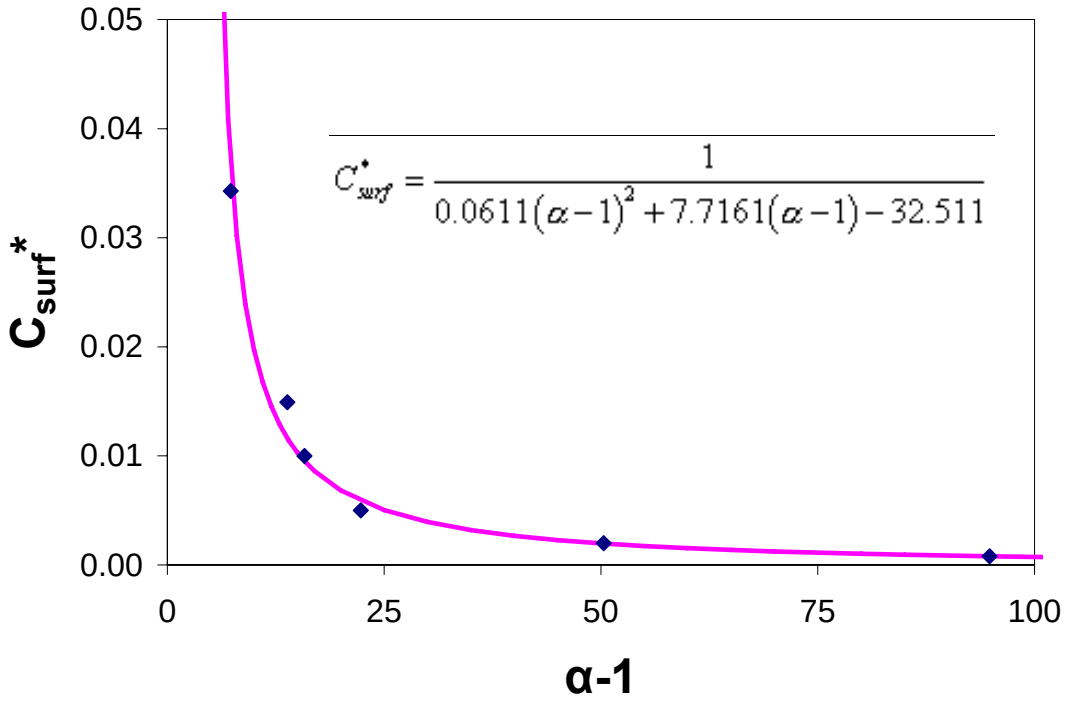

Fig. 5.10 Transformation factors for a surfactant system (see Fig. (5.9)). The transformation is applied to the oil component.

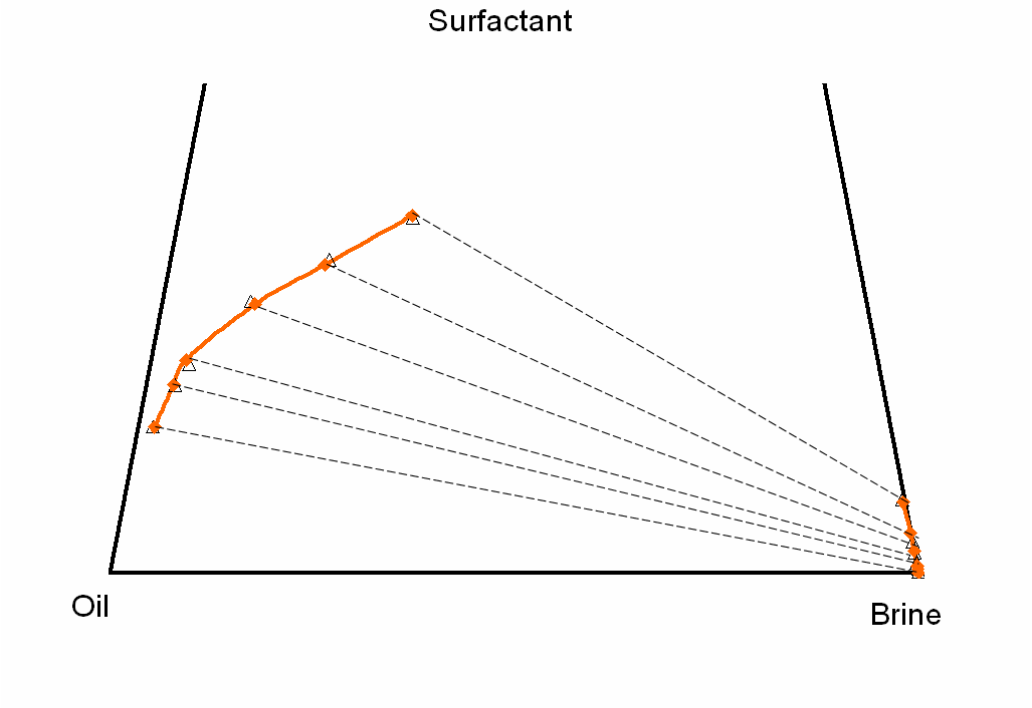

Fig. 5.11 Comparison of the non-iterative transformation method (diamonds with tie lines) with the experimental data (triangles).

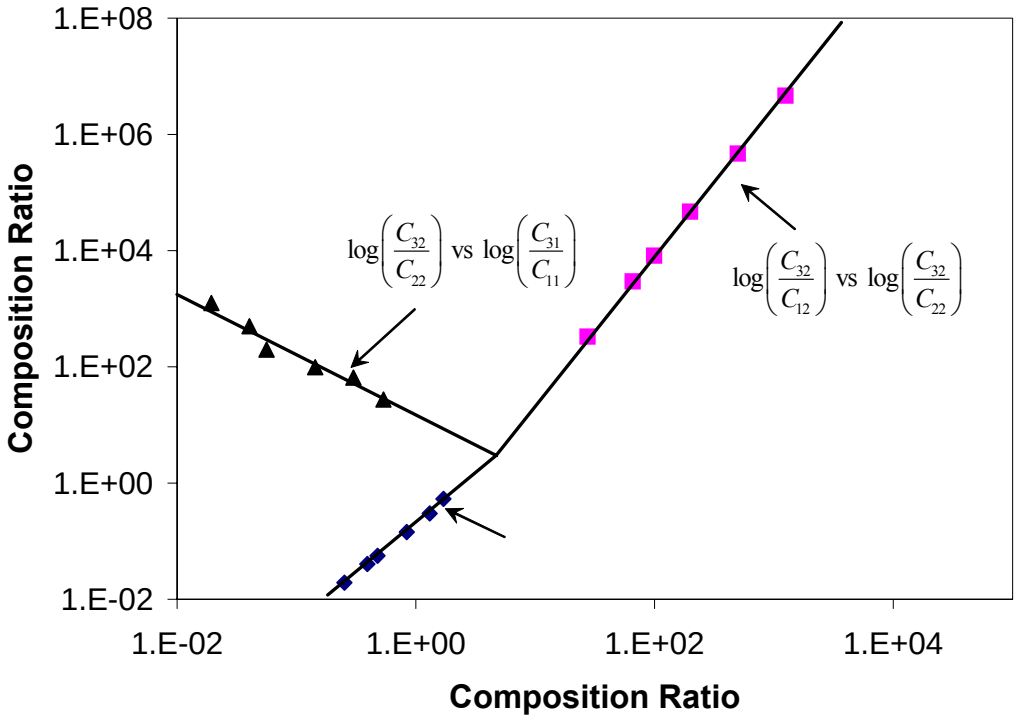

Fig. 5.12 Hand's plot (1930) for the ternary diagram of chemical flood in Fig. (5.9).

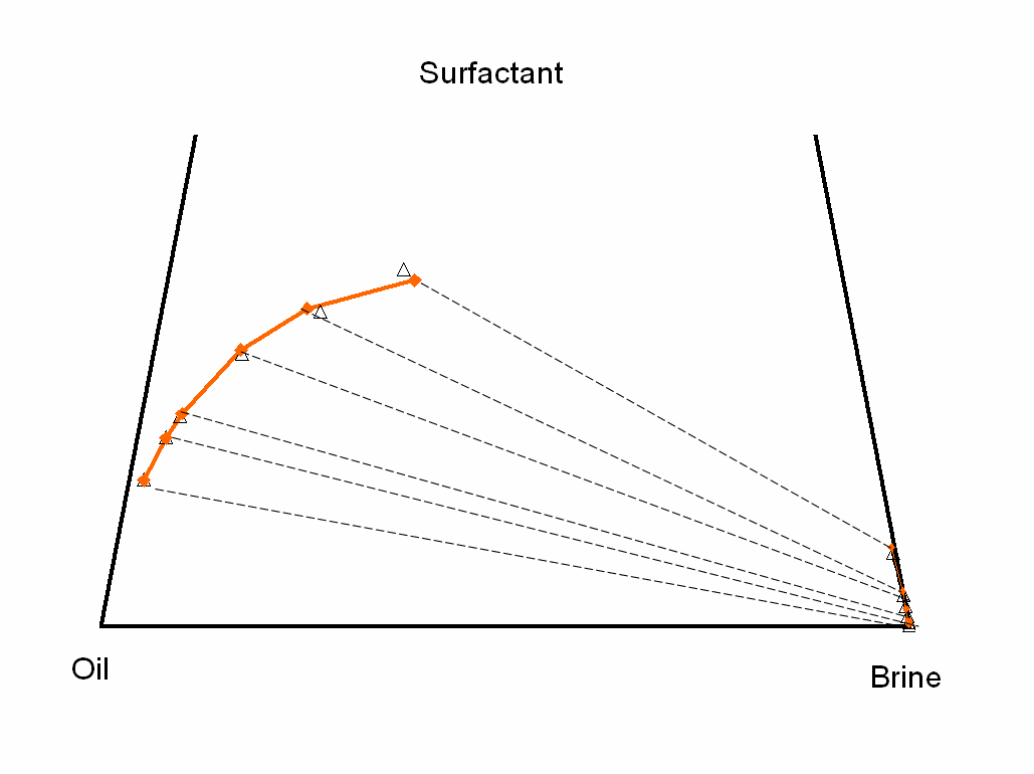

Fig. 5.13 Comparison of Hand's method (diamonds with tie lines) and the experimental data (triangles). Hand's method is less accurate than the transformation method in Fig. (5.11).

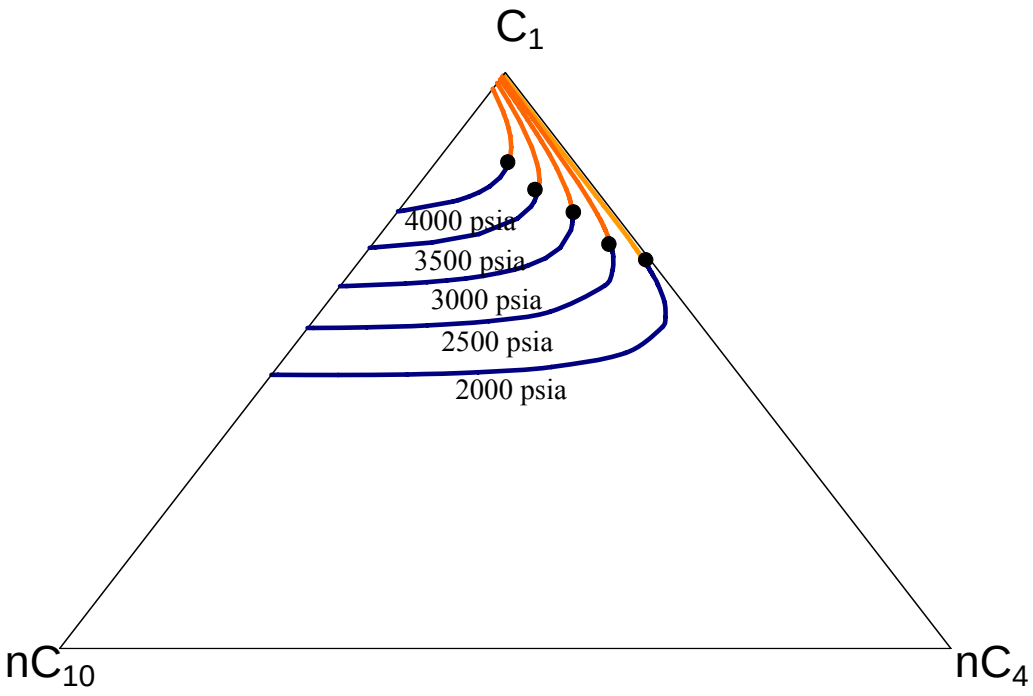

Fig. 5.14 Ternary diagram for C_1- nC_4 - nC_{10} system at different pressures from 2000 psia to 4000 psia at 150°F. The critical points at each pressure are shown by solid circles.

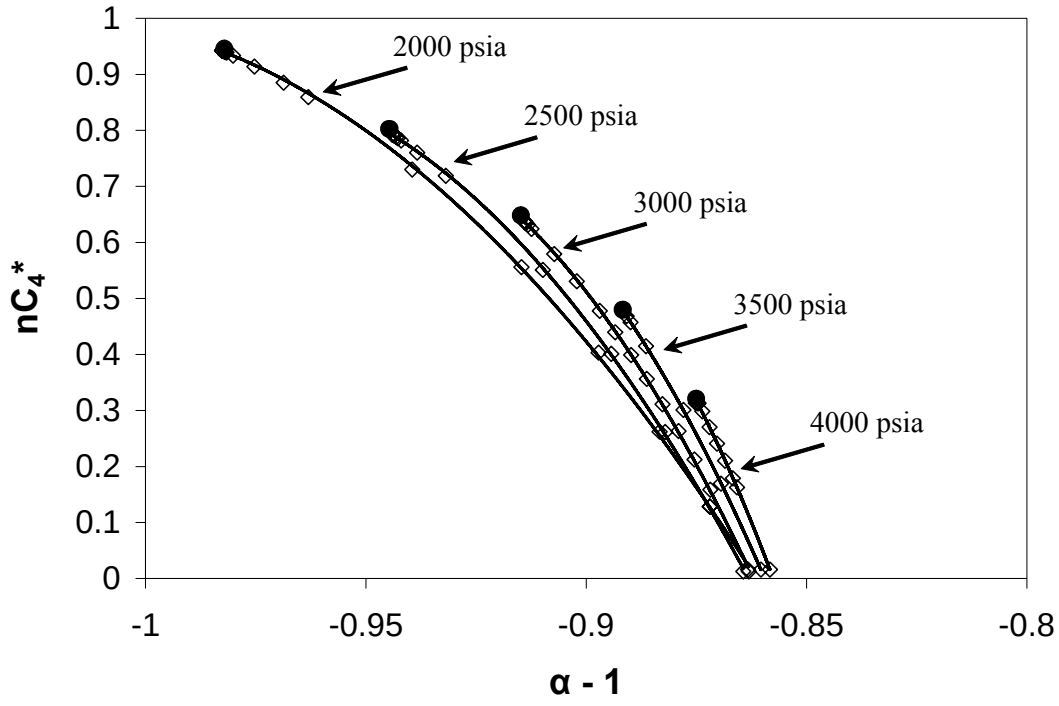

Fig. 5.15 Transformed nC_4 composition as a function of transformation factor for the ternary diagram in Fig. (5.14) at different pressures. The critical point is always at the maximum value for nC_4^*.

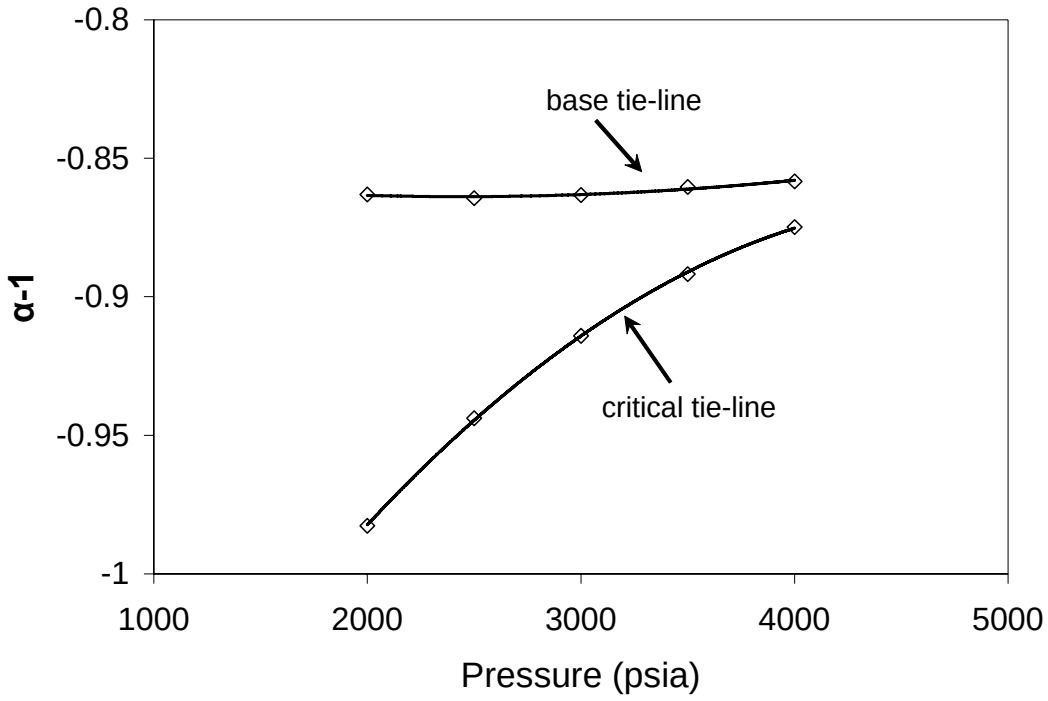

Fig. 5.16 The minimum transformation factor (the critical tie line) and the maximum (the base tie line) as a function of pressure. The calculated transformation factors must lie within this range.

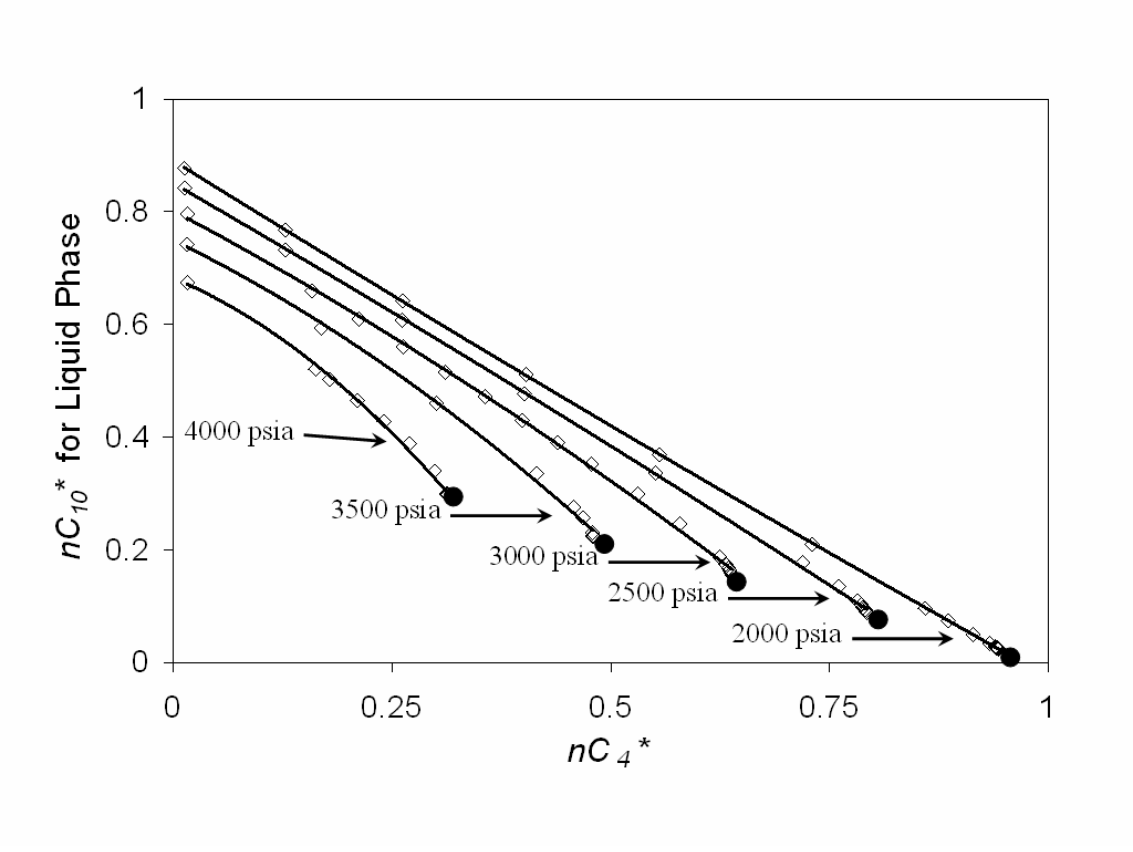

Fig. 5.17 Bubble-point curves in the transformed space at different pressures for the phase behavior in Fig. (5.14). All curves are accurately fitted using quadratic functions.

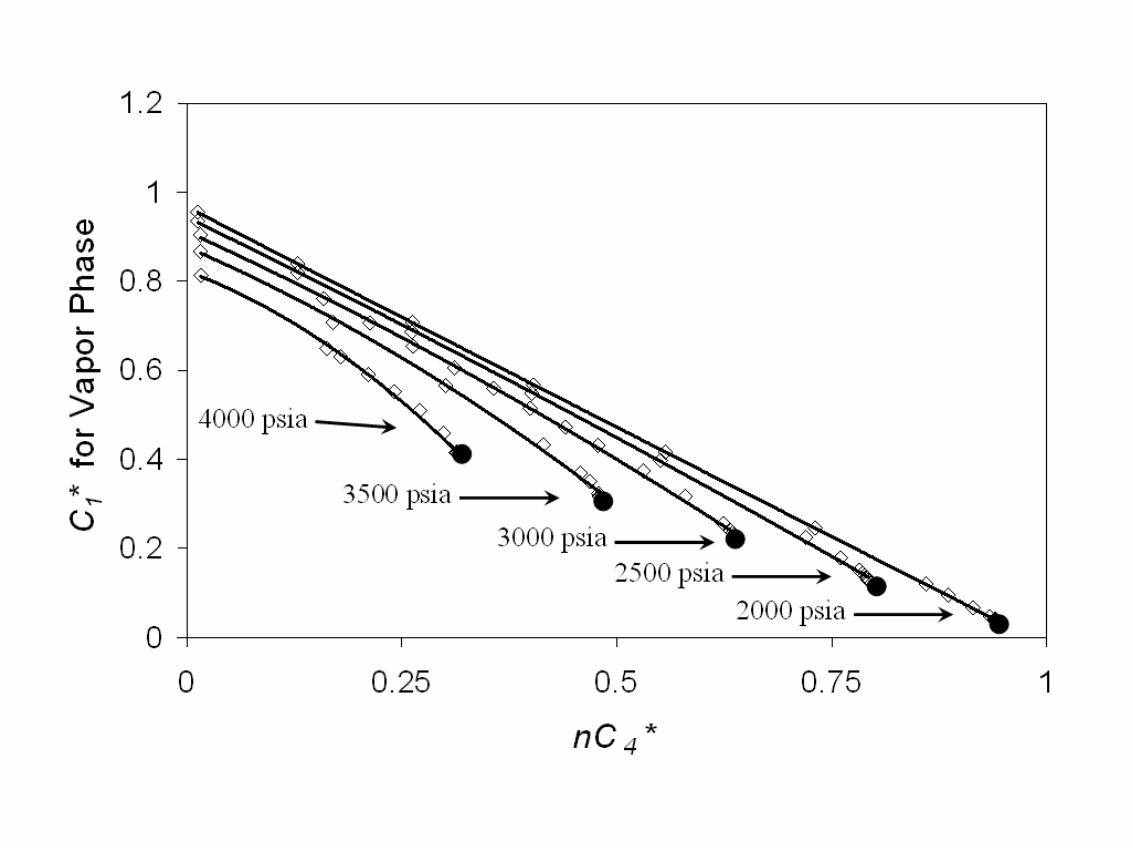

Fig. 5.18 Dew-point curves in the transformed space at different pressures for the phase behavior in Fig. (5.14). All curves are accurately fitted using quadratic functions.

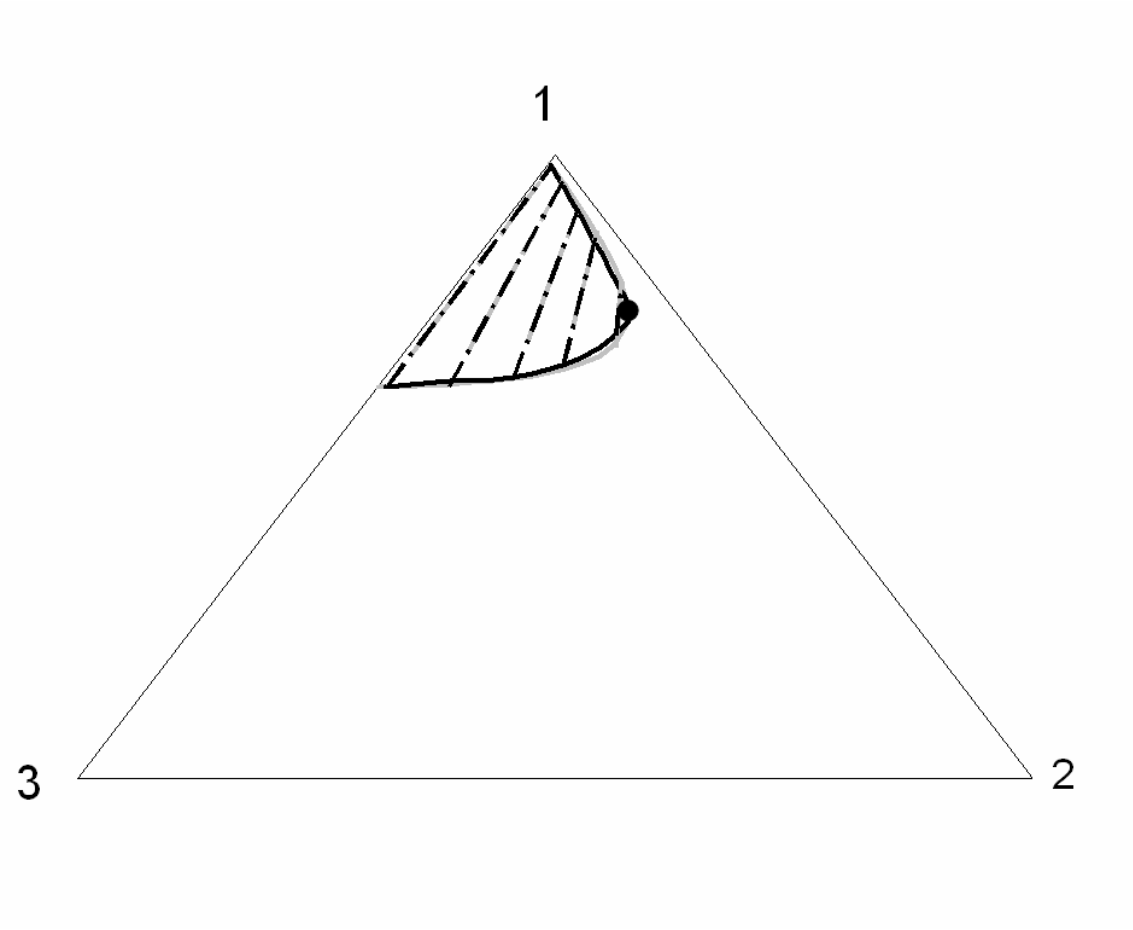

Fig. 5.19 Equilibrium compositions calculated using the transformation method at pressure of 3000 psia and 150^{o}F. The transformation method is accurate. The original data from the PR EOS (1977, 1978) is shown in grey and the calculated data using the transformed method is in black.

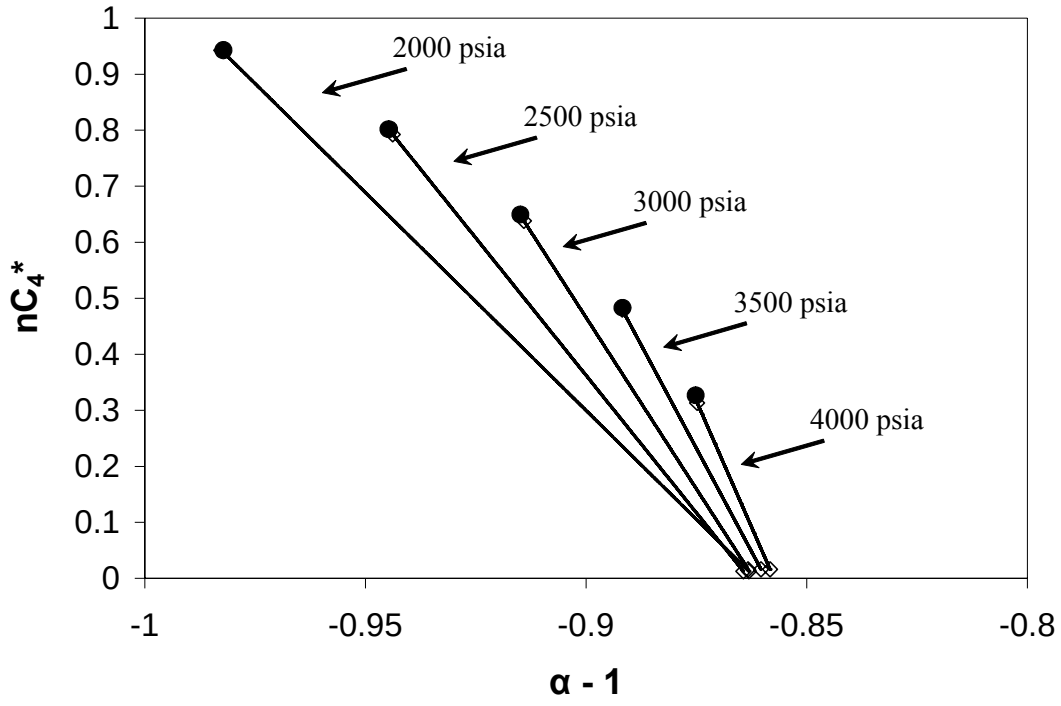

Fig. 5.20 Transformed nC_4 composition as a function of the transformation factor for the ternary system in Fig. (5.14) at different pressures. We linearly interpolate the relationship at each pressure from the base tie line to the critical tie line in this example.

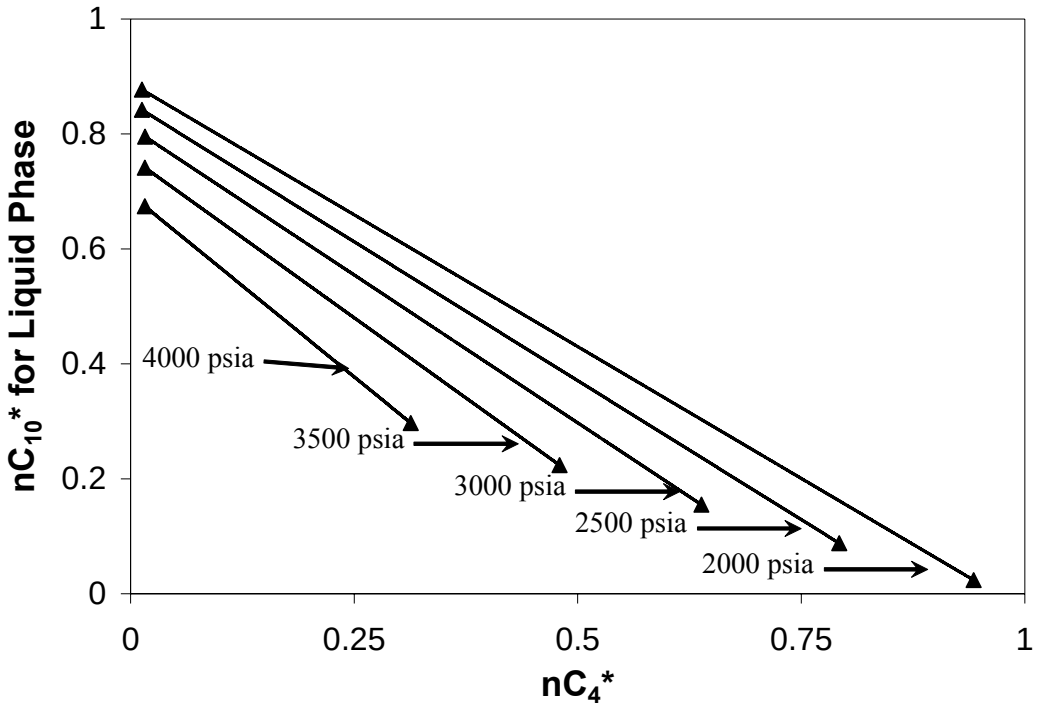

Fig. 5.21 Bubble point curves in the transformed space using linear interpolation for the oil in Fig. (5.14).

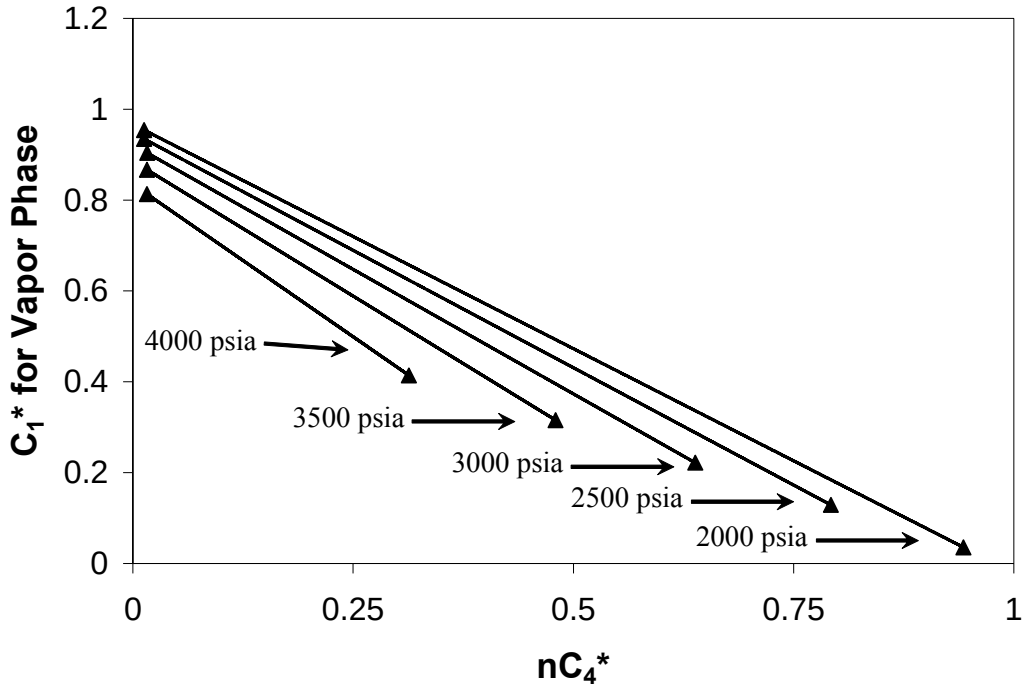

Fig. 5.22 Dew point curves using linear interpolation in the transformed space for the oil in Fig. (5.14).

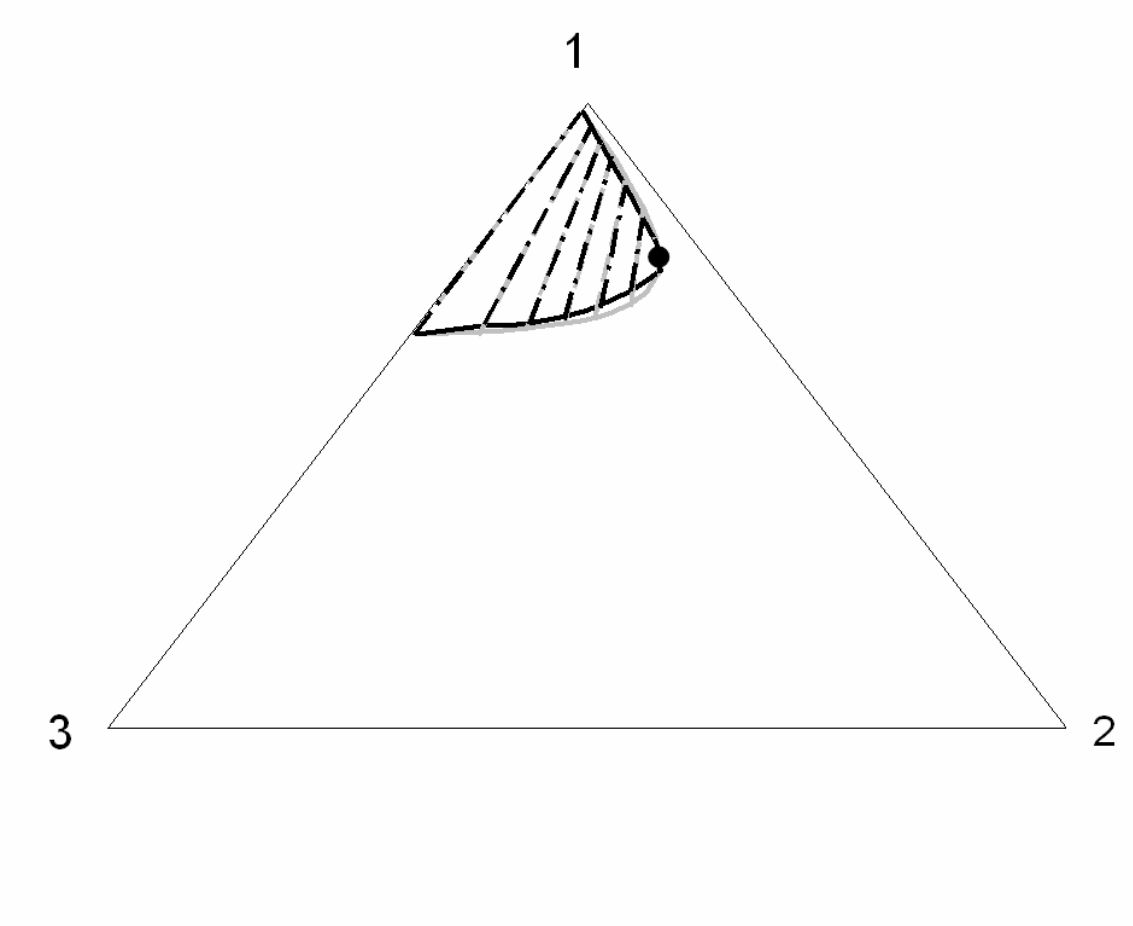

Fig. 5.23 Equilibrium compositions calculated using the transformation method at 3000 psia and 150°F. We linearly interpolate the phase behavior from the limiting tie line to the base tie line on the 1-3 axis. The transformation method using linear interpolation yields accurate results.

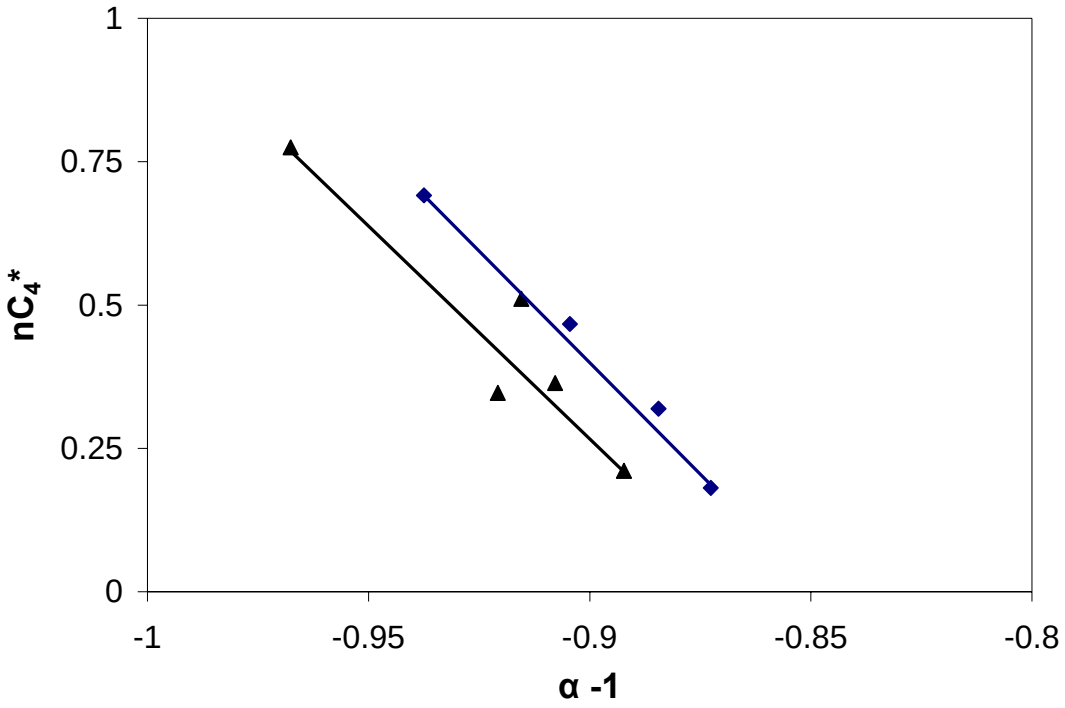

Fig. 5.24 Transformed nC_4 composition as a function of transformation factor for the CO_2-nC_4-C_{10} ternary system (Metcalfe and Yarborough, 1979) at 1000 psia (diamonds) and 1400 psia (triangles).

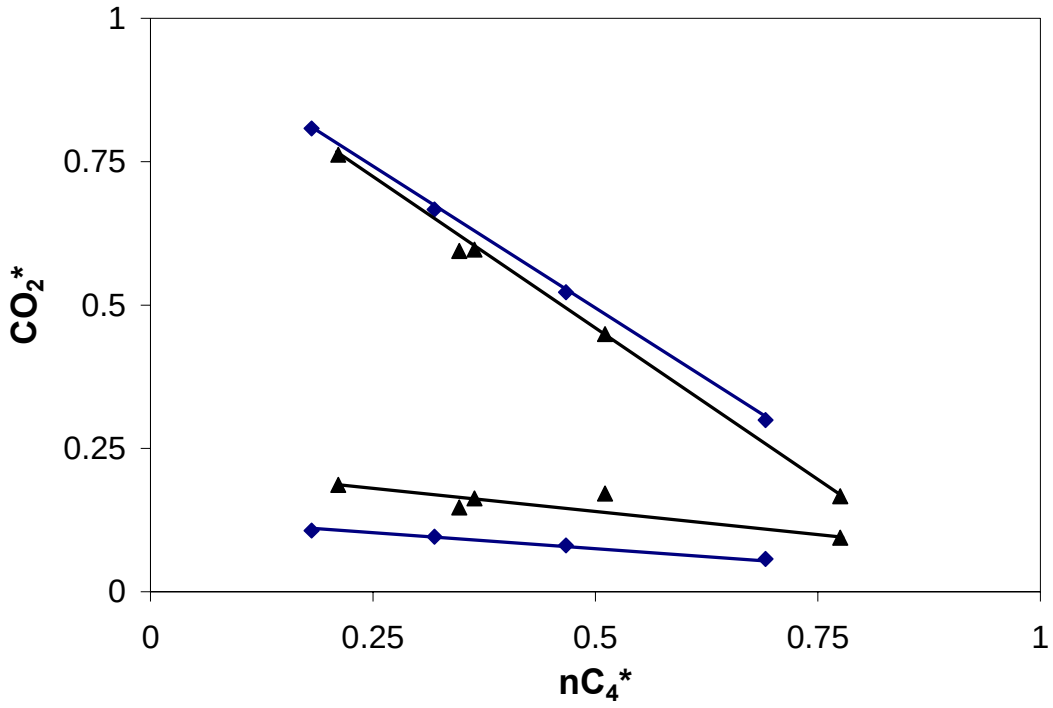

Fig. 5.25 Binodal curves in the transformed space at pressures of 1000 psia (diamonds) and 1400 psia (triangles). Linear interpolation is used for the binodal curves between two tie lines at each pressure.

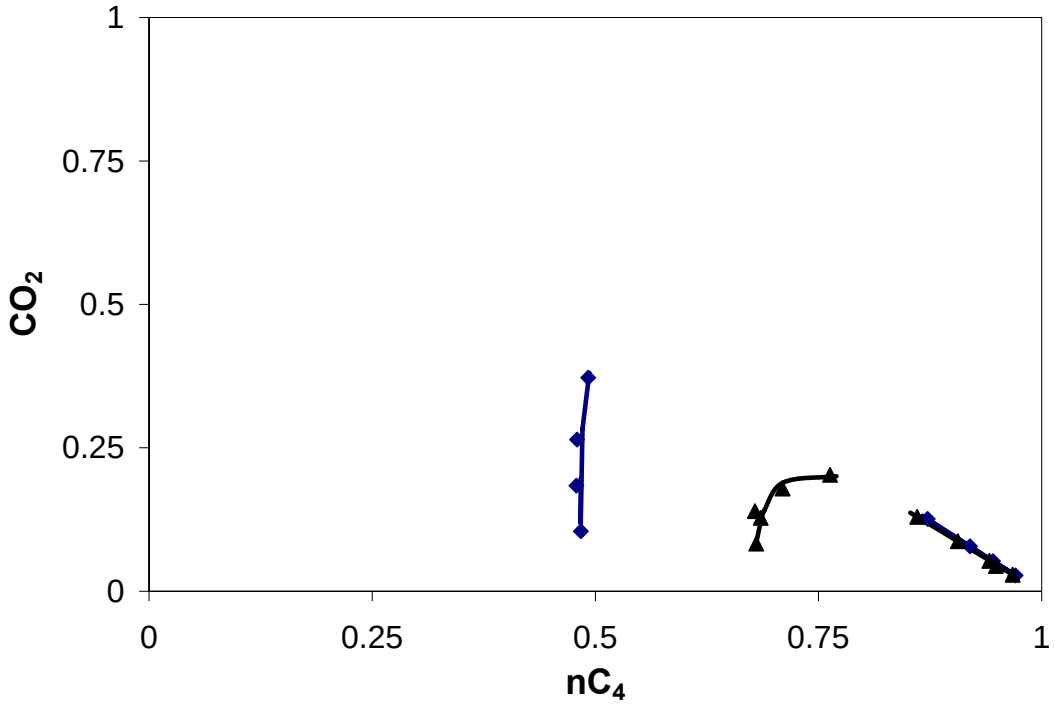

Fig. 5.26 Equilibrium compositions calculated at 1000 psia (diamonds) and 1400 psia (triangles) using the transformation method. The experimental data is shown in dots and the calculated equilibrium compositions are in curves. The new method predicts the phase behavior accurately.

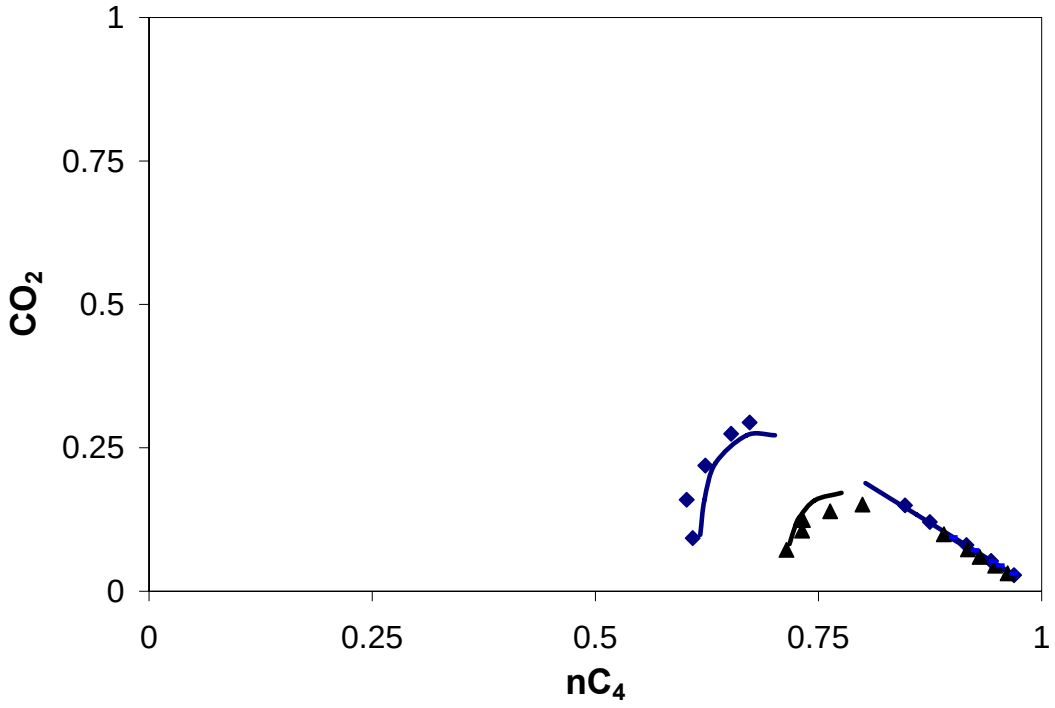

Fig. 5.27 Equilibrium compositions calculated at 1250 psia (diamonds) and 1500 psia (triangles) using the transformation method. The experimental data is shown in dots and the calculated equilibrium compositions are in curves. The new method is accurate.

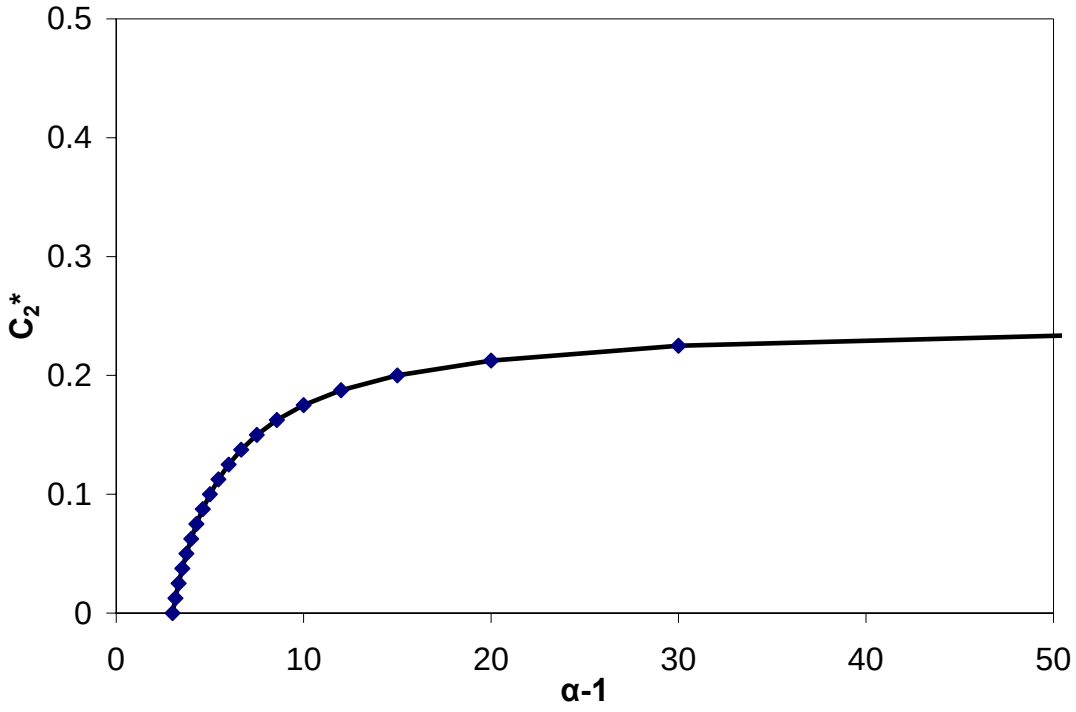

Fig. 5.28 Transformed intermediate composition as function of the transformation factor for a ternary system with constant *K*-values of $K_1 = 5.0$, $K_1 = 2.0$ and $K_3 = 0.5$.

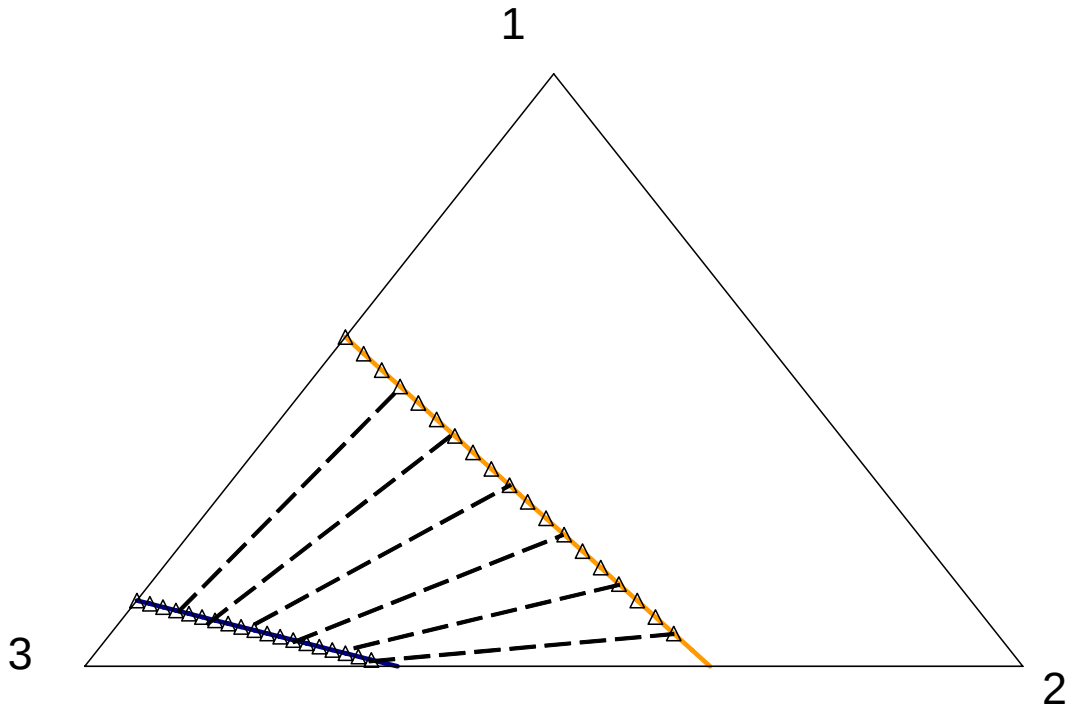

Fig. 5.29 Calculated equilibrium compositions using the transformed method for the ternary system with constant *K*-value in Fig. (4.1). Triangles are from the Rachford-Rice method (1952), and the lines are from the transformation method. The transformation method is very accurate.

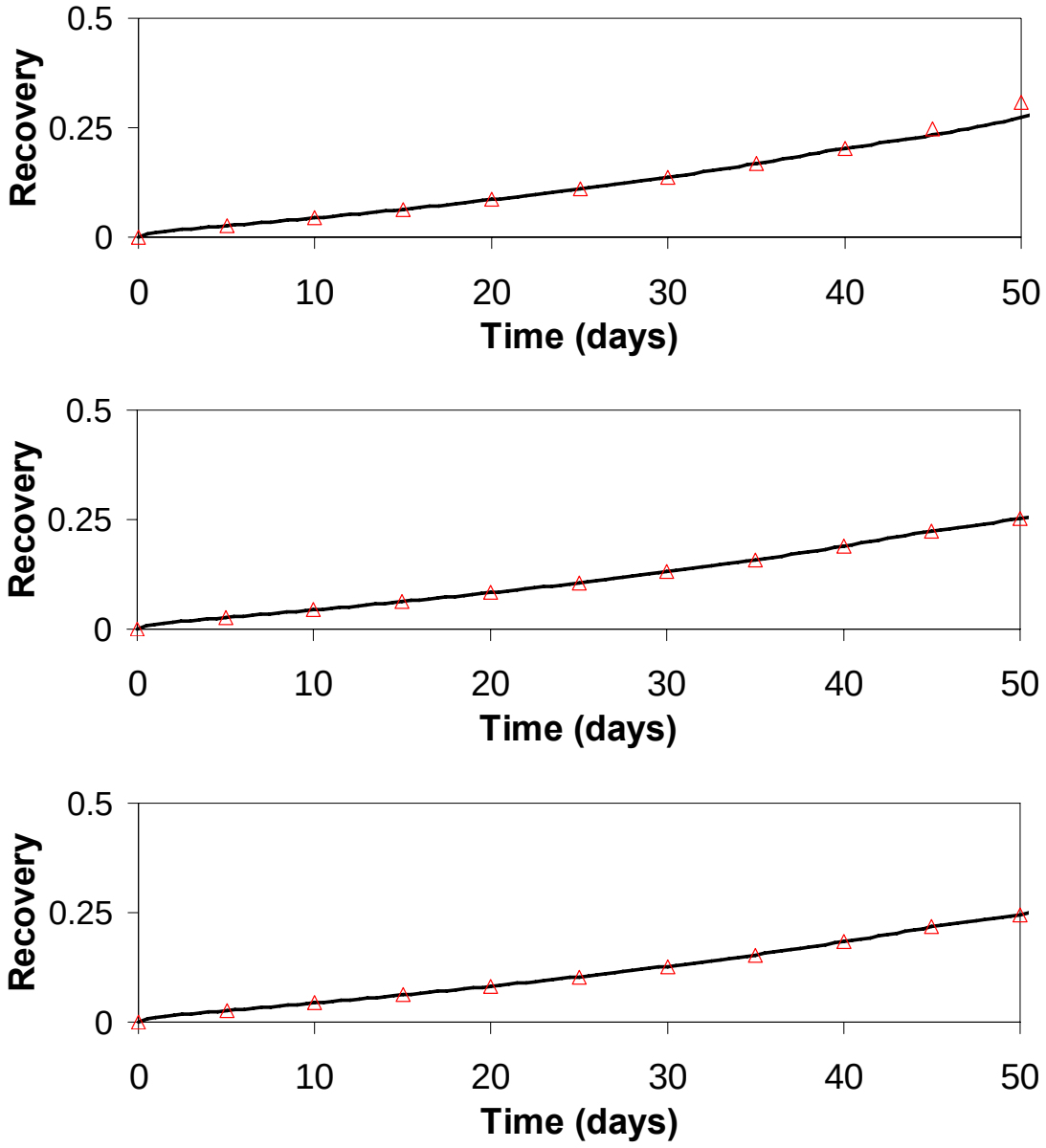

Fig. 5.30 Comparison of the C_{10} recovery using the standard EOS model (triangles) and the transformation method (lines) at different numbers of grid blocks. The numbers of grid blocks are 10, 20 and 40, respectively, from the top. The transformation method agrees well with the conventional method.

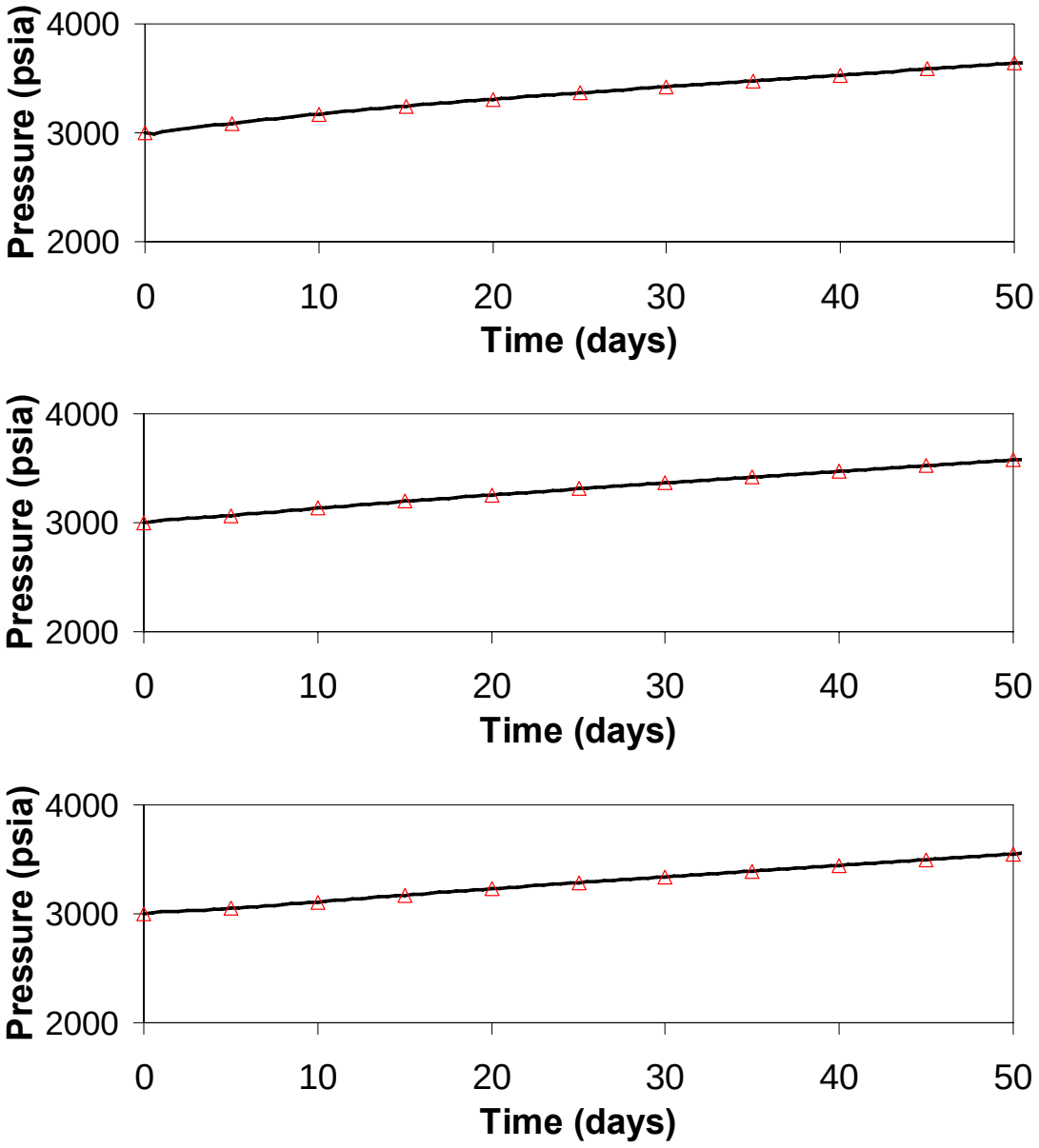

Fig. 5.31 Comparison of the average reservoir pressure in psia using the standard EOS model (triangles) and the transformation method (lines). The number of grid blocks are 10, 20 and 40, respectively, from the top. The transformation method agrees well with the conventional simulation.

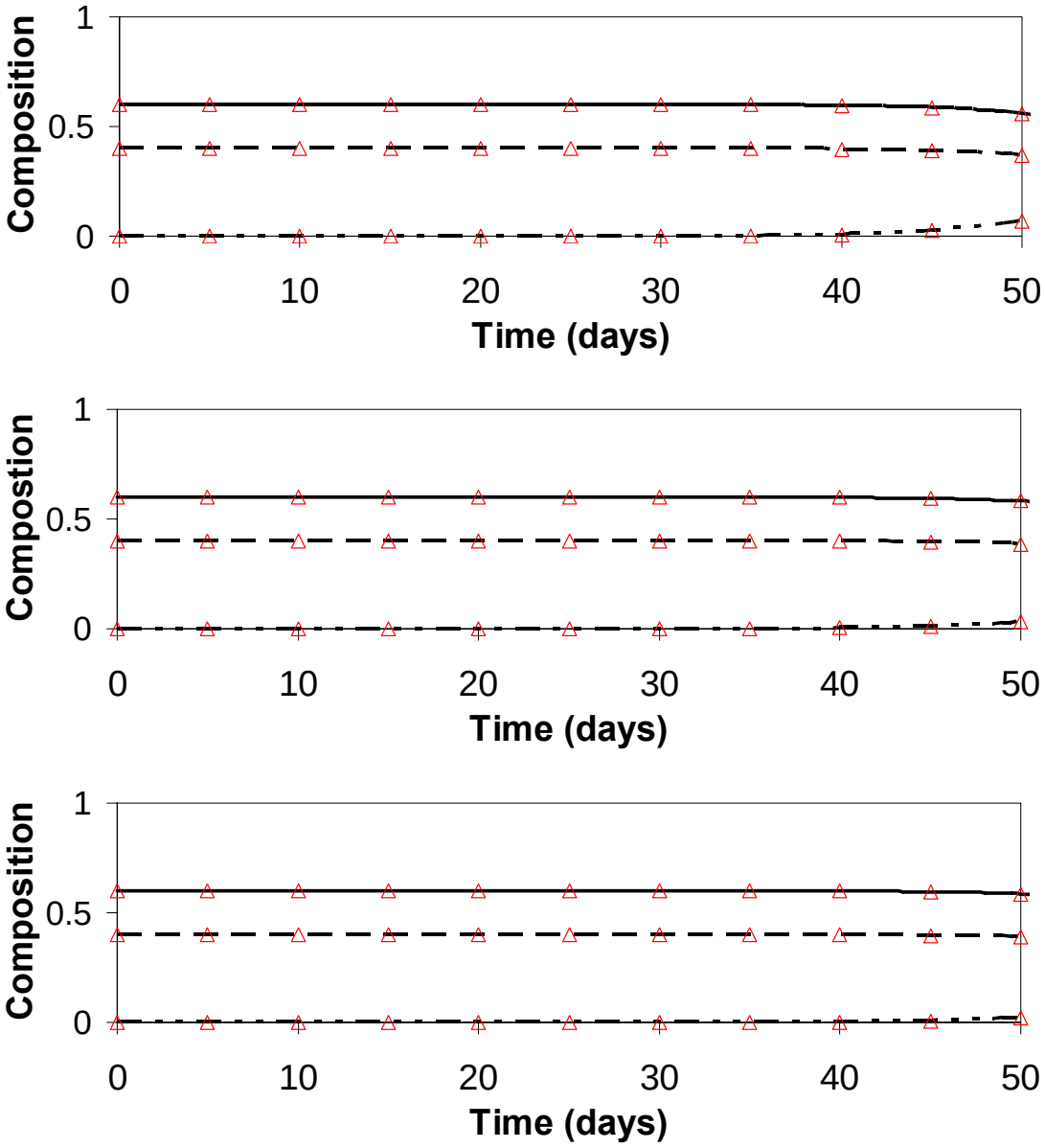

Fig. 5.32 Comparison of the compositions measured at the production well using the standard EOS model (triangles) and the transformation method (curves). The nC_4 compositions are the solid lines, nC_{10} are the dash lines and C_1 are the double dash lines.

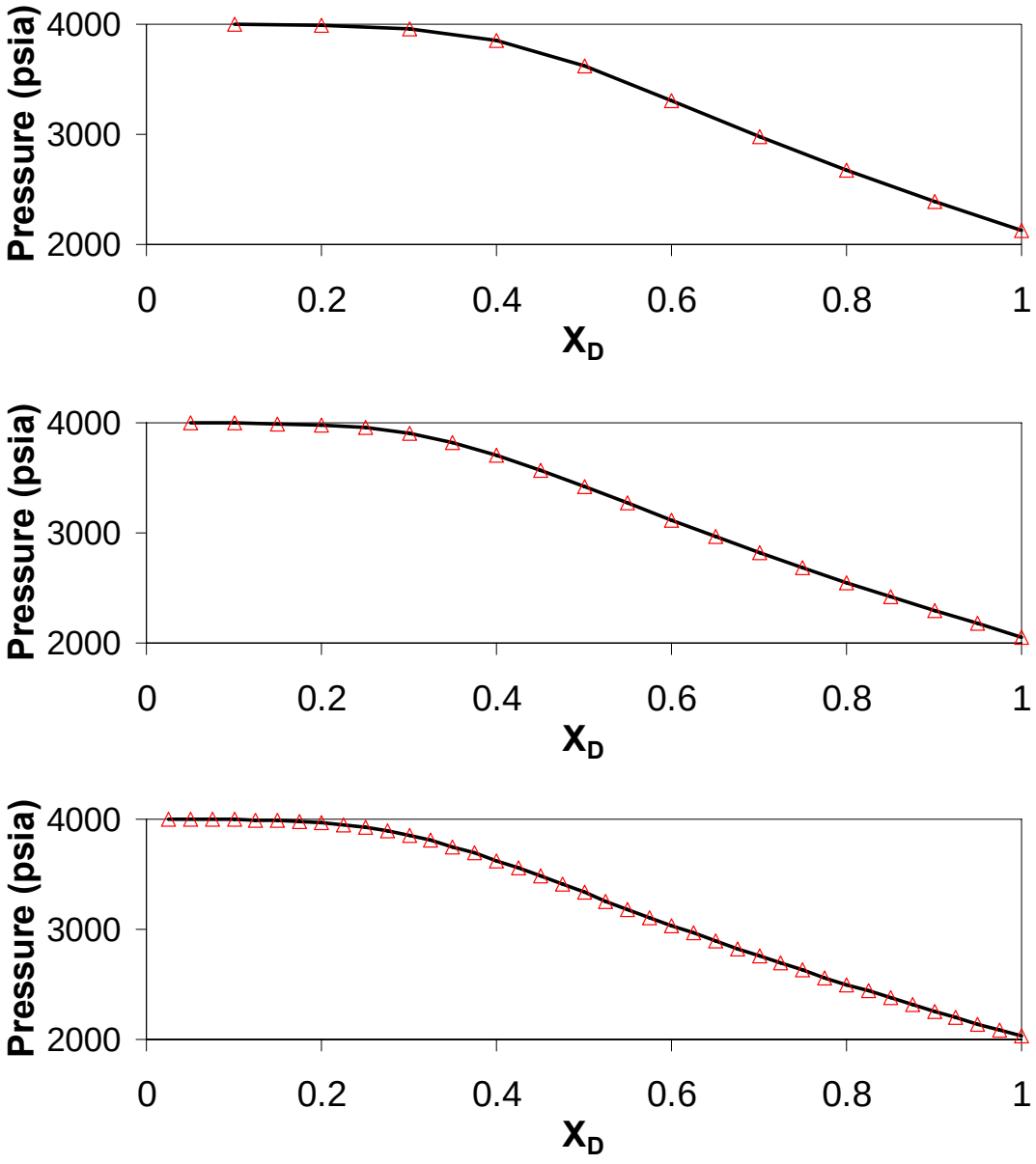

Fig. 5.33 Comparison of pressure profile at 20 days using 10 (top), 20 (middle) and 40 (bottom) grid blocks. The standard UTCOMP results are in triangles and the transformation method results are in curves. The non-iterative transformation method is almost identical as the conventional method.

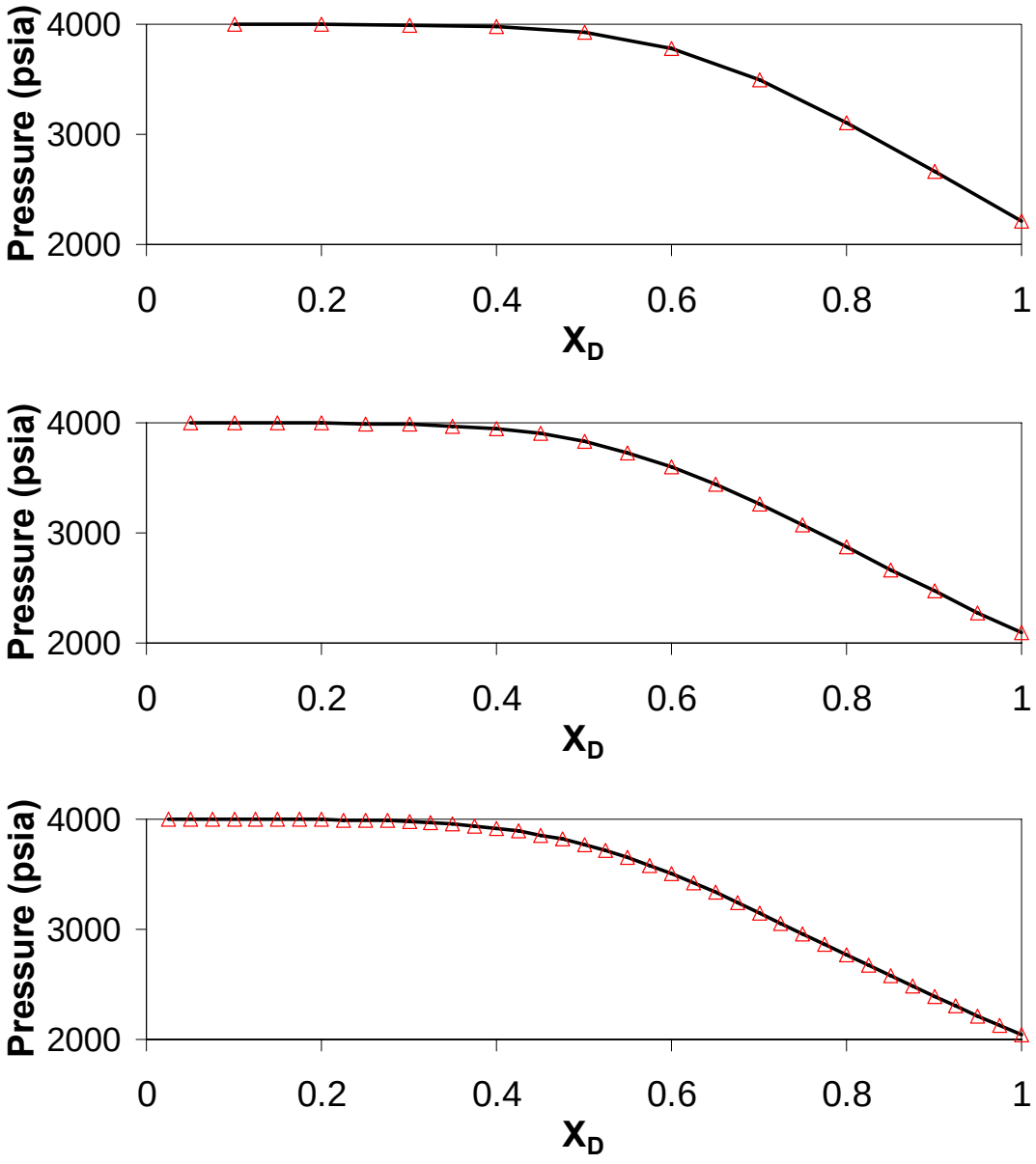

Fig. 5.34 Comparison of the pressure profile at 40 days using 10 (top), 20 (middle) and 40 (bottom) grid blocks. The standard UTCOMP results are in triangles and the transformation method results are in curves. The non-iterative transformation method is very accurate.

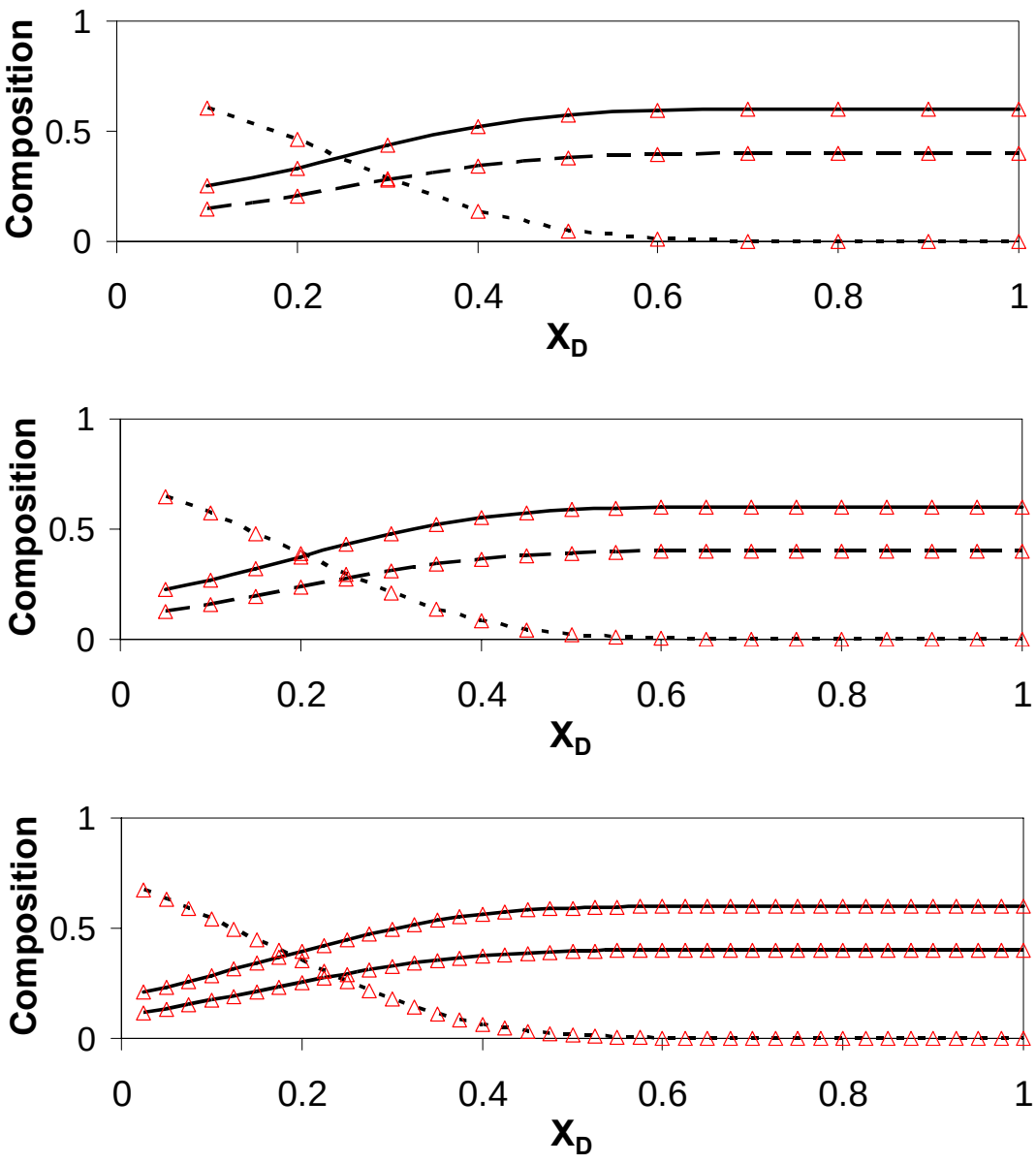

Fig. 5.35 Comparison of the overall composition profile at 20 days using 10 (top), 20 (middle) and 40 (bottom) grid blocks. The standard UTCOMP results are in triangles. The results using the transformation methods are: nC_4 in solid curves, nC_{10} in dash curves and C_1 in double dash curves.

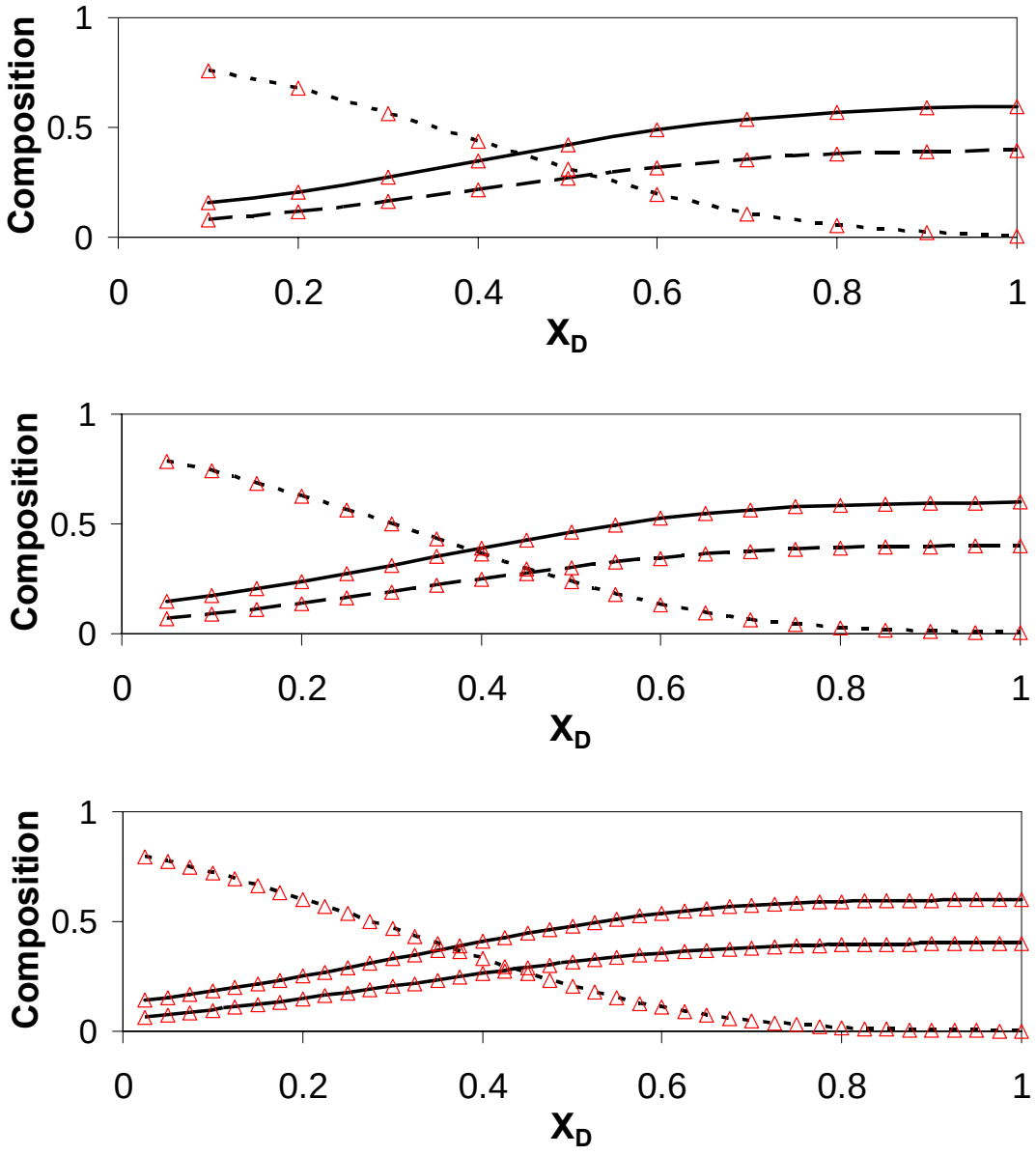

Fig. 5.36 Comparison of the overall composition profile at 40 days using 10 (top), 20 (middle) and 40 (bottom) grid blocks. The standard UTCOMP results are in triangles. The results using the transformation methods are: nC_4 in solid curves, nC_{10} in dash curves and C_1 in double dash curves.

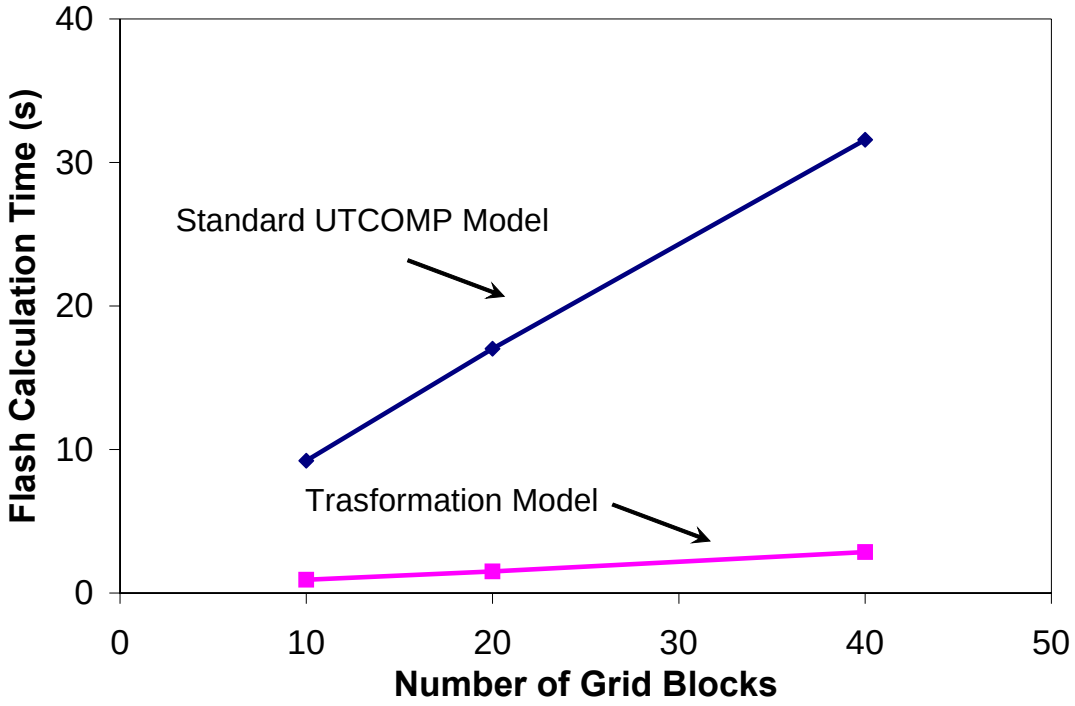

Fig. 5.37 CPU time used for the flash calculations in simulation using the standard UTCOMP method and the transformation method. The new method is approximately 10 times faster than the conventional flash calculation.

Chapter 6: Conclusions and Future Work

In this work, several practical phase behavior models have been developed for flash calculations using EOS, constant *K*-values, and non-iterative transformation factors. The implementation of these different models and their impacts on speed, accuracy and robustness were examined. Compared with conventional models, all these new approaches show significantly improved speed and robustness.

6.1 KEY CONCLUSIONS

6.1.1 EOS-Based Reduced Method

1 A new, rapid, accurate, simple and robust model is developed to perform flash calculations with arbitrary non-zero binary interaction parameters (BIPs). The new model requires a maximum of six reduced variables in phase-split calculations, and five in stability analysis calculations regardless of the number of components;

2 In flash calculations, the new method significantly improves the speed by a factor of 1.3 for seven-component systems, and approximately 14 for thirty-five component systems compared with the conventional method. In stability analysis calculations, the new method also improves the speed by a factor of 1.9 for seven-component systems and 24 for thirty-five component systems;

3 In flash calculations, the new method has improved robustness close to the critical point;

4 In flash calculations, the reduced method will yield the exact solution compared with conventional method when the same BIPs are used. Significant improvement in speed and robustness without sacrificing accuracy are the major advantages of this new method;

5 The new method is also shown to be easily applied to three-phase flash calculations.

6.1.2 Constant K-value Flash Calculations

1 A simple, fast and accurate objective function is developed to replace Rachford-Rice and similar approaches.

2 The correct solution lies within a predetermined window, the range of which is derived in this dissertation;

3 The new objective function is continuous and almost linear in the solution window. Because of improved linearity, the new method is significantly faster than Rachford-Rice, and often requires less iterations. Based on batch calculations, the research shows that the new method needs approximately 25% less time for three-component fluids, and 40% less for fifteen-component fluids;

4 The new objective function is scaled near the critical point so that neither the objective function nor its derivative change significantly when *K*-values approach 1.0;

5 Simulations in GPAS show that this new objective function requires approximately 5% fewer iterations than the Rachford-Rice procedure;

6 The robustness is also improved that the new objective function can always converge to a correct tie line regardless the overall composition.

6.1.3 Transformation Method for Limited Compositional Simulators

1 A simple, accurate, non-iterative, rapid and robust transformation method is developed for ternary systems for limited compositional simulators;

2 The new method is over 100 times faster than conventional EOS flash calculations, and approximately 10 times faster than flash calculations with constant *K*-values. No iterations are used in calculating equilibrium compositions. As a result this method is very fast and robust even at the critical point.

3 An investigation window is proposed to guarantee the uniqueness of the solution. This window is also used in phase stability test;

4 The new method can model both partial miscible and full miscible flooding processes using pressure- and temperature-dependent transformation factors and binodal curve functions. The new model is much more accurate compared with Hand's model, and almost exact as EOS flash calculations;

5 Because the method is direct, the new method always gives an accurate solution when the overall composition is on a tie line or tie-line extension;

6 Even with simplified transformation model by linear interpolation between base tie line and critical tie line, the new method is practically accurate;

7 Reservoir simulations confirm that this model is much faster than conventional EOS models without sacrificing accuracy. For example, simulation shows that the new method is approximately 10 times faster than the conventional flash calculations in UTCOMP for a ternary system;

8 The new method could be used to simulate miscible gas injection that requires complicated phase behavior with a few pseudocomponents and requires a large number of grid blocks. Some accuracy will be lost, however, by using only three pseudocomponents.

6.2 FUTURE RESEARCH

Additional research that could be addressed are:

1 Implementation of the new reduced method into an IMPEC and fully implicit reservoir simulator is of practical interest to illustrate the efficiency and accuracy of this new model;

2 Implementation of the new reduced method for three or more phases is of growing importance;

3 Optimization of the iterative techniques in reduced method is also important, so that the number of iterations could further be reduced;

4 Expansion of the non-iterative transformation method to at least four pseudocomponents would greatly improve its accuracy in compositional reservoir simulations.

Appendix: Flash Calculations with Negative Compositions

When we calculate MMP or MME, it may require flash calculations with constant K-values where at least one component has a negative overall composition. In this case, there may be multiple tie lines passing through that overall composition and in MMP/MME calculations it is important to locate all of them. The conventional method using Rachford-Rice (1952) has convergence problems for these cases because the correct solutions are not within the Whitson-Michelsen window (1989).

We can extend the new objective function in Chapter 4 to this case to guarantee convergence. A similar investigation window can also be derived within which all correct solutions must lie. Let us assume that the K-values of the overall composition are sorted from the lightest component (with the largest K-value) to the heaviest component (with the smallest K-value), that is $K_1 > ... > K_j > 1 > K_{j+1} > ... > K_{N_C}$.

The same objective function as Eq. (4.12) applies in this case. However, the investigation window of Eq. (4.13) is different. From Eq. (4.7), we have for each component in the equilibrium liquid phase

$$x_i = \frac{\left(K_1 - 1\right) z_i x_1}{\left(K_i - 1\right) z_1 + \left(K_1 - K_i\right) x_1} \quad i = 2,..., N_C - 1 \tag{A.1}$$

Further, we want $0 \le x_i \le 1$ for each equilibrium composition. As a result,

$$0 \le \frac{\left(K_1 - 1\right) z_i x_1}{\left(K_i - 1\right) z_1 + \left(K_1 - K_i\right) x_1} \le 1 \quad i = 2,..., N_C - 1 \tag{A.2}$$

When the overall composition for component *i* is positive,

$$\frac{(K_i-1)z_1+(K_1-K_i)x_1}{(K_1-1)z_i x_1}\geq 1 \qquad i=2,...,N_C-1 \text{ and } z_i>0 \tag{A.3}$$

From Eq. (A.3), the primary variable x_1 must fall into the following window,

$$x_1\begin{cases} < \dfrac{(K_1-1)z_1}{(K_1-1)z_i-(K_1-K_i)} & \text{when } z_i>0 \text{ and } (K_1-1)z_i-(K_1-K_i)>0 \\ \geq \dfrac{(K_1-1)z_1}{(K_1-1)z_i-(K_1-K_i)} & \text{when } z_i>0 \text{ and } (K_1-1)z_i-(K_1-K_i)<0 \end{cases} \tag{A.4}$$

Similarly, when the overall composition for component *i* is negative, the primary variable x_1 must lie within

$$x_1\begin{cases} < \dfrac{(K_1-1)z_1}{(K_1-1)z_i-(K_1-K_i)} & \text{when } z_i\leq 0 \text{ and } (K_1-1)z_i-(K_1-K_i)<0 \\ \geq \dfrac{(K_1-1)z_1}{(K_1-1)z_i-(K_1-K_i)} & \text{when } z_i\leq 0 \text{ and } (K_1-1)z_i-(K_1-K_i)>0 \end{cases} \tag{A.5}$$

The final window of the primary variable x_1 are obtained from Eqs (A.4) through (A.5) together with $0\leq x_1\leq 1$ by

$$x_1\begin{cases} \leq \min[1, \dfrac{(K_1-1)z_1}{(K_1-1)z_i-(K_1-K_i)}] & \text{when } z_i\left[(K_1-1)z_i-(K_1-K_i)\right]>0 \\ \geq \max[0, \dfrac{(K_1-1)z_1}{(K_1-1)z_i-(K_1-K_i)}] & \text{otherwise} \end{cases} \tag{A.7}$$

All the correct solutions fall into the above window. The objective function is continuous in the window of Eq. (A.7), however, the function is no longer necessary positive at the lower limit of the window or negative at the upper limit.

We present several example flash calculations where at least one composition is negative. We considered the overall compositions that are along the same tie-line extension as those in Fig. (4.1). The overall compositions studied are point A (-0.171, 0.020, 1.151) and point B (1.322, 0.500, -0.822). We examined the objective functions and the investigation window for each overall composition using different methods.

Point A has two valid tie lines that pass through it. Figure (A.2) shows the Rachford-Rice (1952) objective function with the Whitson-Michelsen window (1989). Both roots corresponding to the different tie lines are not within the Whitson-Michelsen window. Figure (A.3) compared the Wang and Orr function (1997, 1998) and our new function. As is shown, the two different roots lie within the window of Eq. (A.7). The Wang and Orr function has a trivial solution at $x_1 = 0$.

Point B has only one tie line that passes through it. Figure (A.4) shows the Rachford-Rice (1952) objective function with the Whitson-Michelsen window (1989). The correct solution is not in that window. Figure (A.5) compared the Wang and Orr function (1997, 1998) and our new method. As is shown, the two different roots lie within the window in Eq. (A.7). Wang and Orr method also has the trivial solution of $x_1 = 0$.

In both examples, the correct solutions lie within the window defined by Eq. (A.7), and the new objective does not have a trivial solution as does Wang and Orr (1997)

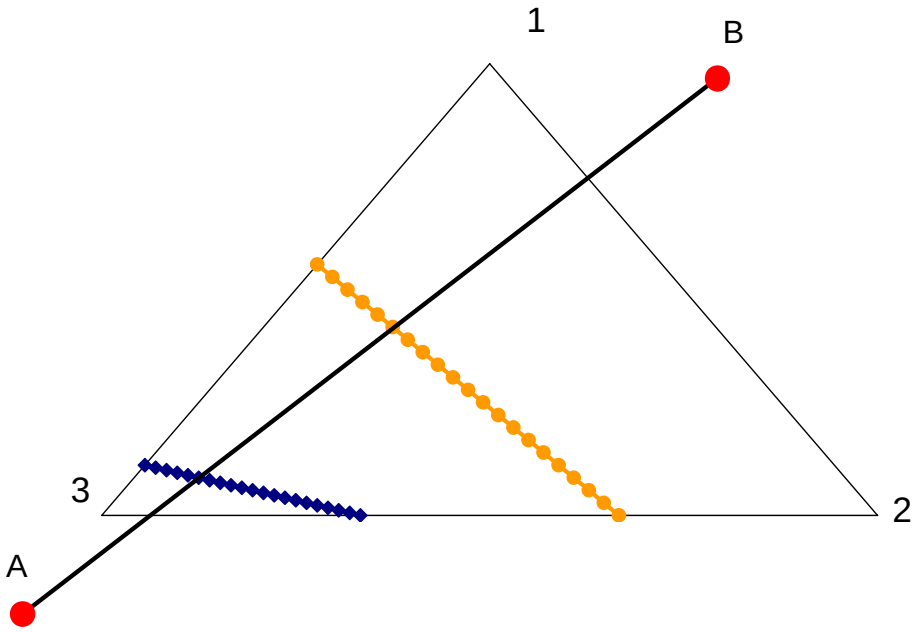

Fig. A.1 Ternary diagram with K_1 =5.0 , K_2 =2.0 , and K_3 =0.5 . The two compositions shown lie on the same tie-line extension as that point in Fig. (4.1).

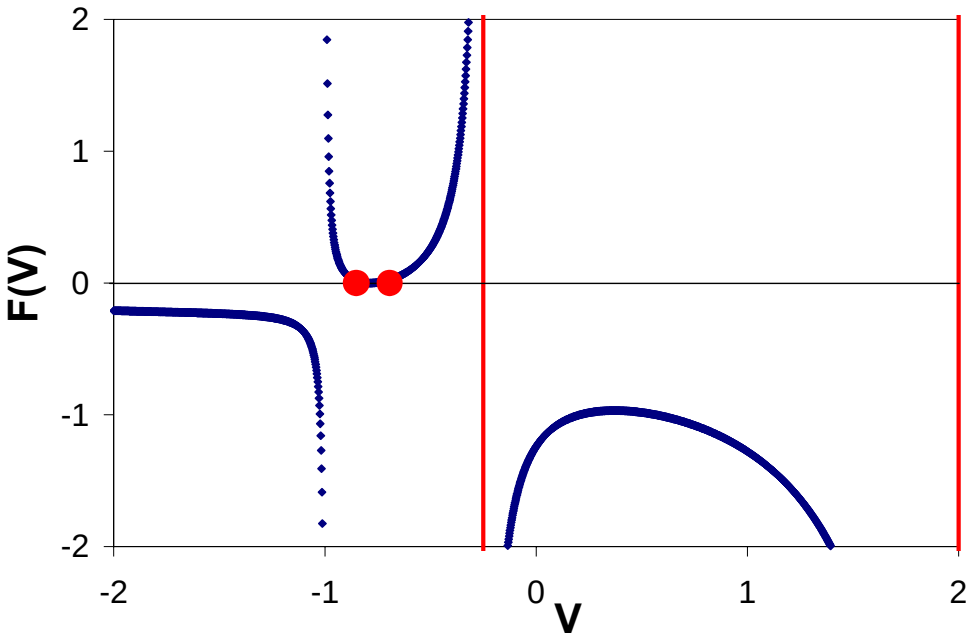

Fig. A.2 Rachford-Rice function (1952) for point A in Fig. (A.1). The vertical lines are the limits of the Whitson-Michelsen window (1989). There are two roots (solid dots) corresponding to different tie lines and both are not within that window.

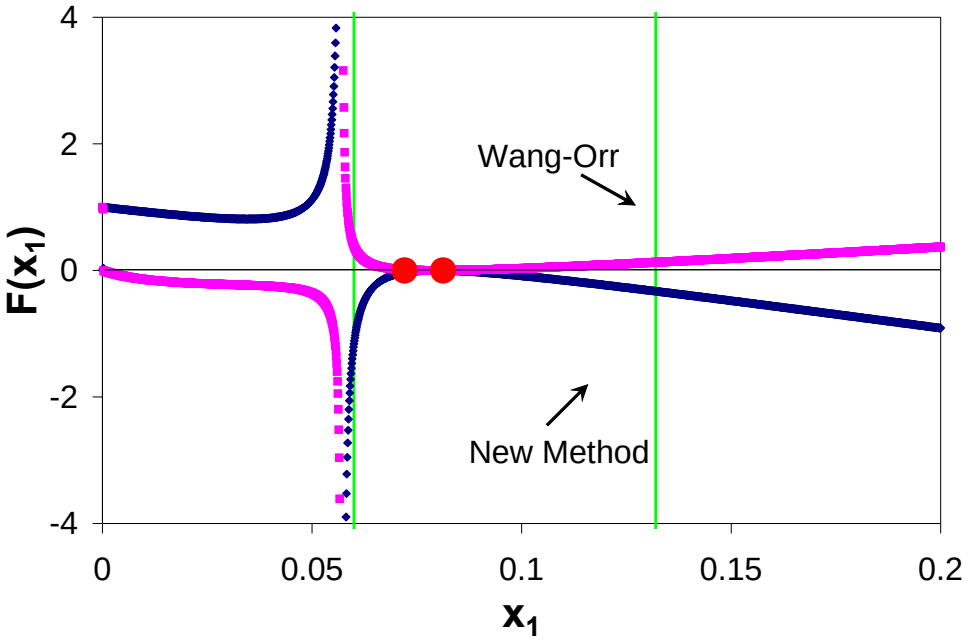

Fig. A.3 Objective functions for point A in Fig. (A.1) based on the new objective method and that given by Wang and Orr (1997, 1998). The two correct roots (the solid dots) lie within the window given by Eq. (A.7). The new objective function is very linear.

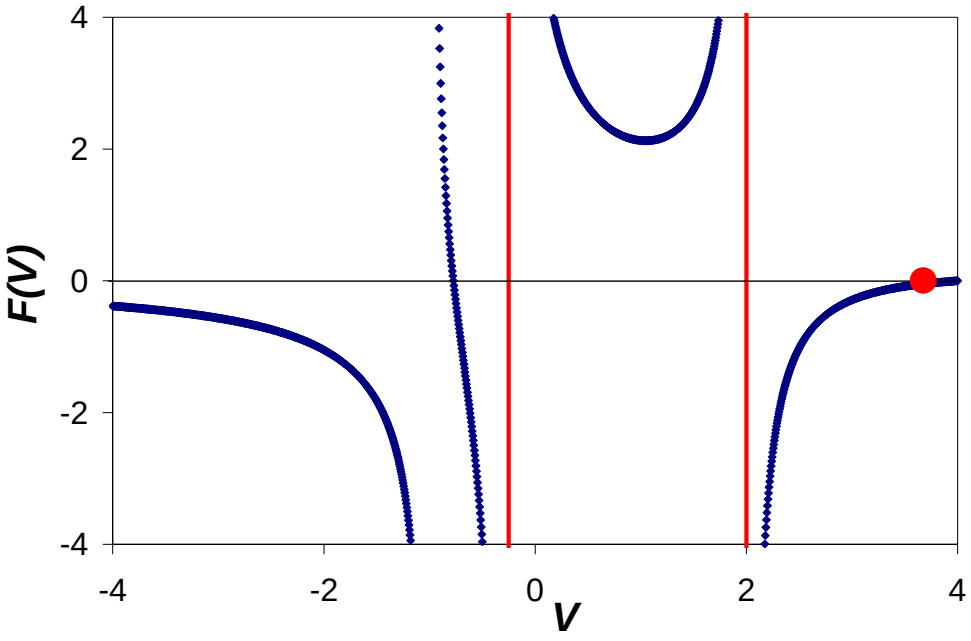

Fig. A.4 Rachford-Rice function (1952) for point B in Fig. (A.1). The vertical lines are the limits of the Whitson-Michelsen window (1989). The correct root (solid dot) is not within the window.

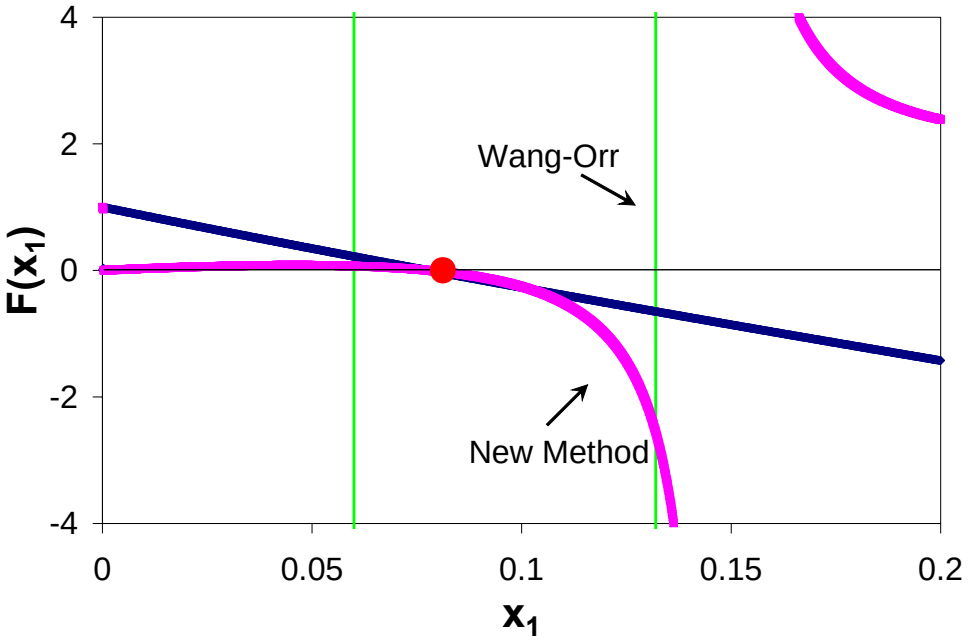

Fig. A.5 Objective functions for point B in Fig. (A.1) based on the new objective method and that given by Wang and Orr (1997, 1998). The correct root (the solid dot) lies within the window given by Eq. (A.7). The new objective function is very linear.

Glossary

a	attraction parameter for EOS, $psia \cdot ft^3 / lbm - mol$
A	attraction parameter for EOS, dim.
b	repulsion parameter for EOS, $ft^3 / lb - mol$
B	repulsion parameter for EOS, dim.
C	transformed composition, dim.
d	dimensionless chemical potential, dim.
D	dimensionless chemical potential, dim.
e	error or objective function
F	objective function
$\hat{f}$	component fugacities, psia
g	binary interaction parameter for new model, see Eqs. (2.5), dim.
h	binary interaction parameter for new model, see Eqs. (2.5), dim.
J	Jacobian matrix, dim.
k	binary interaction parameter, dim.
K	K-value, dim.
L	liquid mole fraction, dim.
N_C	number of components
N_P	number of phases
MW	molecular weight, dim
P	reservoir pressure, psia
q	reduced variable for pure components, dim.
R	gas constant, $psia \cdot ft^3 / lb - mol \cdot R$

T	temperature, ^{o}F
$\bar{V}$	molar volume, $ft^3 / lb - mol$
V	vapor mole fraction, dim.
x	liquid phase molar composition, dim.
X^*	transformed liquid phase molar comopsition, dim.
y	vapor phase molar composition, dim.
$\tilde{y}$	composition at the stationary point, dim.
Y	modified primary variable in stability analysis
Y^*	transformed vapor phase molar comopsition, dim.
$\tilde{Y}$	modified stationary points in stability analysis
z	overall composition, dim.
Z^*	transformed overall molar comopsition, dim.
α	transformation parameter,dim.
δ	Kronecker delta function
δ_1	EOS parameter, see Eq. (2.3)
δ_2	EOS parameter, see Eq. (2.3)
ϕ_i^j	component fugacity coefficient, dim.
Θ	reduced parameters, various dimensions
ω	acentric factor, dim.
μ	chemical potential, J/mol

Superscripts and Subscripts

*	transformed composition
i,j	species index
k,l	index for reduced parameters
c	critical properties

D	dimensionless quantity
j,l	phase index
L	liquid phase
m	mixture property
max	upper boundary of the investigation range
min	lower boundary of the investigation range
ref	reference component
T	total property of multi-phase mixture
V	vapor phase

Bibliography

Baker L.E., Pierce, A.C. and Luks, K.D.: "Gibbs Energy Analysis of Phase Equilibria," *SPEJ,* **22**: 731-742, 1982.

Bullard, L. G. and Biegler, L. T.: "Iterated Linear Programming Strategies for Non-smooth Simulation: a Penalty Based Method for Vapor-liquid Equilibrium Applications," *Comp. & Chem. Eng.,* **17** (1), 95-109, 1993.

Chang, Y.: "Development and Application of an Equation of State Compositional Simulator," Ph.D. dissertation, the University of Texas at Austin, 1990.

Coats, K.H.: " Simulation of Gas Condensate Reservoir Performance," *JPT*, 1870-1886, 1985

Egwuenu, A.M., Johns, R.T., and Li, Y.: "Improved Fluid Characterization for Miscible Gas Floods," SPE 94034 presented at 2005 SPE Europec Conference, Madrid, Spain, June 13-16.

Firoozabadi A. *Thermodynamics of Hydrocarbon Reservoirs.* New York, NY: McGraw-Hill; 1999.

Firoozabadi, A. and Pan, H.: "Fast and Robust Algorithm for Compositional Modeling: Part I: Stability Analysis Testing," *SPEJ* (Mar 2002), 78-89.

Gautam, R. and Seider, W. D.: "Computation of Phase and Chemical Equilibrium. Part I. Local and Constrained Minima in Gibbs Free Energy," *AIChE J*., **25:** 991-999, 1979.

Han, G. And Rangaiah, G. P.: " A Method for Calculation of Vapor-Liquid and Liquid-Liquid Equilibria," *Comp. & Chem. Eng.*, **21** (8): 905- 913, 1997.

Hand, D.B.: " Dineric Distribution," *J.Phy.Chem*., **34** (9): 1961-2000, 1930.

Harding S.T. and Floudas C.A.: "Phase Stability with Cubic Equations of State: A Global Optimization Approach," *AIChE J.,* **7**:1422-1440, 2000.

Hearn, C.L and Whitson, C.H.: "Evaluating Miscible and Immiscible Gas Injection in the Safah Field, Oman," SPE 29115 presented at the 1995 SPE Symposium on Reservoir Simulation, San Antonio, TX, Feb 12-15.

Heidemann, R. A. Three-phase Equilibria Using Equations of State. *AIChE J.***, 20**:847-855,1974.

Hendriks, E.M.: "Reduction Theorem for Phase Equilibrium Problems," *Ind.Eng.Chem.Res*., **27**:1728-1733, 1988.

Hendriks, E.M. and Van Bergen, A.R.D.: "Application of a Reduction Method to Phase Equilibria Calculations," *Fluid Phase Equilib.*, **74**:17,1992.

Hong, K.C.: "Lumped-Component Characterization of Crude Oils for Compositional Simulation," SPE 10691 presented at 1982 SPE/DOE Enhanced Oil Recovery Symposium, Tulsa, OK, Apr 4-7.

Hoteit, H. and Firoozabadi, A.: " Simple Phase Stability-Testing Algorithm in the Reduction Method," *AIChE J.,* **52**(8), 2909-2920, 2006.

Hua J.Z., Brennecke J.F., Stadtherr M.A.: "Reliable Prediction of Phase Stability Using an Interval Newton Method," *Fluid Phase Equilib.,* **116**:52-59,1996.

Hua J.Z., Brennecke J.F., Stadtherr M.A.: "Reliable Computation of Phase Stability Using Interval Analysis: Cubic Equation of State Models," *Comput. Chem Eng.,* **22**:1207-1214,1998

Jensen, B.H. and Fredenslund, A.: "A Simplified Flash Procedure for Multicomponent Mixtures Containing Hydrocarbons and One Non-hydrocarbon Using Two-parameter Cubic Equations of State," *Ind.Eng.Chem.Res*., **26**: 2129-2134,1987.

Jessen,K., Michelsen, M.L. and Stenby, E.H.: "Global Approach for Calculation of Minimum Miscibility Pressure," *Fluid Phase Equilibria*., **153**(2):251-263, 1998.

Johns, R.T., Dindoruk, B. and Orr, F.M. Jr.: "Analytical Theory of Combined Condensing/Vaporizing Gas Drives," *SPE Adv. Tech. Series,* **1**: 7-16, 1992.

Johns, R.T. and Orr, F.M. Jr.: "Miscible Gas Displacement of Multicomponent Oils," S*PEJ* (Mar 1996), 39-46.

Johns, R.T., Fayers, F.J., and Orr, F.M. Jr.: "Effect of Gas Enrichment and Dispersion on Nearly Miscible Displacement in Condensing/Vaporizing Drives," *SPE Adv. Tech. Series,* **2**: 26-34, 1993.

Leibovici, C.F. and Neoschil, J.: "A Solution of Rachford-Rice Equation," *Fluid Phase Equilibria*, **74**(1): 303-308, 1992.

Leibovici, C.F. and Neoschil, J.: "A New Look at the Rachford-Rice Equations for Multiphase Systems," *Fluid Phase Equilibria*, **112**(2): 217-221, 1995.

Li, Y.K. and Nghiem, L.X.: "The Development of a General Phase Envelope Construction Algorithm for Reservoir Fluid Studies," SPE 11198 presented at

1982 SPE Annual Technical Conference and Exhibition in New Orleans, LA, September 26-29.

Liu, K.: "Reduce the Number of Components for Compositional Reservoir Simulation," SPE 66363 presented at the 2001 SPE Reservoir Simulation Symposium, Houston, TX, Feb 11-14.

Litvak, M.L. and Wang. C.H.: "Integrated Reservoir and Surface Pipeline Network Compositional Simulations," SPE 48859 is presented at the 1998 SPE International Conference and Exhibition in Beijing, China, November 2-6.

McDonald CM, Floudas CA.: "Global Optimization for the Phase Stability Problem," *AIChE J.,* **41**:1798-1814,1995

Michelsen, M.: "The Isothermal Flash Problem. Part I: Stability," *Fluid Phase Equilib*., **9**:1-19, 1982.

Michelsen, M.: "The Isothermal Flash Problem. Part II: Phase Split Calculation," *Fluid Phase Equilib*., **9**: 21-40, 1982.

Michelsen, M.: "Simplified Flash Calculation for Cubic Equations of State," *Ind.Eng.Chem.Proc.Des.Dev*., **25**: 184-188, 1986.

Monroy-Loperena, R. and Vargas-Villamil, F.D.: "On the Determination of the Polynomial Defining Vapor-Liquid Split of Multi-Component Mixtures," *Chem.Eng.Sci.*, **56**(20): 5865-5868, 2001.

Nagarayan, N. R., Cullik, A. S. and Griewank, A.: "New Strategy for Phase Equilibrium and Critical Point Calculations by Thermodynamic Energy Analysis. Part I. Stability Analysis and Flash," *Fluid Phase Equilib.,* **62**: 191-210,1991

Nichita, D.V.: "A Reduction Method for Phase Equilibrium Calculations with Cubic Equations of State," *Brazilian J. of Chemical Engineering*, **23**(3): 427-434, 2006

Nichita, D.V., Broseta, D., and Hemptinne, J.C.: "Multiphase Equilibrium Calculation Using Reduced Variables," SPE 89439 presented at the 2004 SPE/DOE 14th Symposium on Improved Oil Recovery, Tulsa, OK, April 17-21.

Nichita, D. V., Broseta, D., de Hemptinne, J.-C. and Lachet, V.: "Efficient Phase Equilibrium Calculation for Compositional Simulation: the Direct Reduced Flash," *Petro. Sci. & Tech.*, **25**(3): 315-342, 2007.

Nichita, D.V., De Los Angeles Duran Valencia, C. and Gomez, S.: "Volume-based Thermodynamics Global Phase Stability Analysis," *Chem. Eng. Comm.*, **193**(10): 1194-1216, 2006.

Nichita, D.V., Gomez, S. and Luna, E.: "Multiphase Equilibria Calculation by Direct Minimization of Gibbs Free Energy with a Global Optimization Method," *Comp. & Chem. Eng.*, **26**(12), 1703-1724, 2002.

Nichita, D.V., Gomez S. And Luna, E.: "Phase Stability Analysis with Cubic Equations of State by Using a Global Optimization Method," *Fluid Phase Equilib.*, **194**: 411-437, 2002.

Nichita, D.V. and Minescu, F.: "Efficient Phase Equilibrium Calculation in a Reduced Flash Context," *Can. J. Chem. Eng.*, **82**(6), 1225-1238, 2004.

Okuno, R. Private communications, 2007.

Pan, H. and Firoozabadi, A.: "Fast and Robust Algorithm for Compositional Modeling: Part II: Two-phase Flash Computations," SPE 71603 presented at 2001 ATCE, New Orleans, LA, September 30 – October 3.

Peng, D.Y. and Robinson, D.B.: "A Rigorous Method for Prediction the Critical Properties of Multicomponent Systems from an Equation of State," *AIChEJ*, **23:** 137, 1977.

Pope, G.A., Tsaur, K, Schechter, R.S. and Wang, B: "The Effect of Several Polymers on the Phase Behavior of Micellar Fluids," *SPEJ*, 1982 Dec, 816-830.

Rachford, H.H. and Rice, J.D.: "Procedure for Use of Electronic Digital Computers in Calculating Flash Vaporization Hydrocarbon Equilibrium," *Petroleum Transactions AIME*, **195**: 237-238, 1952.

Rasmussen C.P., Krejbjerg K., Michelsen M.L. and Bjurstrom K.E.: "Increasing Computational Speed of Flash Calculations with Application for Compositional, Transient Simulations," *SPERE,* 2006 February, 32-38.

Redlich, O., and Kwong, J.S.: "On the Thermodynamics of Solutions. V: An Equation of State. Fugacities of Gaseous Solutions, " *Chem. Rev.*, **44**: 233, 1949.

Soave, G.: "Equilibrium Constants from a Modified Redlich-Kwong Equation of State," *Chem. Eng. Sci.* , **27**: 1197, 1972.

Solano, R., Johns, R.T., and Lake, L.W.: "Impact of Reservoir Mixing on Recovery in Enriched-Gas Drives Above the Minimum Miscibility Enrichment," *SPEREE*, **4**(5), 358-365, 2001.

Stenby, E.H. and Wang, P.: "Noniterative Phase Equilibrium Calculation in Compositional Reservoir Simulation," SPE 26641 presented at 1993 ATCE, Houston, TX, October 3-8.

Sun A.C. and Seider W.D..: "Homotopy-continuation Method for Stability Analysis in the Global Minimization of the Gibbs Free Energy," *Fluid Phase Equilib.,* **103**: 213-249, 1995.

Tang, D.E. and Zick, A.A.: "A New Limited Compositional Reservoir Simulator," SPE 25255 presented at 1993 SPE Symposium on Reservoir Simulation, New Orleans, LA, February 28 – March 3.

Trangenstein, J.A.: "Minimization of Gibbs Free Energy in Compositional Reservoir Simulation", paper SPE 13520, presented at the SPE 1985 Reservoir Simulation Symposium, Dallas, TX.

Von Rossenberg, D.U.: "Determination of the Polynomial Defining Vapor-Liquid Split of Multi-Component Mixtures," *Chem. Eng. Sci.*, **18**(4): 219-222, 1963.

Von Rossenberg, D.U.: "On the Determination of the Polynomial Defining Vapor-Liquid Split," *Chem.Eng.Sci.*, **32**(12): 1546-1547, 1977.

Voskov, D.V. and Tchelepi,H.A.: "Compositional Space Parameterization for Flow Simulation," SPE 106029 presented at 2007 SPE Reservoir Simulation Symposium, Houston, TX, February 26-28.

Wang, Y. and Orr, F.M. Jr.: "Calculation of Minimum Miscibility Pressure," SPE 29683 presented at 1998 SPE/DOE Improved Oil Recovery Symposium, Tulsa, OK, April 19-22.

Wang, Y. and Orr, F.M. Jr.: "Analytical Calculation of Minimum Miscibility Pressure," *Fluid Phase Equilib.*, **139**(1):101-124, 1997.

Warren, J.H. and Adewumi, M.A.: "Polynomial Objective Fucntions for Flash Calculations: Binary, Ternary and Quaternary Systems," *Ind.Eng.Chem.Res.*, **32**(7), 1528-1530, 1993.

Whitson, C.H. and Michelsen, M.L.: "The Negative Flash," *Fluid Phase Equilib.*, **53**(1): 51-71, 1989.

Yuan, H. and Johns, R.T.: "Simplified Method for Calculation of Minimum Miscibility Pressure or Enrichment," *SPEJ,* December 2005: 416-425.

Zick, A.A.: "A Combined Condensing/Vaporizing Mechanism in the Displacement of Oil by Enriched Gases," SPE 15493 presented at 1986 ATCE, New Orleans, LA, October 5-8.

Vita

Yinghui Li was born on September 27, 1976 in Handan, Hebei province, China, the son of Qi Li and Naibo Liu. In 1994, he entered Tsinghua University in Beijing, China, and received the degree of Bachelor of Science in Chemical Engineering in 1999 in this five-year program. In the same year, he was admitted to Chinese Academy of Science Graduate School in Beijing for a three-year graduate program in Chemical Engineering in the Institute of Process Engineering. He received a Master of Science degree in 2002, and then entered the Department of Petroleum and Geosystems Engineering at the University of Texas at Austin in 2003. He has authored and co-authored three SPE papers. He was awarded Pre-emptive Fellowship in 2003 and Conoco-Phillips Fellowship in 2004.

Permanent address: 1624 W 6th Street, Apt M, Austin, TX, 78703

This dissertation was typed by Yinghui Li.